“Mutated neo-antigens as targets for individualized cancer immunotherapy”

Dissertation
zur Erlangung des Grades
“Doktor der Naturwissenschaften”

Im Promotionsfach Pharmazie
am Fachbereiche Chemie, Pharmazie und Geowissenschaften
der Johannes Gutenberg-Universität
in Mainz

Mathias Vormehr
geb. in Worms

Mainz, 2016

Dekan: [redacted]

Erster Berichterstatter: [redacted]

Zweiter Berichterstatter: [redacted]

Dritter Berichterstatter: [redacted]

Datum der mündlichen Prüfung: 09.06.2016

Summary

Carcinogenesis is largely driven by somatic gene mutations. Accumulating evidence suggests that a significant subset of mutations result in neo-epitopes recognized by tumor-specific T cells and thus may constitute the Achilles' heel of malignant cells. T cells directed against mutations have been shown to have a key role in spontaneous immune responses against cancer and in the clinical efficacy of potent cancer immunotherapy modalities, such as adoptive transfer of autologous tumor infiltrating lymphocytes and immune checkpoint inhibitors. Whereas these findings strengthen the idea of a prominent role of neo-epitopes in tumor rejection, the systematic therapeutic exploitation of mutations was hampered until recently by the uniqueness of the repertoire of mutations ("the mutanome") in every patient's tumor. Our group pioneered to set up a process for an individualized immunotherapy approach to target the full spectrum of a patient's personal tumor-specific mutations by combination of exome and transcriptome sequencing, bioinformatic target identification and selection followed by RNA based tumor vaccination.

In this thesis, it was shown that tumor mutations, in particular single nucleotide variations (SNVs), insertions, deletions (indels) and gene fusions are frequently immunogenic. Moreover, it was demonstrated for the first time that SNVs are predominantly recognized by $CD4^+$ T cells. Neo-epitopes can be targeted by customized RNA-based monotope or poly-neo-epitope vaccines with substantial therapeutic effects in mouse tumor models. Notably, CD4 neo-epitope vaccination was shown to positively affect the tumor microenvironment of the CT26 colon carcinoma by decreasing the ratio of $FoxP3^+$ regulatory T cells to $CD4^+$ T cells and augmenting $CD4^+$ and $CD8^+$ T-cell infiltration. In addition, anti-tumoral efficacy of neo-epitope specific $CD4^+$ T cells in CT26 colon carcinoma tumors was shown to critically depend on $CD8^+$ T cells and CD40L signaling. CD40-CD40L interaction between activated $CD4^+$ T cells and dendritic cells (DCs) mediates the upregulation of costimulatory molecules on DCs which in turn supports the priming of naive, tumor specific $CD8^+$ T cells. A meta-analysis revealed that immunogenic SNVs and indels have a significantly better binding prediction for MHC class II than their non-immunogenic counterparts. Vaccination against mutations selected for favorable MHC class II binding prediction and abundant mutated mRNA expression resulted in tumor-control without prior immunogenicity testing.

The preclinical data shown here for three different mouse tumor models established the feasibility of individualized cancer vaccines and raised hopes that this concept will be effective in humans as well. This study paved the way and directly influenced the design of clinical studies in melanoma and triple-negative breast cancer patients.

Zusammenfassung

Somatische Genmutationen sind eine Hauptursache der Karzinogenese. Darüber hinaus häufen sich Hinweise, dass eine signifikanter Anteil von Mutationen zu Neo-Epitopen führen, die von tumorspezifischen T-Zellen erkannt werden und daher die Achillesferse maligner Zellen darstellen könnten. Mutationsspezifische T-Zellen spielen eine Schlüsselrolle in der spontanen Immunantwort gegen Krebs und in der klinischen Wirksamkeit erfolgreicher Immuntherapien wie dem adoptiven Transfer von tumorinfiltrierenden T-Zellen oder Immun-Checkpoint-Inhibitoren. Obgleich diese Erkenntnisse die Idee einer prominenten Rolle von Neo-Epitopen in der Abstoßung von Tumoren stärken, war eine therapeutische Nutzung bis vor kurzem durch die Einzigartigkeit des Mutatiosrepertoires ("Mutanom") in jedem individuellen Tumor eingeschränkt. Unsere Gruppe konnte erstmals einen Prozess für eine individualisierte Immuntherapie etablieren, der das volle Spektrum tumorspezifischer Mutationen eines jeden Patienten adressiert. Mittels Exom- und Transkriptom-Sequenzierung sowie bioinformatischer Mutationsidentifizierung und Selektion wird das Mutanom eines Patienten bestimmt und durch eine RNA basierte Impfung targetiert.

Diese Arbeit zeigt, dass Tumormutationen, insbesondere einzelnukleotid Variationen (SNVs), Insertionen, Deletionen (Indels) und Genfusionen häufig immunogen sind. Zudem wird zum ersten mal demonstriert, dass SNVs hauptsächlich von $CD4^+$ T-Zellen erkannt werden. Neo-Epitope können durch eine maßgeschneiderte RNA-basierte Monotop- oder Poly-Neo-Epitop-Vakzine adressiert werden, die einen bedeutenden therapeutischen Effekt in murinen Tumoren hervorruft. Es konnte gezeigt werden, dass eine CD4 Neo-Epitop-Vakzinierung das Tumormikromilieu des CT26 Kolonkarzinoms durch Reduzierung des Verhältnisses von suppressiven $FoxP3^+$ regulatorischen T-Zellen zu $CD4^+$ T-Zellen und durch Steigerung der $CD4^+$ und $CD8^+$ T-Zellinfiltration positiv beeinflusst. Zudem wurde gezeigt, dass der antitumorale Effekt mutationsspezifischer $CD4^+$ T-Zellen entscheidend von $CD8^+$ T-Zellen und CD40L Signalisierung abhängt. Der CD40-CD40L Singalweg zwischen aktivierten $CD4^+$ T-Zellen und dendritischen Zellen (DCs) führt zur Hochregulierung kostimulatorische Moleküle auf DCs das wiederum das Priming naiver, tumorspezifischer $CD8^+$ T-Zellen fördert. Eine Metaanalyse konnte zeigen, dass immunogene im Vergleich zu nicht-immunogenen SNVs sowie Indels eine signifikant bessere Bindungsvorhersage für MHC-Klasse-II haben. Vakzinierung gegen Mutationen mit prädizierter MHC-Klasse-II Bindung sowie hoher Expression von mutierter mRNA im Tumor führte zu einem antitumoralem Effekt ohne einer vorherigen Immunogenitätstestung.

Die hier gezeigten präklinischen Studien in drei verschiedenen Maus-Tumormodellen beweißen die Durchführbarkeit einer individualisierten Krebsvakzine und wecken Hoffnungen, dass dieses Konzept ebenfalls bei Menschen erfolgreich sein wird. Diese arbeit bereitete den Weg und beeinflusste das Design von klinischen Studien in Melanom- und dreifach negativen Brustkrebspatienten.

Publications

Parts of this thesis (including some figures and text fragments) were previously published in on of the following articles:

Kreiter S, Vormehr M, van de Roemer N, Diken M, Löwer M, Diekmann J, Boegel S, Schörs B, Vascotto F, Castle JC, Tadmor AD, Schoenberger SP, Türeci Ö, Sahin U, **Mutant MHC class II epitopes drive therapeutic immune responses to cancer.** *Nature* 2015, 520:692-696.

Vormehr M, Diken M, Boegel S, Kreiter S, Türeci Ö, Sahin U, **Mutanome directed cancer immunotherapy.** *Curr Opin Immunol.* 2015, 39:14-22

Vormehr M, Schrörs B, Boegel S, Löwer M, Türeci Ö, Sahin U, **Mutanome Engineered RNA Immunotherapy: Towards patient-centered tumor vaccination.** *J Immunol Res.* 2015, Article ID 595363.

Türeci Ö, Vormehr M, Kreiter S, Huber C, Sahin U, **Targeting the roots of cancer with individualized neo-epitope vaccines.** *Clin Cancer Res.* 2016, 22(8).

Kloke B, Kreiter S, Vormehr M, Diken M, Kuhn AN, Sahin U, **Actively personalized cancer vaccines - the step into clinical application.** *Pharmazie* 2015, 10:1-5.

Contents

List of Figures

List of Tables

Abbreviations

4T1-Luc	4T1-luc2-tdtomato
ACT	Adoptive cell transfer
ANN	Artificial neural network
AP	Alkaline phoshatase
APC gene	Adenomatous polyposis colon gene
APC	Antigen-presenting cell
ATP	Adenosine triphosphate
BCIP	5-Bromo-4-chloro-3-indolyl phosphate
BLI	Bioluminescence imaging
BSA	Bovine serum albumin
CD	Cluster of differentiation
CDK4	Cyclin-dependent kinase 4
CEA	Carcinoembryonic antigen
CGA	Cancer germline antigens
CLL	Chronic lymphocytic leukemia
CNS	Central nervous system
CombLib	Combinatorial peptide libraries
ConA	Concanavalin A
CTL	Cytotoxic T lymphocyte
DC	Dendritic cell
DMEM	Dulbecco's Modified Eagle Medium
DMSO	Dimethyl sulfoxide
DNA	Deoxyribonucleic acid
EDTA	Ethylenediaminetetraacetic acid
ELISA	Enzyme-linked immunosorbent
ELISpot	Enzyme-linked immunospot
EMA	European medicines agency
ERAP	ER aminopeptidase
FACS	Fuorescence-activated cell sorting
FBS	Fetal bovine serum
FDA	U.S. food and drug administration
FFPE	Formaldehyde-fixed, paraffin-embedded
FSC	Forward scatter
GFP	Freen fluorescent protein
GM-CSF	Granulocyte-macrophage colony-stimulating factor
GMP	Good manufacturing practice
HEPES	4-(2-hydroxyethyl)-1-piperazineethanesulfonic acid
HMGB1	High-mobility group protein B1
HPLC	High-performance liquid chromatography
HPV	Human papillomavirus
IDO	Indoleamine-pyrrole 2,3-dioxygenase
IEDB	Immune epitope database
IF	Immunofluorescence
IFN	Interferon
IL	Interleukin
Indel	Insertion and deletion
IP	Intraperitoneal
IV	Intravenous
Luc	Firefly Luciferase
MACS	Magnetic-activated cell sorting
MCA	Methyl-cholanthrene
MDA5	Melanoma differentiation-associated protein 5
MDSC	Myeloid-derived suppressor cells
MEM	Minimum Essential Medium Eagle
MHC	Major histocompatibility complex
miRNA	MicroRNA
MITD	MHC class I trafficking domain
mRNA	Messenger RNA
MSI	Microsatellite instable
MSS	Microsatellite stable
NBT	Nitro blue tetrazolium chloride
NGS	Next-generation-sequencing
NMD	Nonsense-mediated mRNA decay
NSCLC	Non–small-cell lung cancer
nsSNV	Non-synonymous SNV
NVRC	Normalized variant read counts
ORF	Open reading frame
PBL	Peripheral blood lymphocytes
PBS	Phosphate buffered saline
PKR	Protein kinase R
PMA	Phorbol 12-myristate 13-acetate
PVDF	Polyvinylidene difluoride
Ras	Rat sarcoma
RB	Retinoblastoma
RIG-I	Retinoic acid-inducible gene 1
RNA	Ribonucleic acid
ROC	Receiver operating characteristic
ROI	Region of interest
ROS	Reactive oxygen species
RPKM	Reads per kilobase per million mapped reads
RPMI	Roswell Park Memorial Institute
RTK	Receptor tyrosine kinase
RT	Room temperature
s.e.m.	Standard error of the mean
SC	Subcutaneous
SEC	Secretion domain
SEREX	Serological identification of antigens by recombinant expression cloning

SMM	Stabilized matrix method
SNVs	Single nucleotide variations
SP	Signal peptide
SSC	Sideward scatte
TAA	Tumor associated antigens
TAM	Tumor-associated macrophage
TAP	Transporter associated with antigen processing
TCGA	The Cancer Genome Atlas
TIL	Tumor-infiltrating lymphocyte
TLR	Toll-like receptor
TME	Tumor microenvironment
TP53	Tumor protein 53
Treg	Regulatory T cell
TRP-1	Tyrosinase-related protein-1
TSA	Tumor specific antigens
UTR	Untranslated region
VEGF	Vascular endothelial growth factor

1 Introduction

1.1 Cancer

Cancer is a group of diseases characterized by cells with limitless uncontrolled and invasive growth. The hallmarks of cancer which are present in almost every cancer type are summarized in Figure 1.1.

According to the WHO cancer a leading couse of death worldwide. The lifetime risk of developing cancer is approximately 50 % for men and 43 % for women in Germany. Five year survival rates strongly depend on the tumor type. Whereas 90 % of patients suffering from malignant melanoma survive at least five years, only 10 % of pancreatic cancer patients survive more than five years. The most common cancer type for men is prostate cancer (25 %). Women most often suffer from breast cancer (32 %). Second and third most prevalent tumor types irrelevant of sex is colon and lung cancer [1].

The cause of cancer are genetic and epigenetic changes facilitating the detrimental properties of cancer cells [2]. During tumor initiation non-synonymous mutations in tumor suppressor genes such as TP53 [3], RB [4] or APC [5] and proto-oncogenes (e.g. the Ras genes [6]) allow for uncontrolled growth and amplification of genetic instability. Epigenetic silencing of tumor suppressor gene promoters by hypermethylation of CpG dinucleotides, miRNA mediated downregulation of DNA repair genes or viral infections are yet other ways that initiate uncontrolled tumor growth and genetic instability [7, 8]. Tumor progression through acquisition of additional mutations that result in further malignant properties can be promoted by constant inflammatory or growth signals. For example, while chronic liver inflammation during hepatitis C virus infection promotes liver cancer [9], chronic asbestos exposure that causes airway inflammation is known to promote lung cancer [10].

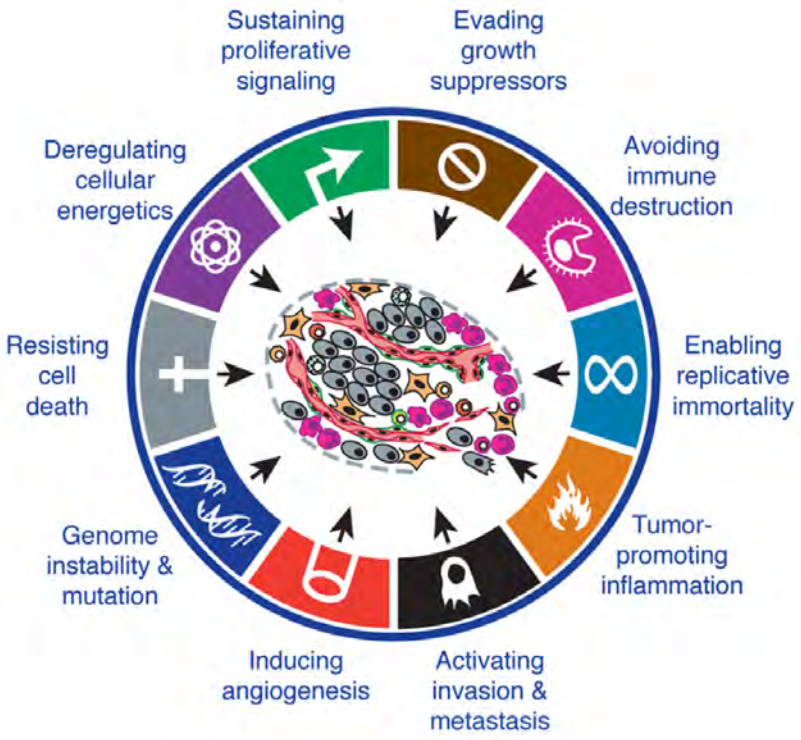

Figure 1.1: The Hallmarks of Cancer. Cancer cells have acquired several functional properties that contribute to their destructive potential. Modified after Hanahan and Weinberg [11].

1.2 Cancer Immunotherapy

Cancer immunotheraphy has its roots in the late 19th century. Although the mechanism of action was yet unknown, WILLIAM B. COLEY showed that cancer regressed when patients were stimulated with a mixture of attenuated bacteria (*Coley's toxin*) [12, 13]. At the beginning of the 20th century, PAUL EHRLICH then first suggested that the immune system was able to repress cancer [14]. However, only the discovery of the major histocompatibility complex (MHC) [15] in 1948 and the establishment of inbred mice [16, 17] enabled experiments showing for the first time the immune rejection of transplanted syngeneic tumors in mice [15, 18, 19]. Subsequently, BURNET and THOMAS formulated the famous theory of cancer immunosurveillance in 1959. They speculated that lymphocytes are responsible for the elimination of continuously arising, nascent transformed cells [20]. Nevertheless, it took four decades until the theory was generally excepted (reviewed in detail by Dunn et al. [21]). Experiments by the group of ROBERT D. SCHREIBER showed that tumors formed in the absence of an intact immune system are more immunogenic (unedited) compared to cancer that arises in immunocompetent hosts (edited) [22]. They proposed that in a first step, the immune system eliminates tumor cells (*elimination*). Similar to DARWINS' theory of "survival of the fittest", the immune system then selects for tumor cell variants with increasing capacities to survive immune attacks (*equilibrium*). Finally, the tumor expands in an uncontrolled manner in the immunocompetent host (*escape*) [21]. Mechanisms leading to immune escape are summarized in Table 1.1.

Several methods to overcome immune escape mechanisms and to induce a strong anti-cancer immune

Table 1.1: Immune Escape Mechanisms. The table lists examples of menchanisms that block anti-tumor immune responses. [23–26]. APC: antigen-presenting cell, TME: tumor microenvironment. T_{reg}: regulatory T cell, MDSC: myeloid-derived suppressor cell, TAM: tumor-associated macrophage, TLR: Toll-like receptor, HMGB1: High-mobility group protein B1, TGF: Transforming growth factor, LFA1: Lymphocyte function-associated antigen 1, ICAM1: intercellular adhesion molecule 1, IDO: indoleamine-pyrrole 2,3-dioxygenase, VEGF: vascular endothelial growth factor, FasL: Fas ligand, ROS: reactive oxygen species.

Step	Mechanism
Release of cancer antigens	Tolerogenic cell death
	Low amounts of released tumor antigen
Antigen presentation, T-cell priming and activation	"Type 2 phenotype" of APC (IL-10, IL-4, IL-13)
	Low levels of proinflammatory cytokines (e.g. TNF-α, IFN-α, IFN-γ)
	Low expression of costimulatory and MHC molecules
	Missing endogenous adjuvants (TLR ligands, HMGB1, ATP, etc.)
	Expression of checkpoint inhibitors (CTLA-4, PD-L1/2),
	Suppressive molecules (IDO, Arginase, TGF-β)
T-cell trafficking and tumor infiltration	Low levels of T-cell chemokines (CX3CL1, CXCL9, CXCL10, CCL5)
	Low levels of LFA1:ICAM1, selectins on tumor endothelium
	VEGF, Endothelin1
Tumor cell recognition by T cells	Reduced peptide-MHC expression
Tumor cell killing	Expression of checkpoint inhibitors (CTLA-4, PD-L1/2, TIM3, LAG-3, VISTA, BTLA)
	Suppressive molecules (IDO1, Arginase, TGF-β, FasL, ROS, Adenosine)
	Suppressive cells (TAMs, MDSCs, T_{regs})
	Hypoxia

response are now emerging [27]. For example, administration of activatory cytokines like IFNα, IL-2, IL-7, IL-12 or IL-15 and microbiological adjuvants such as Toll-like receptor ligands cause an inflammation and enhance the performance of antigen-presenting cells. Thus, they are promoting anti-tumoral T-, B- and NK-cell responses and attenuate immunosuppression. Similarly, neutralization of immune inhibitors (e.g. TGF-β, IL-10, Arginase or IDO1) results in reduced immune suppression and improved performance of several immune cell subsets. The blockade of immune checkpoints such as CTLA-4, TIM3, LAG3 or the PD-1/PD-L1 axis or immune stimulation via CD137, OX40, GITR or CD40 agonists was shown to activate primed T cells, increase the number and infiltration of tumor-specific T cells and diminish tumor immunosuppressive mechanisms. Cancer vaccines or the adoptive transfer of tumor-specific T cells aim at generating or increasing the number of tumor-specific T cells.

It is important to state that several synergistic combinations of immunotherapies might exist that potentiate the effect of the individual treatments [27]. For example, the combination of the CTLA-4 blocking antibody Ipilimumab with the PD-1 blocking antibody Nivolumab was shown to induce an objective response in almost 60 % of melanoma patients. In comparison, the objective response rates of the monotherapies were with 19 % for Ipilimumab and 48 % for Nivolumab significantly lower [28].

Common to the majority of cancer immunotherapies is that they more or less depend on tumor-specific T cells which recognize tumor antigens presented on APCs or tumor cells. Especially for cancer vaccination the selection of an adequate tumor antigen is key for its success. Thus, T cell-defined tumor antigens will be discussed in more details in the next sections.

1.2.1 T Cell-Defined Tumor Antigens

T cell-defined tumor antigens can be categorized in three major groups mainly differentiated by the pattern of expression, whether or not they are shared between tumor patients and the extent to which central tolerance affects the T-cell response (Table 1.2). T cells are educated in the thymus through a process called negative selection to prevent the recognition of autoantigens [29]. Thus, T cells readily recognize foreign antigens, but in general are unable to recognize self-antigens, including most shared tumor antigens, with a high avidity.

An ideal tumor antigen is solely expressed on tumor tissue preventing autoimmune side effects and the restriction of the T-cell repertoire by central tolerance. In addition, antigens should be shared by a broad patient cohort in order to facilitate a therapy for a meaningful number of cancer patients.

Table 1.2: Categories of tumor antigens. Tumor antigens can be broadly categorized into three classes. [A]For some CGA or point mutations tolerance might play a role (see 1.2.1.2). [B]Autoimmunity against CGA has rarely been observed [30]. [C]Some mutations are shared like BCR-ABL or certain p53 mutations.

Category	Subcategory	Shared	Self-Tolerance	Auto-immunity	Examples
Tumor associated (TAA)	Over-expressed	Yes	Yes	Yes	HER2 [31], Survivin [32], VEGF [33], Telomerase [34]
	Differ-entiation	Yes	Yes	Yes	Tyrosinase [35], NY-BR-1 [36], Melan-A/MART-1 [37], TRP-1/gp75 [38], CEA [39]
Cancer germline (CGA)		Yes	No[A]	No[B]	MAGE-A1 [40], MAGE-A3 [41],BAGE-1 [42], NY-ESO-1/LAGE-2 [43]
Tumor specific (TSA)	Mutated	No[C]	No[A]	No	BCR-ABL [44], β-Catenin [45], Kras [46], p53 [47], CDK4 [48], IVAC antigens [49, 50]
	Viral	Yes	No	No	E6, E7 (HPV) [51], HBs (HBV) [52]

Tumor-associated antigens (TAAa)

Tumor-associated antigens TAAs are also present on healthy tissue and can be further subcategorized into *overexpressed* and *differentiation* antigens. Overexpressed antigens such as HER2 [31] are present on healthy tissue but to a much higher extent on tumor cells. Differentiation antigens, for

example Tyrosinase [35] are mainly expressed on the tissue from which the tumor originated. TAAs are shared between patients which allows the application of T-cell immunotherapy for a broad group of patients. A major drawback, however, is the restricted T-cell repertoire due to central tolerance. As a result, T-cell responses against TAAs are usually weak. Moreover, T-cell immunotherapy against TAAs can lead to severe autoimmunity, especially if the antigen is expressed in organs like the brain, heart or eye [53–56].

Cancer germline antigens (CGA)

Cancer germline antigens (CGAs, also called Cancer testis (CT) antigens) are solely present in the tumor, in male germ cells, placenta or in early stages of embryonic development. CGAs are shared tumor antigens and in many cases tolerance does not play a role due to lack of thymic expression (some CGAs like MAGE-A1 are also expressed in the thymus [57]). In addition, lack of expression in healthy tissue (germ cells do not express MHC molecules) renders them suitable targets for T-cell immunotherapy.

Tumor-specific antigens (TSAs)

In comparison to TAAs, tumor-specific antigens (TSAs) such as viral or mutated antigens are solely expressed by malignant cells. Thus, T-cell responses are less likely to be affected by central tolerance and auto-immune side effects are not expected (see also 1.2.1.2). Viral antigens such as the HPV-16 derived E6 and E7 proteins present in cervical or head and neck carcinomas are attractive targets as they are shared by many patients [58]. Nevertheless, viral TSAs expression is limited to only a fraction of cancers. Moreover, in most cases only a few viral epitopes can be targeted per tumor which might result in tumor escape by downregulation or mutation of viral antigens. In comparison to viral antigens, tumors express 10s to 1000s of non-synonymous mutations, representing a huge repertoire of ideal targets for tumor immunotherapy (Figure 1.2). Unfortunately most of those mutations are unique to each patient requiring a personalized approach (exceptions are for exampe the BCR-ABL fusion protein [44], some p53 [47], Kras [46] or CDK4 point mutations). This used to be the major obstacle for exploiting mutations as targets for T-cell based immunotherapy but changed with the advent of next-generation-sequencing (NGS) (see also 1.2.2.2).

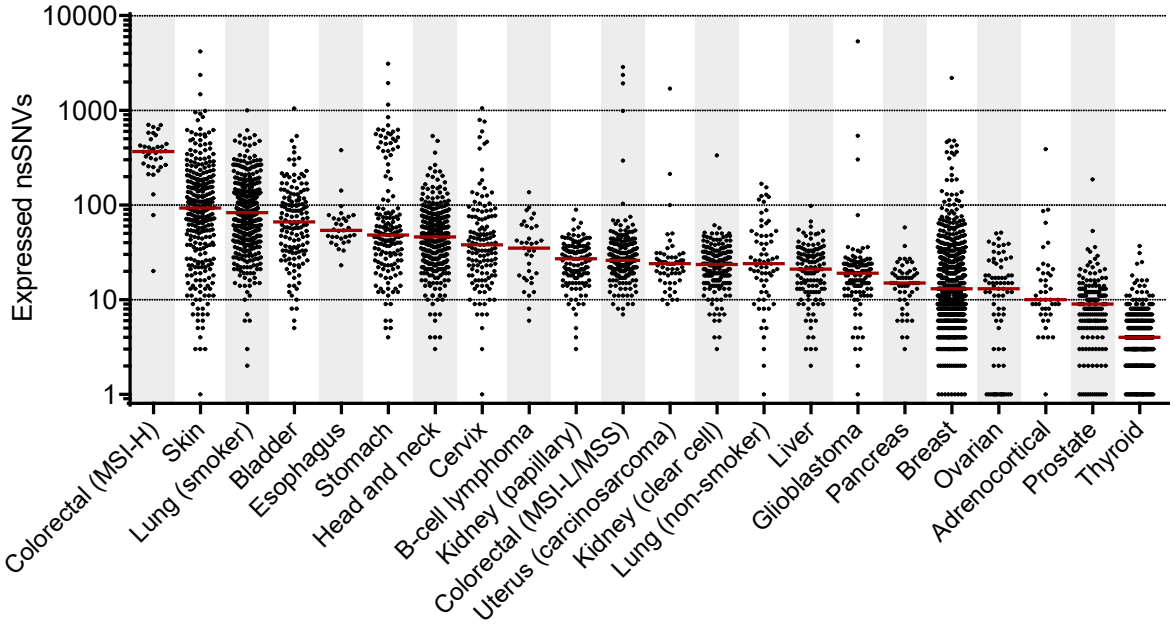

Figure 1.2: The number of expressed tumor mutations across different cancer types. DNA and RNA sequencing data obtained from The Cancer Genome Atlas (TCGA) was used in order to retrieve the number of non-synonymous SNVs (nsSNVs) in several tumor types as described in [49]. Each dot represents the number of expressed nsSNVs in a patient's tumor, the red line shows the median. The figure was adopted from Vormehr et al. [59].

1.2.1.1 Mutation Types

As explained in section 1.2.1 mutations represent a rich source of tumor antigens with ideal properties as targets for cancer immunotherapy. Several mutation types exist which are summerized in Figure 1.3 and Table 1.3. Single nucleotide variations (SNVs) constitute the majority of tumor mutations [60]. SNVs can be synonymous (silent) so that the amino acid sequence in not altered or can cause non-synonymous missense (amino acid is altered) or nonsense (a stop codon is generated) mutations. In addition to SNVs, small insertions and deletions (indels) or large chromosomal aberrations, like gene fusion are regularly identified in tumors. A minority of indels and fusions are in frame. In-frame indels may result in neo-epitopes by insertion or deletion of one or more amino acid. In-frame gene fusions can cause breakpoint-spanning neo-epitopes, as shown for the BCR-ABL fusion protein [44]. The majority of indels and fusions cause a frameshift which, if present in an exon and not affected by nonsense-mediated mRNA decay (NMD) [61], results in several new amino acids. NMD is a post-transcriptional quality control mechanism to ensure transcriptome fidelity. A premature termination codon approximately 24 nucleotides upstream of a splicing-generated exon-exon junction triggers the decay of aberrant mRNA. In addition to a frameshift, gene fusions can lead to the translation of intronic sequences that might result in a number of new amino acids as well. Gene fusions can be the outcome of large deletions or translocations. Moreover, indels or SNVs can cause splice site mutations at the exon-intron boundary leading to an altered open reading frame (ORF).

Mutations that give rise to longer neo-antigen stretches may harbor multiple immune recognition motifs therefore inducing polycloncal T-cell responses that are in general not restricted by central tolerance (see 1.2.1.2).

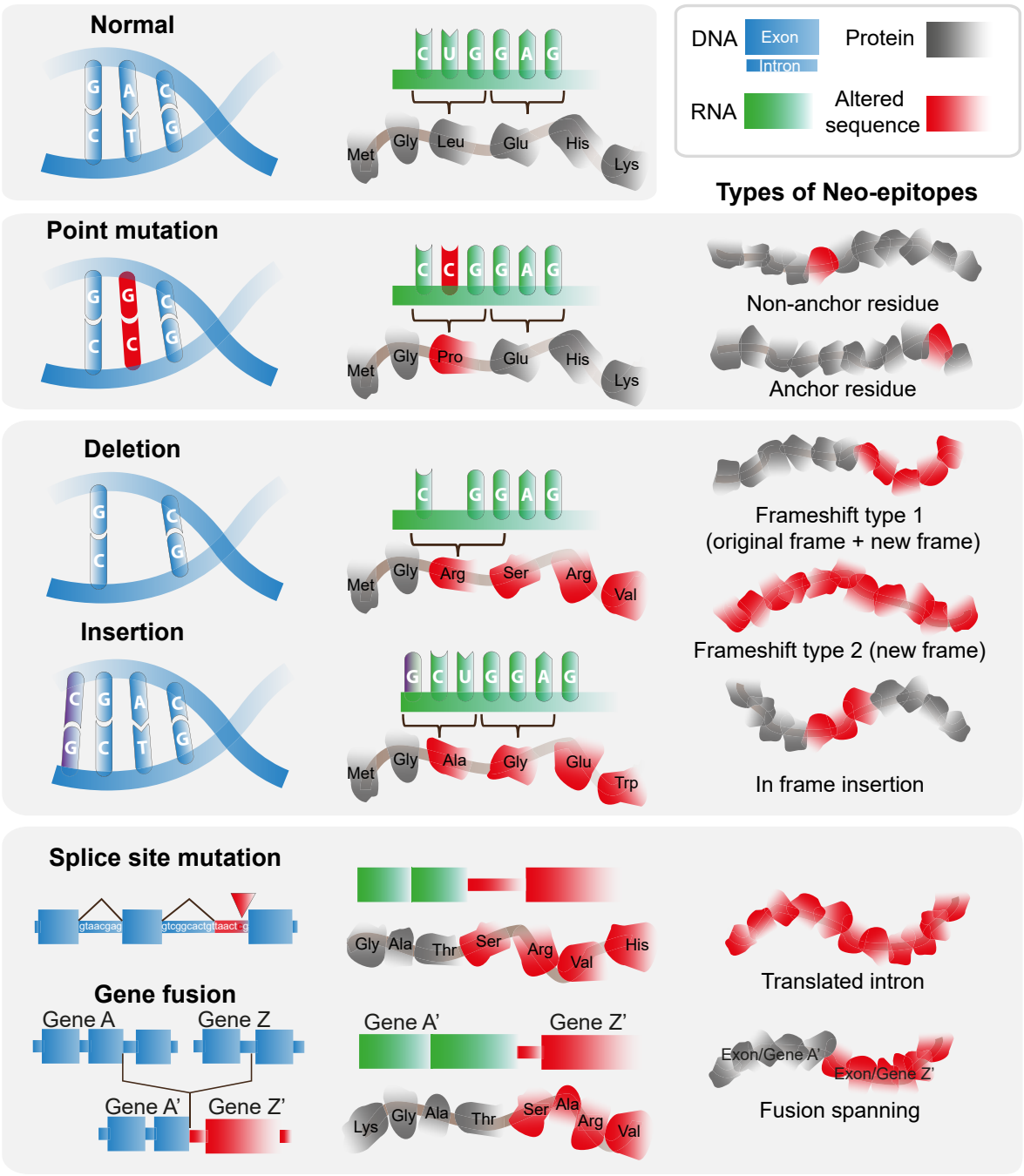

Figure 1.3: Types of genomic mutations and T-cell neo-epitopes resulting from them. Non-synonymous point mutations in the coding sequence of a gene alter a single amino acid. By creating an anchor residue or changing the TCR binding properties (non-anchor residue) a neo-epitope may be formed. Insertion of three or a multiples of three nucleotides in frame introduces novel amino acids into the protein sequence potentially generating a T-cell response. Insertion or deletions of exonic nucleotides, mutations in intronic regions that affect RNA splicing or gene fusions can cause inclusion of introns into mRNA and a shift of the open reading frame. Resulting T-cell epitopes may be in part (type 1) or fully (type 2) comprised of an altered amino acid sequence. In addition, T cells may target neo-epitopes formed by translated introns or fusion of distant exons and genes as a result of splice site mutations and gene fusion.

Table 1.3: Types of gene mutations.

Type	Subtype	New Amino Acids	Potentially Immunogenic
SNV	Silent	0	No
	Missense	1	Yes
	Nonsense	0	Yes
	Splice site	Plenty	Yes
Indel	Frameshift	Plenty	Yes
	In-frame	0 or few	Yes
	Splice site	Plenty	Yes
Gene fusion	Frameshift	Plenty	Yes
	In-frame	0	Yes
	Intron	Plenty	Yes

1.2.1.2 Mutations in Cancer Cells as a Source for Neo-epitopes

Somatic cancer mutations in exons of expressed genes may alter the sequence of the respective protein exclusively in tumor cells. A subset of these mutations are presented on MHC class I or II molecules. As they are divergent from the germ line sequence, they may be recognized by T cell clones not deleted from the immune repertoire.

A single altered amino acid introduced via a missense mutation may affect T-cell recognition in three ways (Figure 1.4): (I) by enhancing the ability of the peptide to bind to an MHC molecule (e.g. a mutation in an anchor) [62], (II) by changing the TCR binding properties resulting in a conformationally altered MHC/peptide complex [63], (III) by altering processing of the respective protein and its routing through MHC loading compartments, e.g. an altered proteasomal cleavage site preserving a ligand which normally would be degraded [64, 65]. Similar rules might apply for mutations that are recognized by $CD4^+$ T cells, however, yet supporting data is lacking.

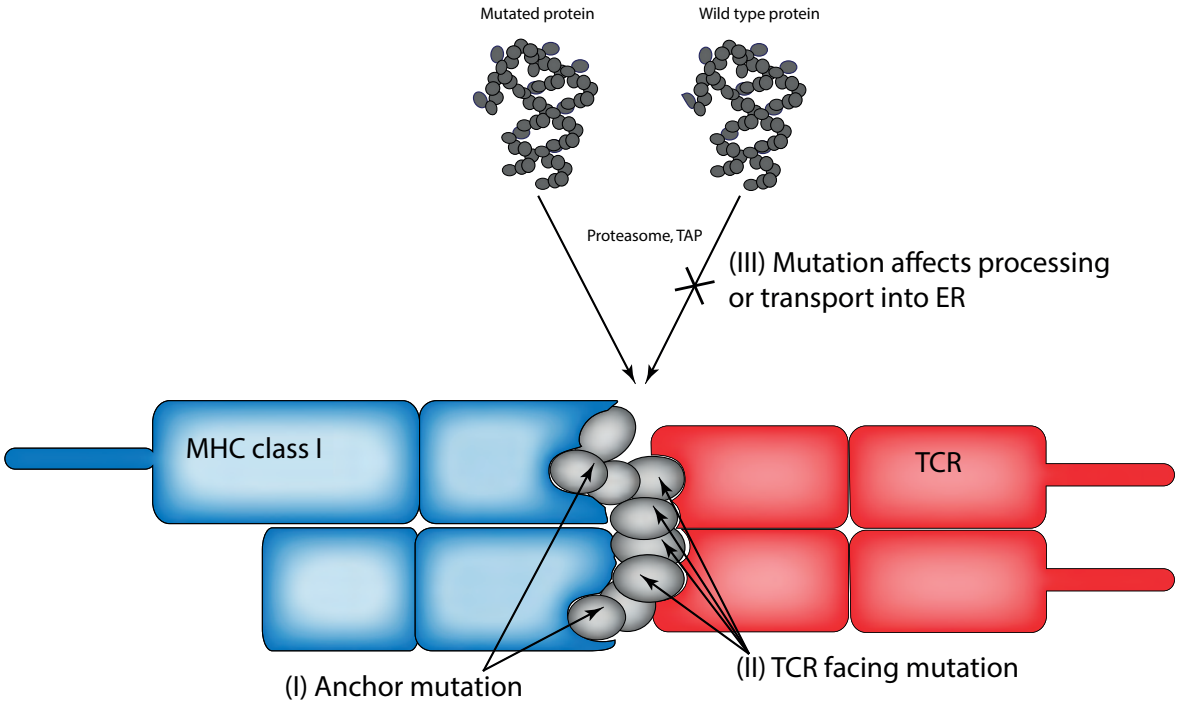

Figure 1.4: SNVs introduce neo-epitopes through distinct mechanisms. Mutations affecting anchor positions (I) or TCR facing residues (II) can create neo-epitopes. Furthermore novel epitopes can occur if a mutation alters the processing of a protein or the transport of a peptide into the ER (III).

1.2.2 Methods to Identify Tumor Antigens and Epitopes

Identification methods for tumor antigens and T-cell epitopes are broadly categorized into *forward* and *reverse* immunology approaches. Forward immunology employs existing immune responses in order to identify new antigens and epitopes. Reverse immunology approaches, on the other hand, use *in silico* prediction tools and subsequent experimental confirmation to identify epitopes from (potential) tumor antigens.

Early methods to identify tumor antigens such as cDNA expression cloning were extremely laborious and time consuming due to the need of T cell clones and tumor cell lines which could be improved by a method called serological identification of antigens by recombinant expression cloning (SEREX). SEREX allowed the screening for tumor antigens using only patient blood and tumor cDNA representing a major improvement in the discovery process. The high throughput discovery of tumor antigens was established only recently with the use of NGS in combination with *in silico* prediction of T-cell epitopes. This methodological breakthrough revolutionized antigen discovery and is the foundation of personalized tumor immunotherapy. The following section will provide a short overview on methods to identify tumor antigens and T-cell epitopes.

1.2.2.1 Forward Immunology Approaches

Forward immunology methods make use of preexisting immune responses in order to identify new tumor antigens.

cDNA expression cloning

The gene encoding for the first characterized human tumor antigen MAGE-A1 [40] was identified by screening of tumor derived cDNA expression libraries with autologous tumor-infiltrating lymphocytes (TILs). Antigen-loss variants of tumor cell lines were transduced with tumor derived cDNA and recognition was tested via autologous T-cell clones. Systematic shortening of the cDNA then finally revealed the minimal T-cell epitope.

HPLC fractionated ligandome

Peptides eluted from the MHC molecules of tumor cells (ligandome) and fractionated via high-performance liquid chromatography (HPLC) are pulsed to HLA-matched cells and tested for the recognition by a tumor-specific T-cell clone. Subsequently, the sequence of the T-cell recognized peptide is decoded via mass spectrometry or Edman degradation [66, 67]. A database search then provides information on the originating antigen. In addition to genetic approaches it is possible to identify posttranslationally modified epitopes [68].

SEREX

A major progress for the identification of tumor antigens was the development of a method called SEREX, serological identification of antigens by recombinant expression cloning developed by UGUR SAHIN and colleagues in 1995 [69]. A phage library encoding the tumor-derived cDNA and screened with autoantibodies lead to the discovery of a plenitude of tumor antigens such as NY-ESO-1 [43], MAGE-C1 [70] and NY-BR-1 [36] (for a full list see [71]). In comparison to the above mentioned methods, SEREX has the advantage that it is less laborious and independent of T-cell clones or tumor cell lines.

Synthetic peptide libraries

Employing synthetic peptide libraries to identify the recognized epitope of a T-cell clone [66] is yet another approach which also allows the finding of mimotopes [72, 73]. Overlapping peptide strings covering the tumor antigen are tested with antigen-specific T-cells thereby identifying the recognized T-cell epitope. Furthermore, an interesting approach was presented by Siewert et al. who cloned TCR sequences into a T-cell hybridoma which expresses the green fluorescent protein (GFP, under the NFAT enhancer) after TCR stimulation. HLA-matched COS-7 cells transfected with plasmids encoding for random peptide sequences served as potential targets. Green fluorescent T cells as well as the surrounding antigen-presenting COS-7 cells encoding for the antigen of interest were isolated using a capillary connected to a micromanipulator. The plasmid coding for the mimotope/epitope can than be isolated from the COS-7 cell and subsequently cloned as well as sequenced.

1.2.2.2 Reverse Immunology Approaches

Reverse immunology approaches try to predict if potential tumor antigens are immunogenic. For many shared antigens identified via forward immunology approaches or for tumor mutations identified by high throughput methods, *in silico* predictions are used to identify T-cell epitopes.

High throughput identification of tumor mutations

As mentioned in section 1.2.1, mutations are a rich source of tumor antigens. However, only recently the concurrence of technological and scientific breakthroughs has opened the way for exploitation of mutations for the development of truly personalized, mutation specific T-cell immunotherapy. While deciphering the first human genome took about 13 years with a cost of about $2.7 billion [74], advances in NGS make it possible today to sequence a genome, exome or transcriptome within hours for approximately $1,000 [75]. Among the hundreds of expressed tumor mutations only a fraction is immunogenic and reverse immunology offers valuable tools to select potential candidates for T-cell based immunotherapy (see also section 1.2.1.2 and 1.3).

In vitro priming

Coculture of PBLs with tumor cells or tumor antigen candidates allows the priming of tumor-antigen specific T cells. Conversely, the induction of a T cells response specific for tumor cells proofs the the relevance of the recognized tumor antigen.

MHC binding prediction

A major prerequisite for the immunogenicity of a tumor antigen is the binding of a potential epitope to an MHC molecule. Furthermore, it was shown that the stability of the MHC-peptide complex correlates with the immunogenicity of the peptide [76]. Several algorithms were developed that employ experimentally validated T-cell epitopes and their binding affinity to the respective MHC molecule to predict the binding (affinity) of a potential T-cell epitope. Examples are SYFPEITHY [67], IEDB [77], NetMHCpan [78] and Rankpep [79]. The IEDB algorithm was used here and therefore described in more detail in section 2.2.4.1. MHC class I molecules bind peptides with very defined properties (length between 8-11 amino acids, conserved anchor residues important for binding) resulting in an efficient binding prediction [80]. Due to the more complex binding properties of MHC class II (open ends allow big variability in the length of epitopes, binding core is not well defined, flanking residues contribute to binding) the efficiency of binding prediction of $CD4^+$ T-cell epitopes is significantly lower [81].

Prediction of proteasome cleavage, TAP transport and TCR binding

Even correct MHC binding prediction does not guarantee immunogenicity of the peptide or recognition of the tumor cells by peptide-specific T cells [82–84]. The latter depends on the expression of MHC molecules on the tumor cells, the correct processing of the epitope for example via the proteasome (C-terminus of $CD8^+$ epitopes) or other proteases (e.g. ER aminopeptidase, ERAP which defines the N-terminus), and the transport into the ER via the transporter associated with antigen processing (TAP) where the loading of the epitope on the MHC molecule takes place. Proteasomal cleavage can be predicted as well by several algorithms (e.g. PAProC [85], NetChop [86], Pcleavage [87] or MAPPP/ FragPredict [88]) but the efficiency so far is not good enough to improve the MHC class I binding prediction. The same holds true for TAP binding prediction [66]. In addition, not every epitope that is correctly processed and binds to MHC molecules can be recognized by the TCR. It

was shown that certain amino acid properties of immunogenic epitopes differ from non-immunogenic epitopes in such that they are usually larger, aromatic and acidic [89]. Nonetheless, these differences are not stringent so that the prediction of TCR recognition so far is rather inefficient [89].

Experimental confirmation of predicted epitopes

Potential epitopes identified *in silico* require experimental confirmation. For human antigens, T cells of vaccinated HLA-transgenic mice can be used to test the recognition of HLA-matched cell lines transduced with the antigen of interest [90]. Moreover, patient derived T cells that recognize the identified epitope can prove the relevance of the predicted epitope [91, 92]. In mice, testing T cells of vaccinated animals for recognition of tumor cells directly proves the relevance of the identified epitope. Similarly, vaccination with RNA or DNA that encodes for sequences longer than the minimal epitope of a murine tumor antigen only then induces T cells when the respective epitope is correctly processed and presented.

1.2.3 Relevance of Neo-Antigen Specific T-Cell Responses in Cancer

Accumulating evidence highlights the importance of neo-antigen specific T cells in spontaneous and therapy-induced immune responses against cancer. Figure 1.5 shows an overview of relevant literature published since 2012.

Spontaneous neo-epitope specific T-cell responses in cancer

First clues that tumor mutations can serve as targets for T cells stem from BOON and KELLERMANN in 1977 [93]. Mutagenesis of a teratocarcinoma line resulted in clones unable to form tumors in syngeneic mice. However, the same tumor clones were able to form cancer in irradiated mice which could be prevented by adoptive transfer of splenocytes of challenged syngeneic mice. It then took almost two decades for the first human mutated antigen to be discovered. WÖLFEL and colleagues screened a cDNA library with an autologous, melanoma specific T-cell clone and revealed the recognition of a point-mutated form of the cyclin-dependent kinase 4 [48]. In the same year of 1995, a minor histocompatibility antigen, HA-2, was identified which was shown to induce graft-versus-host disease (GvHD) after allogeneic hematopoietic stem cell transplantation (HSCT) [94]. Resembling a point-mutation in cancer, a single nucleotide polymorphism in the HA-2 gene resulted in recognition by donor T cells [65]. Similarly, it was shown that SNPs or frameshift polymorphisms may result in T-cell targets responsible for the graft-versus tumor effect after HSCT [95, 96]. In 2005, a study by LENNERZ et al. suggested that neo-antigens are the dominant T-cell targets in human melanoma [97]. Likewise, studies showed that in microsatellite instable (MSI) tumors, neo-antigens are the dominant targets of T cells. In comparison to microsatellite stable (MSS) cancers, microsatellite instable cancers display higher numbers of mutations including frameshift mutations [98] and a better clinical outcome [99]. In line with this, it was demonstrated that the number of frameshift mutations in MSI colorectal cancer patients correlates with intratumoral $CD8^+$ T-cell infiltration [100] which is generally associated with a better disease outcome [101]. More general evidence for the importance of mutation specific T-cell responses in cancer progression was reported in 2014 by the

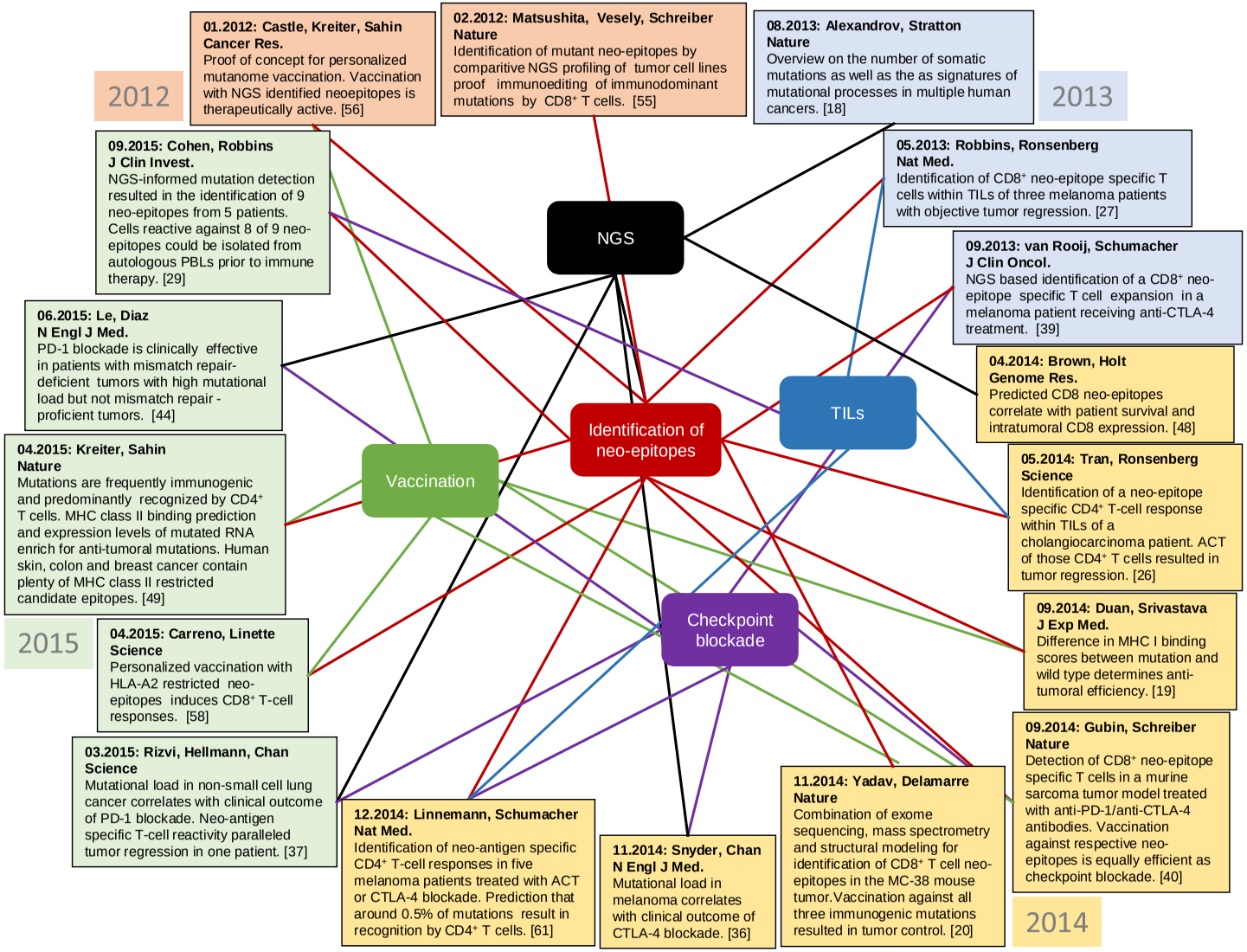

Figure 1.5: A selection of publications related to mutanome directed cancer immunotherapy. Release date, journal, first and last authors as well as key findings are provided. Cross-linked boxes in the center contain terms related to the publication. NGS: next-generation sequencing. TILs: tumor-infiltrating lymphocytes.

group of ROBERT HOLT [102]. They identified SNVs in several cancer types published by The Cancer Genome Atlas (TCGA) and used binding prediction to the respective patient´s HLA-A alleles to identify the tentatively immunogenic ones. Subsequently, they correlated the number of obtained neo-epitope candidates with the level of CD8 expression in the respective tumor as surrogate for T-cell infiltrates. Tumor specimens expressing a high number of mutations predicted to form neo-epitopes were found to contain more $CD8^+$ T cells. Moreover, the number of predicted neo-epitopes, CD8 expression as well as HLA-A expression correlated positively with survival of patients irrespective of the cancer type.

Immunotherapy-induced neo-epitope specific T-cell responses in cancer

Within the last decade several potent immunotherapeutic interventions against cancer have emerged. Promising results have stemmed especially from adoptive cell transfer (ACT) [103–106] of tumor-infiltrating lymphocytes or genetically modified T cells [107, 108] and inhibitory antibodies against CTLA-4 [109, 110] or PD-1/PD-L1 [109–113]. Common for all the aforementioned interventions is that their mode of actions relies on T cells. TIL therapies reinfuse supposedly tumor-reactive T cells after *in vitro* expansion whereas CTLA-4 blockade is thought to enhance anti-tumoral T-cell responses and curtail regulatory T cells *in vivo* [114]. Blockade of the PD-1/PD-L1 axis on the other hand restores T-cell function of pre-existing tumor-specific lymphocytes [115, 116]. With the exception of genetically modified T cells, the tumor antigens targeted as a result of TIL therapy or checkpoint blockade are usually unknown. Studies aiming at identifying corresponding T-cell targets were largely restricted to shared antigens as mutated antigens were technically difficult to identify [103, 104, 117]. However, especially for melanoma, mutation-specific T cells within TILs were frequently discovered [105, 118–121]. With the advent of NGS, several studies have finally confirmed the frequent involvement of mutation-specific T-cell responses after ACT of TILs [106, 122–124]. The possibility of readily identifying mutated antigens via NGS and test their recognition by TILs now also allows the infusion of solely neo-antigen specific T cells. This was first realized by ROSENBERG and colleagues in 2014 showing regression of a metastatic cholangiocarcinoma after ACT of purely neo-antigen specific $CD4^+$ T cells while a prior ACT of a mixed TILs culture resulted in only transient tumor control [106, 124, 125].

Similar to ACT therapies, several studies suggest that checkpoint blockade largely depended on neo-antigen specific T cells [126–130]. SCHREIBER and colleagues for example demonstrated that mutated antigens serve as major class of T cell rejection antigens after CTLA-4 and/or PD-1 blockade in mice. Therapeutic vaccination against identified neo-epitopes was equally efficient as checkpoint blockade [126]. In agreement, it was shown that the degree of clinical benefit of PD-1 and CTLA-4 blockade correlates with the number of identified tumor mutations [128–130].

Together, these findings indicate that the probability of clinical success of a monotherapy with anti-CTLA-4 and anti-PD1 antibodies or the ACT of TILs may be limited to cancers harboring a sufficient number of mutations [131]. Indeed, TIL therapy [103, 104, 132, 133] and checkpoint blockade [28, 109, 110, 112, 113, 116, 134, 135] was so far found to be mainly successful in melanoma, a tumor type with an extremely high mutational load inflicted by UV-mediated DNA damage (Figure 1.2).

Beyond melanoma, checkpoint blockade was shown to be successful especially in smoking induced non–small-cell lung cancer (NSCLC) [112, 116, 129, 136, 137], bladder [138, 139], esophageal [140] and head and neck cancer [141], which were shown to harbor excessive numbers of mutations (Figure 1.2). In accordance, a recent study by Le and coworkers demonstrated that different mismatch-repair deficient tumors that usually harbor hundreds of mutations were much more likely to respond to PD-1 blockade compared to mismatch-repair sufficient colorectal cancers [98]. However, for some tumor types such as liver or renal cancer objective response rates were shown to be fairly good despite of low to medium number of mutations (Figure 1.2) [116, 142, 143]. As indicated earlier, ACT or PD-1/PD-L1 blockade therapies require preexisting T-cell responses [115, 116]. Thus, a logical conclusion would be that further expansion of tumor-specific T cells by vaccination or indirect measures like immunogenic cell death induction through low-dose irradiation, chemotherapy as well as oncolytic virotherapy would expand the functional range to tumor types with lower numbers of mutations. Indeed, Kühnel and coworkers showed that the efficiency of PD-1 immunotherapy was significantly improved by oncolytic virotherapy due to broadening of neo-antigen specific T-cell responses [127].

1.3 The Concept of Individualized Vaccines for Cancer

Due to the importance of T-cell responses in cancer (section 1.2.3), therapeutic vaccination against tumor antigens has been pursued for decades [144]. Clinical trials, however, have so far produced mainly disappointing results [145] which might be explained by the targeting of single or few non-mutated TAAs. As described in section 1.2.1, neo-antigens are ideal targets for cancer immunotherapy as they lack expression in healthy tissues and can potentially be recognized as neo-antigens by the mature T-cell repertoire. Thus, neither on-target toxicity nor immunological tolerance is expected when using them as vaccines. In addition, as tumors contain a plenitude of mutations (Figure 1.2), it is possible to target multiple mutations at once in order to address critical problems in current cancer drug development such as clonal heterogeneity and antigen escape [146, 147]. Putting the concept of personalized cancer vaccination into practice, however, requires several steps (Figure 1.6).

In a first step, the tumor biopsy as source for the individual patient‘s DNA and RNA is retrieved. By comparison of exome sequencing data of healthy tissue and tumor DNA somatic non-synonymous mutations are identified. Transcriptome sequencing of tumor RNA then provides information on the expression levels of identified mutations. Second, those neo-antigens which are likely to induce a T-cell response are to be selected. A vaccine encoding the targets of interest is manufactured, which is finally delivered to professional antigen presenting cells such as dendritic cells (DCs) in combination with an adequate adjuvant. Each step is critical for obtaining efficient and sustained immune responses and will be discussed in more detail below.

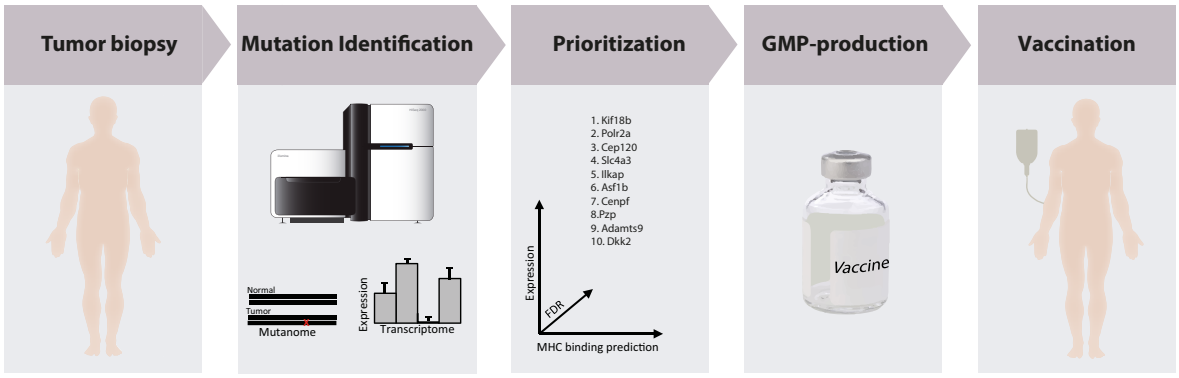

Figure 1.6: Concept of Individualized Vaccines for Cancer (IVAC). NGS of nucleic acid from a tumor biopsy and healthy tissue is used to identify expressed, non-synonymous, somatic mutations. Vaccine targets are selected based on several parameters such as expression, their MHC binding prediction and restriction as well as a false discovery rate (FDR) [148]. Mutations encoded on Pentatope RNAs are produced under GMP conditions and used for therapeutic vaccination. The figure was modified after Vormehr et al. [149].

1.3.1 Mutation Identification

NGS analysis of DNA and RNA for mutation detection requires a representative tumor and a healthy tissue sample. A blood sample is an easy to obtain source for healthy tissue. Tumor biopsies, in particular as fresh frozen samples, in contrast are not always available. Use of formalin-fixed, paraffin-embedded (FFPE) samples as used for routine pathological analysis, for NGS bears the risk of sequencing artefacts. Therefore, our group set up an optimized protocol for the efficient and reproducible isolation of small amounts of nucleic acid from FFPE samples for NGS. Generally speaking, mutation evaluation is error prone and retrieved data depend on the algorithms used [148, 150, 151]. Moreover, correct identification of mutations within tumor biopsies are compromised, by e.g. tumor heterogeneity and contaminations from healthy tissue or necrotic cells. For this reason, we established a statistical value to gauge the "false discovery rate" (FDR) and accurately discriminate true mutations from erroneous calls [148].

1.3.2 Target Selection

Tumors of patients display hundreds of mutations (Figure 1.2). Selecting the right ones as neoantigens for vaccination is challenging and critical, as not every mutation is immunogenic. Therfore, *in vitro* immunogenicity testing of candidate mutations with blood samples of patients is performed. These bioassays identify prevalent immune responses of the patient and thereby validate immunogenicity of mutations of interest. Against many mutations, however, there are no spontaneous immune responses in the patient detectable and their potential as vaccination target is not easily assessable [49]. We addressed this by developing tools for *in silico* selection of targets. Several criteria now used for the prediction of tumor mutations for patients derived from work described here (section 3.3).

1.3.3 Vaccine Format and Production

Effective personalized tumor vaccination requires a suitable vaccine format that bundles the following features: safety, cost-efficiency and scalability under GMP conditions, stability and, most importantly, a reliable induction of a proper T-cell response that depends on the adjuvant capacity and targetability into antigen presenting cells. In this regard, RNA synthesized through *in vitro* transcription is appealing for several reasons. A number of clinical studies proved the safety of RNA vaccines *per se* [152,153]. Furthermore, high amounts of RNA can be manufactured at reasonable cost under GMP conditions, including synthesis of the DNA template, *in vitro* transcription, purification and quality control. For clinical grade RNA as an investigational medicinal product, the correct identity, integrity, sterility, quantity as well as functionality needs to be monitored. RNA can be stable for years in the absence of RNases. The rather short serum half-life of RNA, due to degradation by RNases, has so far compromised the direct *in vivo* use of RNA for vaccination. For this reason, RNA vaccines are usually delivered via adoptive transfer of *in vitro* electroporated DCs [154]. Under GMP conditions and in large scale, this process is demanding and costly. In order to allow for direct use *in vivo*, Sahin et al. introduced several improvements resulting in increased stability and translational efficacy of synthetic RNA by several thousand fold as compared to conventional mRNA [155, 156]. These are e.g. 5'-cap modifications, stabilizing UTR sequences and modified poly(A) tails. A further advantage of RNA is that several mutated epitopes can be easily encoded on the same RNA molecule. Multi-epitopic formats could be beneficial for priming of $CD8^+$ T-cells through improved $CD4^+$ T-cell mediated DC licensing [157]. Moreover, a polyclonal effector T-cell response may act synergistically and allows addressing tumor heterogeneity and immune escape mechanisms. We therefore use synthetic RNA encoding five neo-epitopes comprising selected MHC class I as well as MHC class II binders separated by non-immunogenic 10mer glycine/serine linkers (Figure 1.7). Synthetic mRNA as a class of drug was reviewed in more detail by SAHIN and coworkers [158].

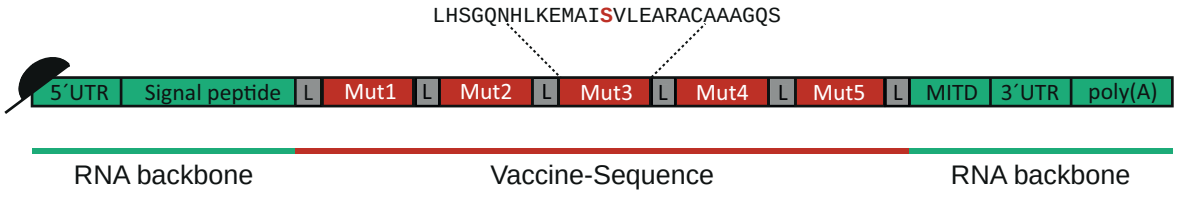

Figure 1.7: Structure of the pentatope RNA vaccine. Several modifications in the 5' cap, 5' and 3' untranslated regions (UTR), poly(A) tail and codon usage increased the translation efficiency and stability of the RNA [155, 156]. Mutated sequences (Mut1-5) encoding 27 amino acids with the mutation in the center (red letter) are separated by non-immunogenic 10-mer linkers. The antigen encoding sequences are flanked by a signal peptide and the MHC class I trafficking domain (MITD, transmembrane and cytoplasmic domain of MHC class I) to ensure optimal antigen presentation [159]. The figure was adopted from Vormehr et al. [149].

1.3.4 Vaccine Delivery and T-Cell Priming

T cells are primed by "professional" antigen presenting cells such as DCs in secondary lymphoid tissue like the spleen and lymph nodes. T-cell priming requires the presentation of processed peptides

of the antigen by MHC class I or II molecules of a DC to a T-cell receptor on T cells. Only in combination with a costimulatory signal by immunogenic DCs are T cells activated. In addition to the costimulatory signal, the cytokine milieu during the priming phase determines the fate of T-cell differentiation [160]. Thus, delivery of the vaccine into sites of T-cell priming and co-delivery of an adjuvant that activates DCs to upregulate costimulatory molecules and secrete the appropriate cytokines are key for obtaining a meaningful vaccine response. RNA not only encodes the antigen, but acts as a DC-maturating adjuvant as well. RNA triggers inflammation by activation of several pattern recognition receptors such as toll-like receptors (TLR) 3,7,8, retinoic acid-inducible gene 1 (RIG-I), protein kinase R (PKR) and melanoma differentiation-associated protein 5 (MDA5) [158]. This results in the maturation of immunogenic DCs and secretion of the proper cytokines for priming of anti-tumor TH1 cells and cytotoxic $CD8^+$ T cells. In order to deliver the RNA vaccine into DCs *in vivo*, two different methods were established in our group. One is the direct injection of naked RNA into the lymph node, where the RNA is taken up selectively and efficiently by DCs via macropinocytosis [161, 162]. The other is intravenous administration of a nanoparticle formulation [49]. Not only does this formulation encapsulate the synthetic RNA, thereby protecting it from degradation, thus optimizing its bioavailability. In addition, the IV route ensures systemic delivery specifically in antigen-presenting cells, most importantly spleen-resident antigen presenting cells. Alternatively, RNA can be administered intradermally [163] or intramuscularly [164]. All those methods are now being actively tested in various preclinical and clinical studies (NCT01684241, NCT02410733). Upon selective uptake by DCs into the cytosol [162], translation of the RNA starts immediately [158]. Cytosolic proteins are usually C-terminally processed via the proteasome and transported by the TAP transporter into the ER, where peptides can be further N-terminally truncated and loaded onto MHC class I molecules. $CD4^+$ T-cell epitopes commonly derive from extracellular proteins loaded onto MHC class II molecules in the late endosome [165]. To ensure optimal antigen presentation of encoded proteins, not only for $CD8^+$ but also for $CD4^+$ T-cell epitopes, we flanked the target sequences with a signal peptide and the trafficking domain (transmembrane and cytosolic domain) of MHC class I. The fusion protein is routed into the ER membrane from which it travels via the Golgi apparatus to the cell membrane and back, until it is degraded and loaded onto MHC class I or MHC class II molecules. This leads to increased antigen presentation, resulting in enhanced $CD4^+$ and $CD8^+$ T-cell responses [159].

1.3.5 Preclinical and Clinical Proof of Concept

Various attempts were made to apply neo-antigen-based vaccine strategies in murine models. Robert Schreiber‘s group demonstrated the feasibility of using genomic and bioinformatic approaches to identify MHC class I neo-epitopes as tumor rejection antigens in a highly immunogenic methylcholanthrene (MCA) induced murine sarcoma model [147]. In a subsequent study his lab showed in immune-edited variants of the sarcoma model that the anti-tumor effect of checkpoint blockade was mediated by MHC class I neo-epitope specific T cells and that vaccination with long synthetic peptides encoding these neo-epitopes induced comparable therapeutic activity as checkpoint inhibition [126]. Srivastava and colleagues selected neo-epitopes for which the wild type counterpart exhibited no predicted MHC binding and demonstrated that prophylactic vaccination against those

neo-epitopes inhibits growth of CMS5 or Meth A tumors in mice [62]. Moreover, Delamarre and coworkers combined mass spectrometry of MHC class I eluted peptides and exome sequencing and demonstrated prophylactic and therapeutic activity of vaccination against identified neo-epitopes in the MC38 tumor model ([63]).

The first preclinical proof of concept for the concept of *Individualized Vaccines for Cancer* (IVAC) integrating the above described aspects into one process was obtained in our group [50]. Sequencing of DNA, as well as mRNA, of the C57BL/6 derived B16F10 melanoma cell line in comparison to healthy tissue revealed hundreds of targetable mutations. Immunogenicity and mouse tumor treatment studies with the SNVs presented as peptide as well as RNA vaccine format revealed that more than a third of the identified mutations were recognized by T cells (16/50) and that a fraction of these T-cell responses were associated with tumor growth control and survival benefit in immunized mice. The confirmation of these studies in the tumor models CT26 and 4T1 of BALB/c background are one part of this thesis and shown in section 3.1.1. A schematic describing mutation discovery and immunogenicity testing is shown in Figure 1.8. Recently, IVAC entered trials in cancer patients and the lessons learned in the preclinical models (see section 3.3) were mirrored into the human setting. In a first-in-human clinical study, in which according to the IVAC approach an actively individualized mutation-based vaccine is manufactured for each and every patient ("IVAC mutanome", Phase I, NCT02035956) and administered intranodally, we are currently assessing the safety and tolerability, as well as the induction of cellular immune responses in melanoma patients. In parallel to the target discovery process and on demand manufacturing of the mutanome vaccine, patients with positive tumors are immunized against two well-known shared antigens (NY-ESO-1 and Tyrosinase). Encoded on two penta-epitopic RNAs, participants subsequently receive a vaccine targeting ten of their mutations. For further information on mutatnome directed cancer immunotherapy and individualized vaccines see reviews by Vormehr et al. [59, 149].

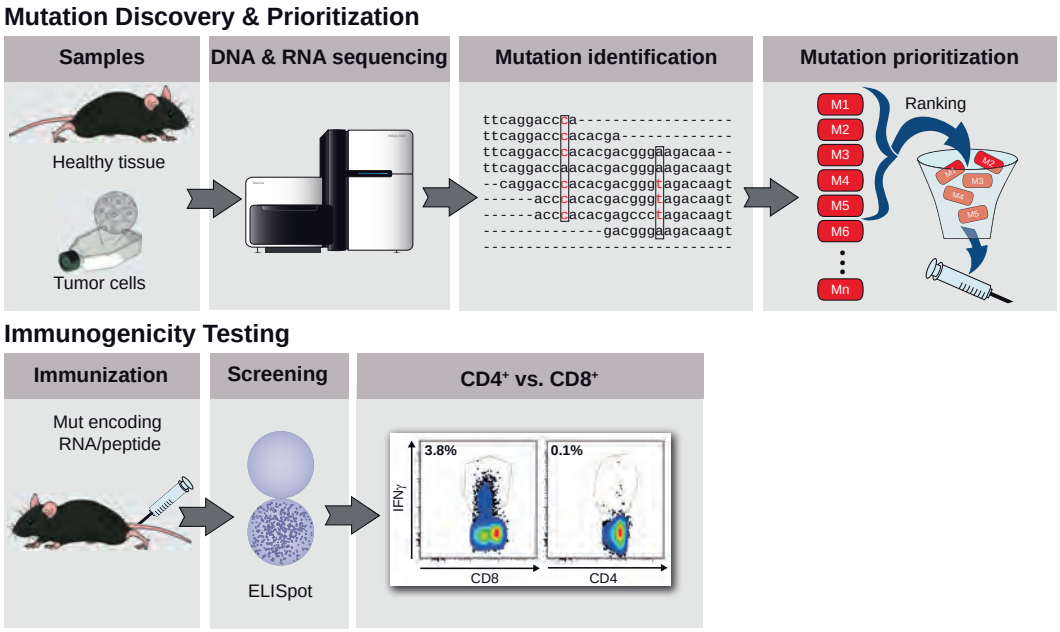

Figure 1.8: Mutation discovery and immunogenicity testing in mice. Exome and RNA sequencing data of the tumor cell line and healthy tissue was compared in order to identify nonsynonymous tumor mutations. Selected mutations were used for immunogenicity testing (2.2.3.3 and 2.2.2.3) and subtyping (2.2.2.5). The figure was modified after Kreiter et al. [49].

1.4 Purpose of the Thesis

This thesis has the following purposes:

1. Validate the preclinical proof of concept for the immunogenicity of Individualized Vaccines for Cancer targeting SNVs in the CT26 colon carcinoma and 4T1 mammary carcinoma tumor models.
    a) Determine the immunogenicity rate of CT26 and 4T1 mutations.
    b) Assess the subtype of neo-epitope specific T-cell responses.
2. Explore polytopic versus monotopic mutanome RNA vaccines.
3. Investigate indels and gene fusions as targets for personalized tumor vaccination in the tumor models B16F10 melanoma, CT26 and 4T1.
    a) Determine the immunogenicity rate of indels and gene fusions.
    b) Characterize whether indels and gene fusions can provide clusters of T-cell neo-epitopes.
4. Test if vaccination against SNVs can induce tumor control in therapeutic tumor models of CT26.
    a) Identify the predominant effector cells.
    b) Dissect the mode of action of tumor control after therapeutic vaccination against neo-antigens.
5. Discover parameters that improve the selection of relevant mutated vaccine targets.

2 Material and Methods

2.1 Material

2.1.1 Antibodies

APC hamster anti-mouse CD11c, clone N418	Miltenyi Biotec, Bergisch-Gladbach, Germany
APC Rat anti-mouse IL-2, clone JES6-5H4	BD Biosciences, Heidelberg, Germany
APC-Cy7 rat anti-mouse CD8a, clone 53-6.7	BD Biosciences, Heidelberg, Germany
Biotin rat anti-mouse IFN-γ, clone R4-6A2	Mabtech, Nacka Strand, Sweden
FITC rat anti-mouse CD4, clone GK1.5	BD Biosciences, Heidelberg, Germany
FITC rat anti-mouse MHC class II, clone M5/114.15.2	Miltenyi Biotec, Bergisch-Gladbach, Germany
Hamster anti-mouse CD40L, clone MR1	Bio X Cell, Lebanon, NH
PE rat anti-mouse CD86, clone GL1	BD Biosciences, Heidelberg, Germany
PE rat anti-mouse IFN-γ, clone XMG1.2	BD Biosciences, Heidelberg, Germany
PE-Cy7 rat anti-mouse TNF-α, clone MP6-XT22	BD Biosciences, Heidelberg, Germany
Rat anti-mouse CD4 antibody, clone YTS191	Bio X Cell, Lebanon, NH
Rat anti-mouse CD8 antibody, clone YTS169.4	Bio X Cell, Lebanon, NH
Rat anti-mouse IFN-γ, clone AN18	Mabtech, Nacka Strand, Sweden
Rat anti-mouse MHC class II (I-A,I-E), clone M5/114	Bio X Cell, Lebanon, NH

2.1.2 Cell Culture Media

Minimum Essential Medium Eagle (αMEM)	Thermo Fisher Scientific, Schwerte, Germany
Dulbecco's Modified Eagle Medium (DMEM)	Thermo Fisher Scientific, Schwerte, Germany
Roswell Park Memorial Institute (RPMI), 1640 GlutaMAX™	Thermo Fisher Scientific, Schwerte, Germany
X-VIVO™ 20	Lonza, Basel, Switzerland

2.1.3 Cell Lines

4T1-WT (CRL-2539 , lot no. 58603185)	ATCC, Wesel, Germany
4T1-luc2-tdtomato (4T1-Luc, 125669, lot no. 101648)	Caliper Life Sciences,Hopkinton, MA
B16F10 (CRL-6475, lot no. 58078645)	ATCC, Wesel, Germany
CT26-Luc (originated from CRL-2638)	TRON, Mainz, Germany
CT26-WT (CRL-2638, lot no. 58494154)	ATCC, Wesel, Germany

2.1.4 Consumables

6-well plates	Nunc, Wiesbaden, Germany
12-well plates	Nunc, Wiesbaden, Germany
24-well plates	Nunc, Wiesbaden, Germany
96-well round-bottom plates	Nunc, Wiesbaden, Germany
Canula (24 G)	Braun, Mesungen, Germany
Canula (27 G)	Braun, Mesungen, Germany
Capillary blood collection tubes (1.3ml, Lithium Heparin)	Sarstedt, Nümbrecht, Germany
Cell culture flask 175 cm^2, 75 cm^2, 25 cm^2	Greiner, Frickenhausen, Germany
Cell strainer 70 µm	Greiner, Frickenhausen, Germany
Centrifuge tubes 50ml, 15 ml	BD Biosciences, Heidelberg, Germany
Cryo tubes 1.8 ml	Nunc, Wiesbaden, Germany
Electroporation tubes, 4mm	VWR, Darmstadt, Germany
Elispot plate, MSIPS45 clear	Millipore, Darmstadt, Germany
FACS tubes, polystyrene, 5ml	BD Biosciences, Heidelberg, Germany
Filter Tips 10 µl, 100 µl, 300 µl, 1000 µl	Eppendorf, Hamburg, Germany
MACS cell separation columns LS	Miltenyi Biotec, Bergisch-Gladbach, Germany
Microhematocrit capillary tubes	Brand, Wertheim, Germany
Petri dish 100x20mm	Greiner, Frickenhausen, Germany
Pipetting reservoire 25 ml	Thermo Fisher Scientific, Schwerte, Germany
Reaction tubes 5 ml, 2 ml, 1.5 ml, 0.5 ml	Eppendorf, Hamburg, Germany
Reaction tubes 5 ml, 2 ml, 1.5 ml, 0.5 ml, protein LoBind	Eppendorf, Hamburg, Germany
Reaction tubes 5 ml, 2 ml, 1.5 ml, 0.5 ml, RNA/DNA LoBind	Eppendorf, Hamburg, Germany
Serological pipettes 5 ml, 10 ml, 25 ml, 50 ml	Greiner, Frickenhausen, Germany
Syringes 5 ml, 1 ml, 0.5 ml	BD Biosciences, Heidelberg, Germany
Syringes, fixed needle, 0.3 ml, 0.5 ml, 1 ml	BD Biosciences, Heidelberg, Germany

2.1.5 Hardware

Automated cell counter Vi-Cell XR	Beckman Coulter, Krefeld, Germany
Anesthetic system, UniVet Porta	Groppler, Deggendorf, Germany
Centrifuge 5810R	Eppendorf, Hamburg, Germany
Centrifuge Heraeus Pico 17	Heraeus, Hanau, Germany
CO_2 incubators HERAcell 150	Heraeus, Hanau, Germany
CTL-ImmunoSpot® S6 Macro Analyzer	CTL, Shaker Heights, OH
Electroporation System ECM 830	BTX, Holliston, MA
ELIspot reader Bioreader 6000-Eγ	BIO-SYS, Karben, Germany
Flow cytometer FACSCalibur	BD Biosciences, San Jose, CA
Flow cytometer FACSCanto II	BD Biosciences, San Jose, CA
Freezer, -80 °C	Heraeus, Hanau, Germany
Freezing container Mr- Frosty	Thermo Fisher Scientific, Schwerte, Germany
IVIS Lumina in vivo imaging system	Caliper Life Sciences,Hopkinton, MA
IVIS Spectrum in vivo imaging system	Caliper Life Sciences,Hopkinton, MA
Laminar flow bench HERAsafe 2020	Heraeus, Hanau, Germany
Microscope CKX31	Olympus, Hamburg, Germany
Restrainer, mouse	LabArt, Waldbüttelbrunn, Germany
Scale Precision Balance CPA 124s	Sartorius, Göttingen, Germany
Vortex mixer	IKA, Staufen, Germany
Water bath	Heraeus, Hanau, Germany

2.1.6 Kits

$CD4^+$ T Cell Isolation Kit, mouse	Miltenyi Biotec, Bergisch-Gladbach, Germany
$CD8^+$ T Cell Isolation Kit, mouse	Miltenyi Biotec, Bergisch-Gladbach, Germany
Compensation particles set anti-rat and anti-hamster	BD Biosciences, Heidelberg, Germany

2.1.7 Mice

Age matched female mice were maintained under specific-pathogen free conditions at the University of Mainz or BioNTech AG Mainz animal facilities. All animal experiments were conducted in accordance to German animal experimentation regulations.

BALB/c	Janvier Labs, Saint-Berthevin, France
C57BL/6	Janvier Labs, Saint-Berthevin, France

2.1.8 Peptides

Peptides were synthesized by JPT Peptide Technologies, Berlin, Germany. Purity was above 90 % as determined by LC-MS with ion trap, quadrupole or TOF detection, MALDI-MS or HPLC. Peptides were delivered as lyophilized powder and stored at -20 °C until usage.

2.1.9 Buffer and Cell Culture Media

CTL nedium

αMEM	
FBS	10 % (v/v)
2-Mercaptoethanol	50 µM
Penicilline/Streptomycin	0.5 % (v/v)

DC medium

RPMI 1640 GlutaMAX™	
FBS	10 % (v/v)
NEAA	1 % (v/v)
Sodium pyruvate	1 % (v/v)
Penicilline/Streptomycin	0.5 % (v/v)
2-Mercaptoethanol	50 µM

Erythrycyte lysis buffer

NH_4Cl	8.25 g
$KHCO_3$	1 g
EDTA	100 µM
H_2O	fill up to 1 l

FACS-buffer

PBS	
FBS	3 % (v/v)
Sodium azide (NaN_3)	10 mM

Freezing medium

FBS	
DMSO	10 % (v/v)

Fekete's solution

Ethanol, 70 %	5 ml
Formalin, 37 %	0,5 ml
Acetic acid, 100 %	0,25 ml

MACS-buffer

PBS	
FBS	1 % (v/v)
EDTA	2 mM

2.1.10 Reagents and Chemicals

2-Mercaptoethanol	Sigma-Aldrich, Saint Louis, MO
4-(2-hydroxyethyl)-1-piperazineethanesulfonic acid (HEPES)	Thermo Fisher Scientific, Schwerte, Germany
5-Bromo-4-chloro-3-indolyl phosphate (BCIP) / nitro blue tetrazolium chloride (NBT) solution	Sigma-Aldrich, Saint Louis, MO
Accutase soluition	Sigma-Aldrich, Saint Louis, MO
Acetic acid, 100 %	Sigma-Aldrich, Saint Louis, MO
Ammonium chloride (NH_4Cl)	Sigma-Aldrich, Saint Louis, MO
Bovine serum albumin (BSA)	Sigma-Aldrich, Saint Louis, MO
Brefeldin A	Sigma-Aldrich, Saint Louis, MO
Concanavalin A (ConA)	Sigma-Aldrich, Saint Louis, MO
Dimethyl sulfoxide (DMSO)	Applichem, Darmstadt, Germany
D-Luciferin	BD Biosciences, Heidelberg, Germany
Ethanol, 98 %	Carl Roth, Karlsruhe, Germany
eFluor 506 fixable viability dye	eBioscience, San Diego, CA
Ethylenediaminetetraacetic acid (EDTA), 0.5M	Sigma-Aldrich, Saint Louis, MO
Erythrosin B	Sigma-Aldrich, Saint Louis, MO
FACS clean	BD Biosciences, Heidelberg, Germany
FACS flow	BD Biosciences, Heidelberg, Germany
FACS Lysing Solution (10X)	BD Biosciences, Heidelberg, Germany
FACS rinse	BD Biosciences, Heidelberg, Germany
Fetal bovine serum (FBS)	PAA Laboratories, Pasching, Austria
Formaldehyde, 37 %	Carl Roth, Karlsruhe, Germany
Ficoll-Paque PREMIUM 1,084	Thermo Fisher Scientific, Schwerte, Germany
Fixation-Buffer	BD Biosciences, Heidelberg, Germany
Human Interleukin-2 (IL-2)	Novartis, Nürnberg, Germany
Lisposomes (F12, L1 or L2)	BioNTech RNA Pharmaceuticals, Mainz Germany
Isoflurane	Baxter, Deerfield, IL
Isopropyl alcohol	Merck, Darmstadt, Germany
Murine Granulocyte-macrophage colony-stimulating factor (GM-CSF)	Peprotech, London, UK
Murine Interferon-γ (IFN-γ)	Peprotech, London, UK
Penicilline-Streptomycin (10.000 U/ml)	Thermo Fisher Scientific, Schwerte, Germany
Phosphate buffered saline (PBS) powder	Biochrom AG, Berlin, Germany
PBS solution	Thermo Fisher Scientific, Schwerte, Germany
Phorbol 12-myristate 13-acetate (PMA)	Sigma-Aldrich, Saint Louis, MO
Potassium bicarbonate (KHC_3)	Sigma-Aldrich, Saint Louis, MO
Sodium azide (NaN_3)	Sigma-Aldrich, Saint Louis, MO

Sodium chloride, 5M	Thermo Fisher Scientific, Schwerte, Germany
Streptavidin-alkaline phoshatase(AP)	Sigma-Aldrich, Saint Louis, MO
Trypan blue	Sigma-Aldrich, Saint Louis, MO
Water, nuclease-free	Carl Roth, Karlsruhe, Germany

2.1.11 RNA

In vitro transcribed RNA was produced by BioNTech Pharmaceuticals, Mainz, Germany as described elsewhere [155]. The schematic layout of antigen encoding RNA was described in detail by Kreiter and colleagues [159] (see also section1.3 and Figure 1.7).

2.1.12 Software and Databases

Adobe Photoshop CS6	Adobe Systems Incorporated, San Jose, CA
Adobe Illustrator CS6	Adobe Systems Incorporated, San Jose, CA
ChemSketch 2015	ACD/Labs, Toronto, Canada
Excel 2010	Microsoft, Redmond, WA
FlowJo X	TreeStar, Ashland, OR
Graphpad Prism 6	GraphPad Software, San Diego, CA
Immune epitope database (IEDB)	Vita et al. [77], `http://www.iedb.org`
IVIS Living Image 4.0	Caliper Life Sciences,Hopkinton, MA
SYFPEITHI database	Ramensee et al. [67], `http://www.syfpeithi.de`

2.2 Methods

2.2.1 Cell Biological Methods

2.2.1.1 Cell Culture

Sterile handling of cells was performed under a laminar flow bench. Working cell banks frozen in liquid nitrogen provided a supply of cell lines. Cell lines were thawed at 37 °C until only a small piece of ice was left, immediately taken up and washed twice with 10 ml sterile PBS. Cells were counted as described in 2.2.1.2, seeded at a concentration of 1 to 5x10^5 cells/cm^2 in sterile cell culture medium (RPMI 1640, GlutaMaxTM) and cultivated at 37 °C and 5 % CO_2 in plastic culture flasks. Every two to three days cells were harvested, centrifuged (4 min, 300 g, RT) and seeded at a concentration of 1 to 5x10^5 cells/cm^2. For experimental studies, cells were kept in culture for at least one week and maximally one month before use. In order to detach cells, 5 ml/175cm^2 accutase sulution was added and incubated for 5-10 min at 37 °C until most cells rounded up and detached. Cells were cetrifuged (300 g, 4 min, RT) and taken up in culture medium or PBS. For cryopreservation, cells were taken up in freezing medium (2.1.9) at a concentration of 5x10^6 cells/ml in cryo tubes, kept overnight at -80 °C in an isopentane filled cryo freezing container and transferred to a liquid nitrogen tank (-196 °C) for long-term storage.

2.2.1.2 Cell Counting

Cell numbers and concentrations were assessed using either a hemocytometer (Neubauer chamber) or an electronic cell counting device (Vi-Cell XR Cell Viability Analyzer). Cells were diluted with the cell viability dye Erythrosin B to an approximate concentration of $1x10^6$ cells/ml and counted in a Neubauer chamber. The mean of four quadrants multiplied with 10^4 equals the concentration per milliliter. The Vi-Cell electronic cell counting device is based on an optical system similar to the Neubauer chamber. Cells can be diluted in the range of 1:1 to 1:20 in a fixed volume of 500 µL. Based on size, contrast, circularity and a trypan blue staining of dead cells the Vi-Cell can determines cell concentration, viability, size distributions and other parameters. In most cases, cell lines and peripheral blood lymphocytes (PBL) were counted with a Neubauer chamber whereas splenocytes were counted with the Vi-Cell analyzer.

2.2.1.3 Generation of Bone Marrow Derived Dendritic Cells

Murine bone marrow derived dendritic cells (BMDCs) were generated as described elsewhere [166] with slight modifications. In brief, tibias and femurs of mice were retrieved under sterile conditions (day 1). Both sides of the bones were cut and the bone marrow was flushed out with DC medium (2.1.9) using a 27G canula. The bone marrow which was then filtered through a 70 µm cell strainer, centrifuged (300 g, 6 min, RT) and incubated in 5 ml erythrocyte lysis buffer (2.1.9) for 3-5 min in order to remove erythrocytes. The lysis reaction was stopped by adding approximately 20 ml PBS. Cells were centrifuged (300 g, 5 min, RT), resuspended in 20 ml DC medium supplemented with GM-CSF (1000 U/ml), counted and seeded at a concentration of $2.5x10^5$ cells/cm^2 (20 ml DC medium per 75 cm^2). Two days later (day three), 5 ml per 75 cm^2 DC medium supplemented with GM-CSF (1000 U/ml) were added. On day five, medium and suspension cells were collected, centrifuged (300 g, 6 min, RT), resuspended in 20 ml DC medium + GM-CSF (1000 U/ml) and added back to the adherent cells. After seven days of culture, BMDCs were harvested and directly used for *in vitro* assays or frozen at a concentration of $1x10^7$ cells/ml as described above. For quality control, BMDCs were stained for CD11c, CD86 and MHC class II and analyzed via flow cytometry (2.2.2.1).

2.2.1.4 Electroporation

The treatment of cells with an electrical pulse leads to the formation of pores in the cell membrane which enhances the uptake of DNA or RNA. This method called electroporation is commonly used to transiently transfect cells. Importantly, due to the susceptibility of RNA towards the degradation by RNases, consumables need to be free of RNases. In addition, surfaces as well as equipment needs to be wiped with an cleaning agent for removing RNases and RNA needs to be kept at 4 °C or below. Cells, either BMDCs or tumor cell lines were harvested, washed twice with serum-free X-Vivo 20 medium and diluted to approximately $1x10^7$ cells/ml. 230 µl of cell solution was added to a 4 mm electroporation cuvette containing 20 µg (1 µg/µl) of RNA and pulsed with the settings described in Table 2.1.

Table 2.1: Electroporation settings.

Cells	No. of pulses	Length of pulses [ms]	Voltage [V]
BMDCs	1	5	400
4T1_Luc	1	5	250

2.2.2 Immunological Assays

2.2.2.1 Flow Cytometry

Flow cytometry is a laser based, biophysical method to analyze cells and one of the most commonly used methods in cell biology. Erroneously, this method is sometimes called FACS (fuorescence-activated cell sorting) which represents a special form of flow cytometry to sort labeled cells.

Analyzed cells are taken up in a liquid stream in a way that a single cell passes different laser beams. Emitted or reflected light is than measured by different detectors such as the forward scatter (FSC) or sideward scatter (SSC). The signal detected by the FSC correlates with the size whereas the SSC signal increases with the granularity of the cell. Despite the analysis of size and granularity cells can be labeled with fluorescent dyes. In most cases, fluorescently-labeled antibodies against cell markers of interest are used. In addition, commonly used fluorescent dyes are the green fluorescent protein (GFP), carboxyfluorescein succinimidyl ester (CFSE) or different viability dyes such as propidium iodide (PI) or Annexin V. Being excited by the laser, the fluorescent dye emits light in a defined wavelength restricted to this specific dye. By combination of different fluorescent dyes a multitude of markers can be analyzed simultaneously.

For surface marker stainings cells were taken up in 100 µl FACS buffer (2.1.9) at a concentration of 0.5-4x10^6 cells/ml containing fluorescently-labeled antibodies (v/v: 1:50 to 1:500) and incubated for 15 to 20 min at 2-8 °C. Labeled cells were washed with 200 to 3000 µl FACS buffer, centrifuged (450 g, 6 min, RT) and taken up in 100 µl FACS buffer at a concentration of approximately 1x10^6 cells/ml. Depending on the viability dye, antibody staining was preceded by staining of cells with the fixable dye eFluor 506 for 15 min at 2-8 °C in PBS or was followed by staining with PI for 5 min at RT in FACS buffer. Flow cytometry was performed on a BD FACSCalibur or BD FACSCanto II and data was analyzed using FlowJo X. Compensation for multi-color stainings with BD FACSCanto II was accomplished using the MACS compensation particles set.

2.2.2.2 Intracellular Cytokine and Surface Marker Staining

Antigen stimulated T cells secrete cytokines like IFN-γ, TNF-α or IL-2. Staining against these cytokines in addition to staining for the surface markers CD4 and CD8 allows the detection of activated T cells and the determination of the T-cell subtype. Surface markers can be directly stained whereas detection of intracellular proteins requires the perforation of the cell membrane. In addition, staining of secreted proteins obliges the treatment of secretion inhibitors such as Brefeldin A, a lactone antibiotic that blocks proteins transport from the endoplasmic reticulum to the Golgi apparatus.

In the presence of Brefeldin A (20 µg/ml) $2x10^6$ splenocytes were stimulated with $2x10^5$ RNA transfected BMDC or 2 µg/ml peptide in 200 µl DC medium. Splenocytes treated with phorbol 12-myristate 13-acetate (PMA, 0.5 µg/ml) and Ionomycin (1 µg/ml) served as positive control. Cells were incubated 5 h at 37 °C, washed with 200 µl FACS buffer and stained with the fixable viability dye eFluor 506 for 15 min at 2-8 °C in 100 µl FACS buffer (see Table 2.2). This was followed by one washing step with 200 µl FACS buffer and staining for CD4 and CD8 cell surface markers for 20 min at 2-8 °C in 50 µl FACS buffer. Cells were then permeabilized and fixed using 100 µL BD Cytofix/Cytoperm according to the manufacturer's protocol. Thereafter cells were washed with 200 µl BD perm/wash buffer and stained for IFN-γ, TNF-α and IL-2 cytokines in 50 µl BD perm/wash buffer. Antibody suspensions were centrifuged for 5 min at 13,000 rpm in order to get rid of antibody complexes that bind unspecifically. Samples were acquired on a BD FACSCanto II. For analysis, cytokine secretion among single, living CD4 or CD8 positive lymphocytes was compared to control samples (medium, irrelevant RNA or irrelevant peptide).

Table 2.2: Cytokine and surface marker staining panel.

Marker	Dye	Volume per sample [µl]
CD4	FITC	0.5
CD8	APC-Cy7	0.5
IFN-γ	PE	1
TNF-α	PE-Cy7	1
IL-2	APC	0.2
Dead cells	eFluor 506	0.1

2.2.2.3 Enzyme-Linked Immunospot Assay

The Enzyme-linked immunospot (ELISpot) assay is a sensitive method for the detection of activated T cells. Most commonly ELISpot assays track the cytokine IFN-γ secreted by antigen stimulated T cells. Similar to an enzyme-linked immunosorbent assay (ELISA), an antibody against the protein of interest (IFN-γ) is coated to a membrane (usually polyvinylidene difluoride, PVDF) of a 96-well microtiter plate. The secreted IFN-γ of stimulated T cells binds to the antibody that is attached to the membrane. After discarding the cells, a second biotin-coupled antibody against IFN-γ is added. Enzyme-coupled (e.g. hydrolyse alkaline phosphatase, AP) streptavidin then binds to the biotin and addition of a substrate (e.g. 5-Bromo-4-chloro-3-indolyl phosphate, BCIP and nitroblue tetrazolium NBT) that is converted to a colored precipitate (see Figure 2.1) allows the visualization of the secreted IFN-γ. In comparison to an ELISA where the protein of interest is measured photometrically, every spot represents an IFN-γ secreting T cell. Spot counting is done manually or by using an automated reader that captures images of each well to analyze spot number and size.

PVDF microtiter 96-well plates were treated with 15 µl ethanol (35 % v/v in water), immediately washed twice with 200 µl sterile PBS and coated with 50 µl anti-INF-γ (10 µg/ml in PBS + 0.5 % BSA) overnight at 4-8 °C. The plate was washed twice with 200 µl sterile PBS and blocked for approximately 30 min at 37 °C by addition of 150 µl DC medium. If not otherwise stated, $5x10^5$

splenocytes were added and stimulated with 2-6 µg/ml peptide or with $5x10^4$ syngeneic BMDC electroporated with RNA. As positive control 2 µg/ml Concanavalin A was added. After overnight culture at 37 °C the cell suspension was discarded, the plate was washed three times with 200 µl PBS and cytokine secretion was detected by staining with 60 µl of biotinylated anti–IFN-γ antibody (1 µg/ml in PBS + 0.5 % BSA) for 2 h at 37 °C. After washing three times with 200 µL PBS, 100 µl of a Streptavidin-Peroxidase (1:1000 v/v in PBS + 0.5 %BSA) was added and incubated for 45 min at RT in the dark. The plate waswashed three times with 200 µl PBS and 100 µl BCIP/NBT solution was added for 5-7 min. The reaction was stopped by addition of water and spots were counted on an automated reader.

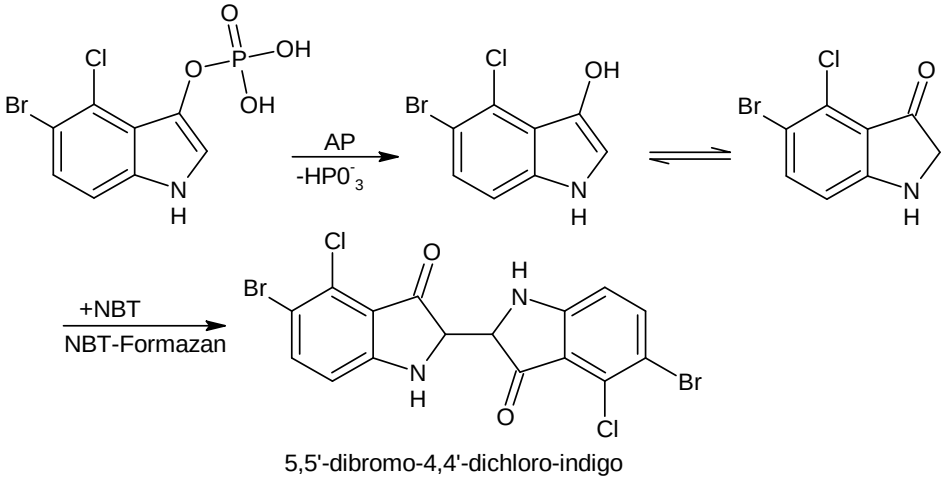

Abbildung 2.1: Reaction of BCIP and NBT. The alkaline phosphatase katalyses the hydrolysation of the phosphoric acid ester at the indole ring of the BCIP. After tautomerisation to the 5-bromo-4-chloro-1,2-dihydro-3H-indol-3-one the substance is oxidized by NBT and dimerizes to the purple-blue indigo dye.

2.2.2.4 Magnetic-Activated Cell Sorting

Monoclonal antibodies coupled with small paramagnetic beads (microbeads) directed to specific surface antigens can be used for cell sorting. The stained cell mixture is added to a column attached to a strong magnet. Antibody labeled cells get stuck in the column by interaction of the magnet with the microbead-coupled antibodies whereas non-labeled cells can be collected in the flow through. After washing and removal of the column from the magnet, antibody labeled cells can be eluted as a separate fraction.

Magnetic-activated cell sorting (MACS) was performed according to the manufacturers protocol. $1x10^8$cells/ml were stained with microbead-coupled antibodies (10 % v/v) in MACS buffer (2.1.9) for 15 min at 2-8 °C. Cells were washed once with 1 to 2 ml of MACS buffer per $1x10^7$cells, taken up in 500 µl MACS buffer and added to a MACS column LS placed in the magnetic field and pretreated with 3 ml MACS Buffer. Subsequently, three times 3 ml of MACS buffer was added and the flow through was collected. The column was removed from the seperator and labeled cells were eluted by addition of 5 ml of MACS buffer by pushing a plunger into the column.

2.2.2.5 Subtyping of T-Cell Responses

For testing wheter $CD4^+$ or $CD8^+$ T cells recognized the respective neo-epitope several methods were applied as indicated in the results section. For subtyping of immunogenic T-cell responses against CT26, intracellular cytokine and surface marker staining (2.2.2.2) was performed. Immune responses against 4T1 derived mutations were subtyped using MACS sorted $CD8^+$ T cells and $CD4^+$T cells (2.2.2.4, flow through after CD8 positive selection) or an MHC class II blocking antibody (20 µg/ml in DC medium) within an IFN-γ ELISpot assay. For the latter method, the blocking antibody was added to the splenocytes and incubated for 15 min at 37 °C before the peptide or RNA elextroporated BMDCs were added.

2.2.2.6 Immunofluorescence Staining

Immunofluorescence (IF) staining was performed by Fulvia Vascotto and Magdalena Brkic. 8 µm sections of cryconserved organs were attached on superfrost slides, dried overnight at RT and fixed in 4 % para-formaldehyde for 10 min at RT in the dark. Sections were washed 3 times with PBS and blocked using PBS supplemented with 1 % BSA, 5 % mouse serum, 5 % rat serum and 0.02 % Nonident for 1 h at RT in the dark. Fluorescent labeled antibodies (FoxP3, clone FJK-16s, eBioscience; CD8, clone 53-6.7, BD; CD4, clone RM4-5, BD) were diluted in staining buffer (PBS supplemented with 1 % BSA, 5 % mouse serum and 0.02 % Nonident) and sections were stained overnight at 4 °C. After washing twice with washing buffer (PBS supplemented with 1 % BSA and 0. 02 % Nonident) and once with PBS, slides were stained for 3 min with Hoechst (Sigma), washed 3 times with PBS, once with distilled water and mounted using Mounting Medium Flouromount G (eBioscience). Immunofluorescence images were acquired using an epifluorescence microscope (ApoTome, Zeiss). Tumor, CD4, CD8 and FoxP3 stained areas were quantified within manually pre-defined tumor regions via computerized image analysis software (Tissue Studio 3.6.1., Definiens). The proportion of marker positive cells in comparison to DAPI positive cells was calculated.

2.2.2.7 Immune Histochemistry

Immune histochemistry was performed by Astrid Spruß and colleagues at Ganymed Pharmaceuticals, Mainz.

Lungs of CT26 tumor bearing mice were fixed overnight in 4 % phosphate buffered formaldehyde solution (Carl Roth) and embedded in paraffin. 50 µm consecutive sections (3 per mouse) were stained for CD3 (clone SP7, Abcam), CD4 (clone 1, cat# 50134-M08H, Sino Biologinal) and FoxP3 (polyclonal, cat# NB100-39002, Novus Biologicals) following detection by a HRP-conjugated antibody (Poly-HRP-anti-rabbit IgG, ImmunoLogic) and the corresponding peroxidase substrate (Vector Nova Red, Vector Laboratories) and counterstained with hematoxylin. $CD3^+$, $CD4^+$, $FoxP3^+$ and tumor areas were captured on an Axio Scan.Z1 (Zeiss) and manually pre-defined tumor and lung regions were quantified via computerized image analysis software (Tissue Studio 3.6.1, Definiens). $CD8^+$ area was calculated by subtracting CD4 stained area from $CD3^+$ area.

2.2.3 Animal Experimental Techniques

2.2.3.1 Anesthesia

Animals were anesthetized using an oxigen-isoflurane vaporizer (2.5 % Isoflurane). Mice were transferred to the anesthesia chamber and kept until movement stopped. Subsequently, mice were taken out of the chamber and the experimental procedure was performed before mice woke up (approximately 5-20 s). For *in vivo* bioluminescence measurements, mice were kept under constant anesthesia until the measurement was completed.

2.2.3.2 Blood Retrieval

Mice were anesthetized and blood was retrieved via the retro-orbital vein using a micro haematocrit capillary tube. Blood was collected in heparin covered capillary blood collection tubes.

2.2.3.3 RNA vaccination

RNA was diluted with H_2O (L1 liposomes) or HEPES(10 mM)/EDTA(0.1 mM) buffer (L2 liposomes) and aqueous 1.5 M NaCl (final concentration 150 mM) solution was added under sterile RNase free conditions. The mixture was inverted several times and liposomes were added. After mixture and approximately 10 min of incubation 200 µl of RNA lipoplexes were injected IV into the retro-orbital plexus. Injected RNA amounts ranged between 5 to 90 µg. For immunogenicity testing, mice were vaccinated weekly for three times. Schedules for therapeutic tumor experiments are indicated in the respective figures.

2.2.3.4 Antibody Administration

Antibodies were administered intraperitoneal (IP, 200 µg in 200 µl PBS).

2.2.3.5 Tumor Models

Tumor cells were cultured and detached as described in section 2.2.1.1and taken up in PBS (see Table 2.3). Cells with a viability below 80 % were discarded. For subcutaneous (SC) tumor models, mice were shaved at the right flank and anesthetized. Subsequently, the skin was lifted with forceps to inject tumor cells with a 0.5 ml syringe under the skin. Tumor growth was measured by caliper every 2-3 days using the formula $\frac{A \cdot B^2}{2}$ (A as the largest and B the smallest diameter of the tumor). For induction of lung tumors, tumor cells were injected intravenously into the tail vain of mice. For this, mice were kept for 1-5 min under red light and transferred into a restrainer. Tumor burden was measured via bioluminescence imaging (BLI, see section 2.2.3.6) for luciferase transgenic tumors. For wild type tumors, tumor nodules were counted after ink staining and formalin fixation (see section 2.2.3.7). After injection, mice were distributed into treatment groups either randomly (B16F10,

CT26-WT) or based on the total flux (2.2.3.6) measurement before the first treatment (ANOVA-P method, Daniel's XL Toolbox V6.53). Health condition of mice was frequently surveilled and documented. Animals were sacrificed as soon as signs of distress, breathing problems or a tumor volume above 1500 mm^3 occurred.

Tabelle 2.3: Cell numbers and injected volumes for used tumor models.

Cells	Cell No.	Injected Volume [µl]	Injection Route
B16F10	$1x10^5$	100	SC
CT26-WT	$2x10^5$	100	SC
CT26-WT	$2x10^5$	200	IV
CT26-Luc	$5x10^5$	200	IV
4T1-Luc	$2x10^4$	200	IV

2.2.3.6 *In Vivo* Bioluminescence Imaging

The firefly (*Photinus pyralis*) luciferase (Luc) is a 61kDa oxidative enzyme that catalyses the bioluminescence reaction of D-Luciferin (Firefly Luciferin) to Oxyluciferin under consumption of ATP and emission of light (Figure 2.2). The emitted light (550-570 nm) can be measured and quantified via a luminometer. Hence, this reaction can be used in order to track the growth of luciferase transgenic tumor cells as the emitted light correlates with the amount of living tumor cells.

Tumor growth of luciferase transgenic cells was traced by bioluminescence imaging after IP injection of an aqueous solution of D-luciferin (250 µl, 1.6 mg in PBS) on an IVIS Lumina or IVIS Spectrum (Caliper Life Sciences). After five minutes, *in vivo* bioluminescence in regions of interest (ROI) were quantified as total flux (photons/sec) (IVIS Living Image 4.0). Additionally, the signal intensity was represented as a pseudocolor image superimposed to grayscale photographic images of mice using the IVIS Living Image software. The acquisition time ranged between 1 s and 3 min at binning 4 or binning 8 depending on the singal intensity.

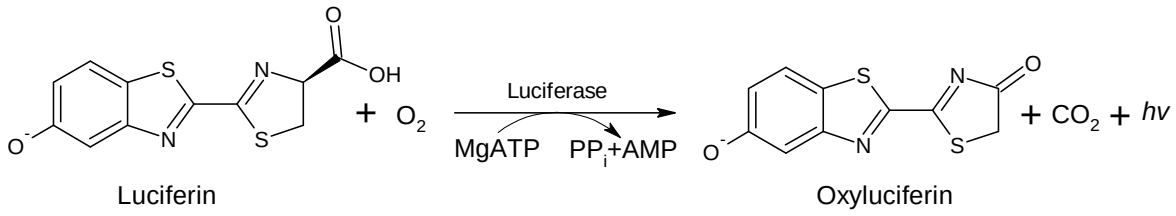

Abbildung 2.2: The luciferase bioluminescence reaction. The firefly luciferase catalyzes the reaction of Luciferin to Oxyluciferin under consumption of ATP and bioluminescence. PP_i: pyrophosphate, *hv*: light.

2.2.3.7 Staining and Counting of Lung Tumor Nodules

Tumor cells injected IV form tumor nodules in the lung. This models, in a simplified manner, metastasis formation of primary tumors. Tumor burden can be either quantified via BLI of luciferase transgenic tumors or by counting of tumor nodules. However, tumor nodules are often difficult to

identify on an untreated lung, especially if they are small. For this reason, ink staining was performed which stains the lung tissue deep blue and the tumor nodules stay colorless. Even if stained with ink, counting remains still difficult due to the soft texture of the lung. This can be improved by fixation with formalin in the presence of ethanol and acetic acid (Fekete's solution 2.1.9, see Figure 2.3). Fekete's solution increases the contrast between tumor nodules and lung tissue and stabilizes the lung tissue.

Mice were sacrificed 14-17 days after tumor inoculation as indicated in the respective figures. The thorax was opened and approximately 0.5 ml ink (diluted 1:10 with PBS) was injected intratracheal. The trachea was pinched of with forceps above the injection site to direct the pressure into the lungs.After injection, the lung was excised, washed with PBS, transferred to approximately 5 ml of Fekete's solution and incubated overnight at 2-8 °C. Thereafter, tumor nodules were categorized by size and counted so that a nodule twice as large as a the smallest nodule in the experiment would count for two tumor nodules and so forth. The maximum number of counted nodules was 500 (everything above was indistinguishable).

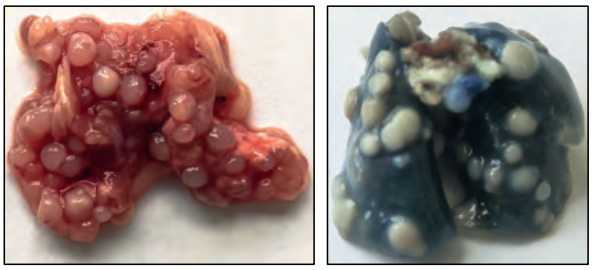

Abbildung 2.3: Lungs with or without ink staining and Fekete's solution treatment. Both lungs are derived from CT26-WT tumor bearing mice. In comparison to the lung on the left, the lung on the right was stained with ink and treated with Fekete's solution

2.2.3.8 Isolation of Spleoncytes

The left lateral abdomen of sacrificed mice was disinfected with 70 % Ethanol and the spleen excised using disinfected forceps and surgical scissors. The obtained organ was kept on ice in a 2 ml reaction tube in PBS and was processed shortly after excision. Under sterile conditions, single cells were acquired by pressing the spleen through a cell strainer placed on a 50 ml tube using a plunger of a 5 ml syringe. The spleen was mashed and rinsed with approximately 20 ml sterile PBS until no more red tissue was left in the cell strainer. The cells were centrifuged (300 g, 5 min, RT), the supernatant discarded and cells resuspended with 5 ml erythrocyte lysis buffer (2.1.9). After 3-5 min the lysis reaction was stopped by addition of 15 ml sterile PBS. The splenocytes were centrifuged (300 g, 5 min, RT), resuspended with 5 ml DC medium and counted with the Vi-Cell cell counter (1:5 dilution with PBS, program "SplenocytesMarc").

2.2.3.9 Isolation of Peripheral Blood Lymphocytes

Blood was retrieved as described in 2.2.3.2 and diluted 1:1 with sterile PBS. Two milliliter of Ficoll-Paque PREMIUM 1,084 was added into a 15 ml tube and the blood solution was carefully layered on top. After centrifugation (400 g, 30 min, RT), peripheral blood lymphocytes (PBL) located at the interlayer between plasma and platelets (upper layer) and granulocytes and erythrocytes (lower layer) were carefully transfered into a new 15 ml tube filled with 5 ml DC medium. The cells were centrifuged (300 g, 5 min, RT), supernatant was removed and PBLs were taken up in the respective volume od DC medium needed for the read out. Cell counting was performed using a Neubauer chamber (2.2.1.2).

2.2.4 *In silico* analysis

2.2.4.1 MHC binding prediction

MHC class I or II binding prediction was performed using the consensus method offered by the Immune Epitope Database (IEDB [77]). The consensus method employs three different prediction algorithms (NetMHC (Artificial neural network, ANN) Version 3.4, Stabilized matrix method (SMM), and Combinatorial peptide libraries (Comblib_Sidney2008)). The output of the IEDB consensus mehtod is the median percentile binding score of the three prediction algorithms. If not otherwise stated, a percentile rank of below 1 for MHC class I and below 10 for MHC class II was utilized.

2.2.4.2 Statistics

Means were compared by using Student's t-test for hypothesis testing to compare individual treatment and corresponding control groups. In case of significantly different variances (F-test, alpha=0.05) Welch's correction was used. For comparison of multiple means one-way ANOVA following Dunnett's test or Tukey's test was applied. Tumor growth was compared by calculating the area under the tumor growth curve (AUC) for single mice. Statistical differences in medians between two groups were calculated with a nonparametric Mann–Whitney U test. Survival benefit was determined with the log-rank test. All analyses were two-tailed and carried out using GraphPad Prism 6.04. n.s.: $P>0.05$, *$P\leq0.05$, **$P\leq0.01$, ***$P\leq0.001$, ****$P\leq0.0001$. In some cases, Grubb's test was used for identification of outliers (alpha=0.05).

3 Results

Whole exomes as well as RNA of B16F10, 4T1 and CT26 tumor cell lines were previously sequenced and compared to healthy tissue in order to identify tumor mutations (see section 1.3) [49, 50, 167]. An overview on the number of identified non-synonymous SNVs (nsSNVs), indels, and gene fusions is summerized in table 3.1. B16F10 mealoma cells, CT26 colon carcinoma cells and 4T1 mamary carcinoma cells express 412, 628 and 157 nsSNVs, respectively. The mutational load of B16F10 and 4T1 tumor cells are in the range of the corresponding human tumors whereas the number of nsSNVs in CT26 corresponds to MSI-H colorectal cancer (Figure 1.2). As demonstrated for human tumors [60] indels and gene fusions are rather rare compared to nsSNVs ranging between 10-20 expressed indels per tumor. 164 expressed gene fusions were predicted in CT26 from which 5 of 11 selected were validated in DNA.

Tabelle 3.1: Identified mutations in the tumor models B16F10, 4T1 and CT26 Whole exome and RNA sequencing data of the tumor cell lines and healthy tissue was compared in order to identify non-synonymous SNVs (nsSNVs, a), small insertion and deletions (indel, b) as well as gene fusions (c) .

Process step	B16F10	4T1	CT26
Somatic nsSNVs in exons	1186	755	628
Expressed nsSNVs	412	157	628

(a) Non-synonymous SNVs (nsSNVs)

Process step	B16F10	4T1	CT26
Somatic indels in exons	30	41	33
Expressed indels	20	19	10
Validated in DNA	13 of 16	3 of 19	22 of 33

(b) Small insertion and deletions (indel)

Process step	CT26
Fusions in RNA with probability >0.66	164
Selected	11
Validated in DNA	5 of 11

(c) Gene fusions

3.1 Immunogenicity Testing

A prerequisite of mutations as targets for an anti-tumoral cancer vaccine is their recognition by T cells (immunogenicity). In its broader meaning, the term immunogenicity is coined by the presence of a T-cell response against a certain antigen. More precisely, *immunogenicity* describes a spontaneous immune response whereas *antigenicity* means the induction of an immune response by vaccination. For the sake of simplicity the term immunogenicity is used in its broader meaning throughout this chapter.

3.1.1 Immunogenicity of Point Mutations

As mentioned in section 1.3.5, B16F10 SNVs were tested as a first proof of concept by Niels van de Roemer. Approximately one third of the 50 SNVs selected for good predicted MHC class I binding were shown to be recognized by T cells after peptide or RNA vaccination. In order to validate these results in a different genetic background, we turned to the CT26 and 4T1 tumor models. BALB/c mice (n=3 for CT26 and 4T1) were repetitively immunized with two RNAs (section 2.2.3.3) encoding each 27 amino acids of a neo-antigen with the mutation in the center. Five days after the last vaccination splenocytes were harvested and analyzed for recognition of the mutated peptide and/or BMDCs electroporated with the respective RNA in an IFN-γ ELISpot assay. Confirmation of immunogenicity and subtyping of T-cell responses was performed via addition of an MHC class II blocking antibody in the ELISpot assay and/or flow cytometric analysis of cytokine release (n=5 for CT26, n=3 for 4T1). 38 of the expressed 4T1 mutations irrespective of MHC I binding prediction were screened. For CT26, 48 of the expressed mutations in analogy to the B16F10 study were selected based on good MHC class I binding ("low score" 0.1-2.1). Another 48 mutations were deliberately chosen for poor binding ("high score" >3.9). Exemplarily, the secretion of IFN-γ by stimulated splenocytes from CT26-M90 ($Aldh18a1_{P145S}$) RNA vaccinated mice is shown in Figure 3.1a. Only the peptide encompassing the mutated but not the wild type amino acid resulted in T-cell recognition. Addition of an MHC class II blocking antibody led to the complete abrogation of IFN-γ secretion, pointing to the fact that CT26-M90 is recognized by $CD4^+$ T cells (Figure 3.1b).

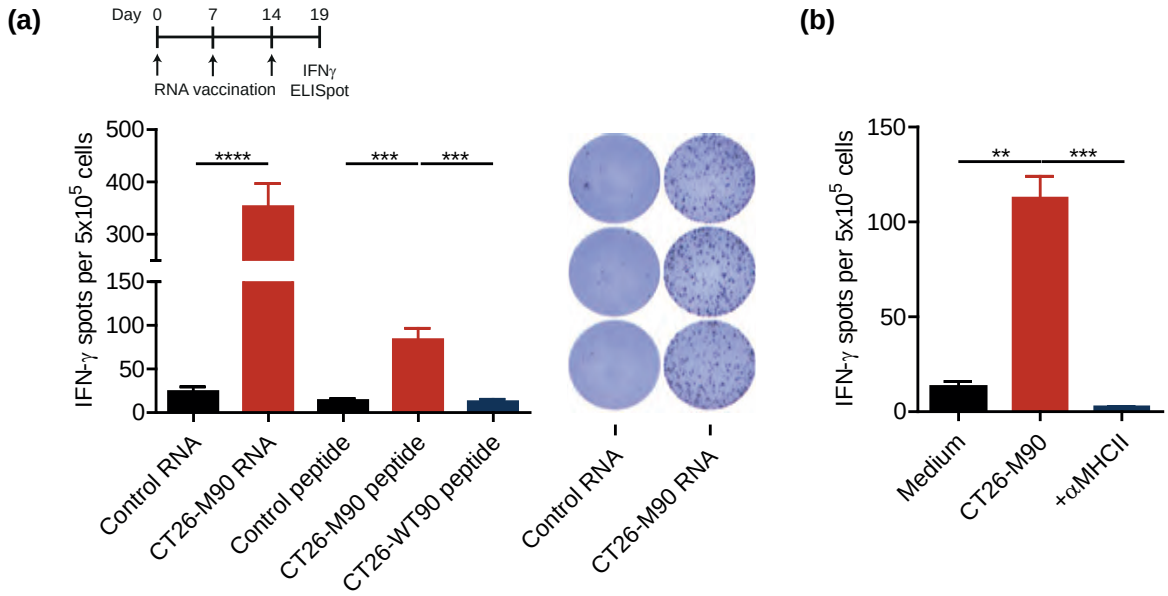

Abbildung 3.1: RNA vaccination induces T-cell recognition of a point mutation in the Aldh18a1 gene. a, BALB/c mice (n=5) were vaccinated three times with 40 µg of RNA encoding for 27 amino acids of the mutated Aldh18a1 gene (contains CT26-M90). Splenocytes were subsequently tested for recognition of mutated or wild type peptides (CT26-M90 peptide and CT26-WT90 peptide, respectively) as well as the RNA electroporated BMDC (CT26-M90 RNA) in comparison to control peptide (SIINFEKL) or irrelevant RNA (eGFP) electroporated BMDC (Control RNA). The image in the center shows the ELISpot data for one mouse. **b,** Splenocytes of vaccinated mice (n=3) were stimulated with CT26-M90 peptide with (+αMHCII) or without (CT26-M90) addition of an MHC class II blocking antibody.

In total, about 45 % of 4T1 mutations and 20 % of CT26 mutations were found to be immunogenic in mice vaccinated with the respective RNA (Figure 3.2, Table 3.2 and 3.3). Surprisingly, the majority of immunogenic mutations were recognized by $CD4^+$ T cells (4T1: 12/17, 71 %; CT26: 16/21, 80 %). For CT26, in the "low" MHC I score subgroup, but not in the "high" score subgroup, several epitopes inducing $CD8^+$ T cells were identified indicating that the MHC class I binding prediction enriched for $CD8^+$ T-cell epitopes (Figure 3.3). MHC class II restricted epitopes, however, were represented in similar frequency in both subgroups.

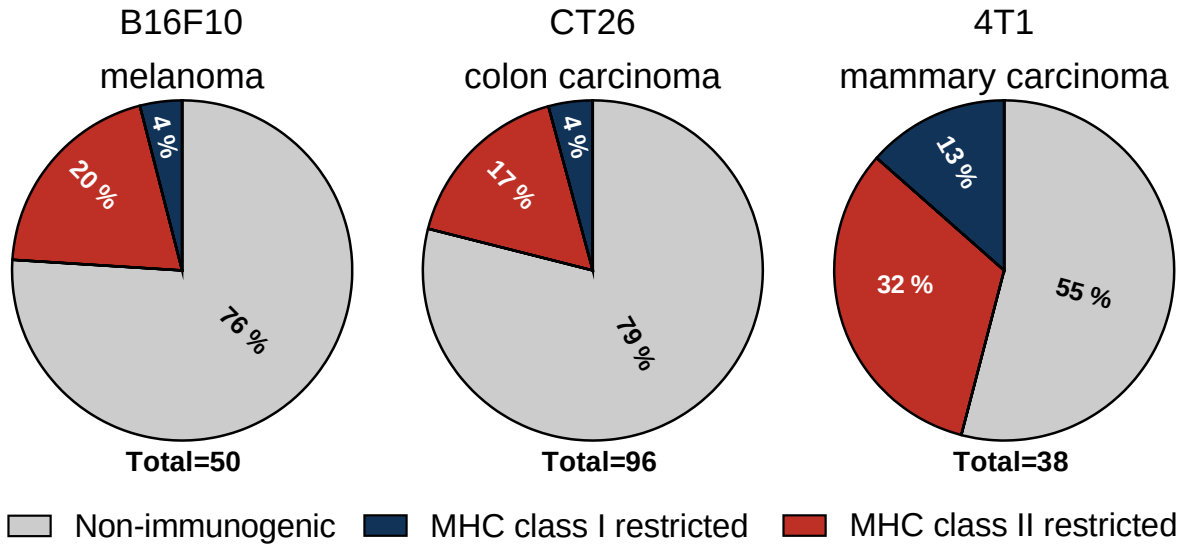

Abbildung 3.2: Prevalence of non-immunogenic, MHC class I or II restricted neo-epitopes.

Table 3.2: Immunogenic 4T1 mutations. 4T1 mutations determined to be immunogenic upon RNA immunization (see Figure 3.2). WT, wild type; AA#, position of mutated amino acid; Mut, Mutation.

Mutation	Gene	Mutated sequence used for vaccination	Substitution (WT, AA#, Mut)	Reactive T cell subtype
4T1-M2	Gen1	IPHNPRVAVKTTNNLVMKNSVCLERDS	K707N	CD4
4T1-M3	Polr2a	LAAQSLGEPATQITLNTFHYAGVSAKN	M1102I	CD4
4T1-M8	Tmtc2	QGVTVLAVSAVYDIFVFHRLKMKQILP	V201I	CD8
4T1-M14	Zfr	AHIRGAKHQKVVTLHTKLGKPIPSTEP	K411T	CD4
4T1-M16	Cep120	ELAWEIDRKVLHQNRLQRTPIKLQCFA	H68N	CD4
4T1-M17	Malt1	FLKDRLLEDKKIAVLLDEVAEDMGKCH	T534A	CD4
4T1-M20	Wdr11	NDEPDLDPVQELIYDLRSQCDAIRVTK	T340I	CD8
4T1-M22	Kbtbd2	DAAALQMIIAYAYRGNLAVNDSTVEQL	T91R	CD4
4T1-M25	Adamts9	KDYTAAGFSSFQKLRLDLTSMQIITTD	I623L	CD4
4T1-M26	Pzp	AVKEEDSLHWQRPEDVQKVKALSFYQP	G1199E	CD8
4T1-M27	Gprc5a	FAICFSCLLAHALNLIKLVRGRKPLSW	F119L	CD8
4T1-M30	Enho	MGAAISQGAIIAIVCNGLVGFLL	L10I	CD4
4T1-M31	Dmrta2	EKYPRTPKCARCGNHGVVSALKGHKRY	R73G	CD4
4T1-M32	Rragd	SHRSCSHQTSAPSPKALAHNGTPRNAI	L268P	CD4
4T1-M35	Zzz3	KELLQFKKLKKQNLQQMQAESGFVQHV	K311N	CD8
4T1-M39	Ilkap	RKGEREEMQDAHVSLNDITQECNPPSS	127S	CD4
4T1-M40	Cenpf	RVEKLQLESELNESRTECITATSQMTA	D1327E	CD4

Table 3.3: Immunogenic CT26 mutations. CT26 mutations determined to be immunogenic upon RNA immunization (see Figure 3.2). MHC class I binding prediction was performed with IEDB consensus. WT, wild type; AA#, position of mutated amino acid; Mut, Mutation.

Mutation	Gene	Mutated sequence used for vaccination	Substitution (WT, AA#, Mut)	Reactive T cell subtype	MHC I score (best prediction)
CT26-M03	Slc20a1	DKPLRRNNSYTSYIMAICGMPLDSFRA	T425I	$CD4^+$	0,3
CT26-M12	Gpc1	YRGANLHLEETLAGFWARLLERLFKQL	E165G	$CD8^+$	1,9
CT26-M13	Nphp3	AGTQCEYWASRALDSEHSIGSMIQLPQ	G234D	$CD4^+$	0,1
CT26-M19	Tmem87a	QAIVRGCSMPGPWRSGRLLVSRRWSVE	G63R	$CD8^+$	0,7
CT26-M20	Slc4a3	PLLPFYPPDEALEIGLELNSSALPPTE	T373I	$CD4^+$	0,9
CT26-M24	Cxcr7	MKAFIFKYSAKTGFTKLIDASRVSETE	L340F	$CD4^+$	1,8
CT26-M26	E2f8	VILPQAPSGPSYATYLQPAQAQMLTPP	I522T	$CD8^+$	0,1
CT26-M27	Agxt2l2	EHIHRAGGLFVADAIQVGFGRIGKHFW	E247A	$CD4^+$	0,2
CT26-M35	Nap1l4	HTPSSYIETLPKAIKRRINALKQLQVR	V63I	$CD4^+$	0,7
CT26-M37	Dhx35	EVIQTSKYYMRDVIAIESAWLLELAPH	T646I	$CD4^+$	0,1
CT26-M39	Als2	GYISRVTAGKDSYIALVDKNIMGYIAS	L675I	$CD8^+$	0,2
CT26-M42	Deptor	SHDSRKSTSFMSVNPSKEIKIVSAVRR	S253N	$CD4^+$	0,3
CT26-M43	Tdg	AAYKGHHYPGPGNYFWKCLFMSGLSEV	H169Y	$CD4^+$	0,3
CT26-M55	Dkk2	EGDPCLRSSDCIDEFCCARHFWTKICK	G192E	$CD4^+$	9,7
CT26-M58	Rpap2	CGYPLCQKKLGVISKQKYRISTKTNKV	P113S	$CD4^+$	11,3
CT26-M68	Steap2	VTSIPSVSNALNWKEFSFIQSTLGYVA	R388K	$CD4^+$	6,8
CT26-M75	Usp26	KTTLSHTQDSSQSLQSSSDSSKSSRCS	S715L	n.d.	5,8
CT26-M78	Nbea	PAPRAVLTGHDHEIVCVSVCAELGLVI	V576I	$CD4^+$	6,3
CT26-M90	Aldh18a1	LHSGQNHLKEMAISVLEARACAAAGQS	P154S	$CD4^+$	8,3
CT26-M91	Zc3h14	NCKYDTKCTKADCLFTHMSRRASILTP	P497L	$CD4^+$	8,8
CT26-M93	Drosha	LRSSLVNNRTQAKIAEELGMQEYAITN	V1189I	$CD4^+$	9,9

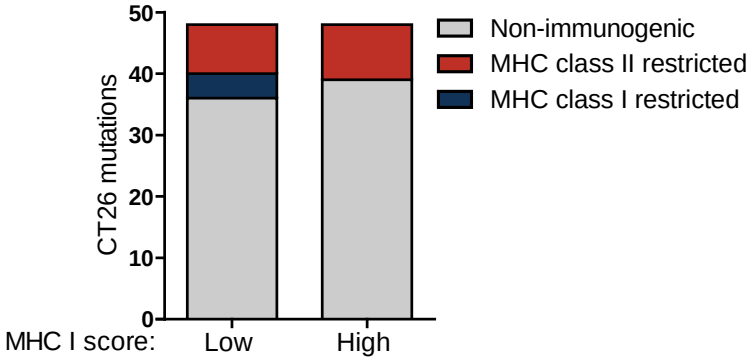

Figure 3.3: Prevalence and subtype of T-cell responses selected for a high or a low MHC I binding score. CT26 mutations were selected based on a good ("low score" 0.1-2.1) or on a unfavorable ("high score" >3.9) MHC class I binding prediction and tested for immunogenicity. Each group is comprised of 48 mutations.

The data shown in this section validate the preclinical proof of concept for the immunogenicity of Individualized Vaccines for Cancer targeting SNVs in the CT26 colon carcinoma and 4T1 mammary carcinoma tumor models. Moreover, they show that SNVs are frequently immunogenic and that the majority of SNVs are recognized by $CD4^+$ T cells rather than $CD8^+$ T cells.

3.1.2 Immunogenicity of Indels and Gene Fusions

As single nucleotide variants are the most abundant cancer mutations, research so far has focused mainly on this subtype. Mutations that introduce long amino acid stretches are even more interesting from an immunological point of view, as they may simultaneously harbor multiple T-cell neoepitopes. For this reason, the prevalence and immunogenicity of two other types of mutations, namely small cancer-associated insertions and deletions (indels) and gene fusions were additionally investigated as targets for personalized cancer vaccination. Indels and fusions were identified in the NGS data of three murine tumor models (Table 3.1b and c). Sanger sequencing of cDNA (fusions) or genomic DNA (indels) was used for validation of the mutation on the sequence level. To investigate the mutations with regard to their potential to elicit immune responses *in vivo*, experiments in mice were conducted (Figure 1.8). To this end, a vaccine for each of the mutations selected for immunogenicity assessment was engineered using antigen-encoding pharmacologically optimized lipoplexed RNA as vaccine format. In-frame indel and fusion mutations were flanked by 15 amino acids of wild-type sequence and frameshift mutations were elongated with 15 wild-type amino acids at the 5' end (Figure 3.4).

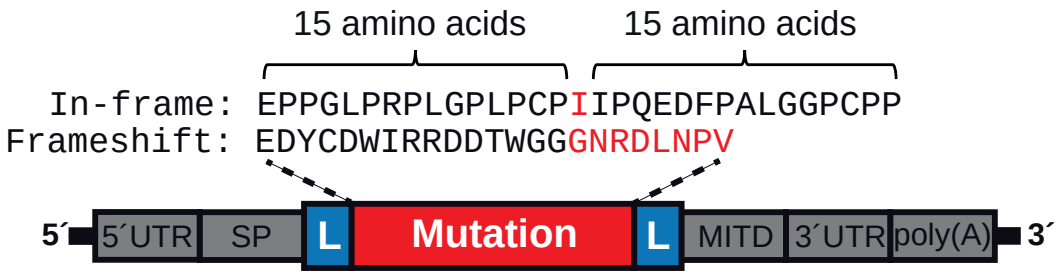

Abbildung 3.4: Structure of vaccine RNA encoding indel or gene fusions. RNA encoded for mutated amino acids including 15 flanking amino acids in case of indel or gene fusions that resulted in an in-frame mutation. In case of frameshift mutations, 15 amino acids were added at the 5' end of the novel amino acids. Red: novel amino acids, black: wild-type amino acids, UTR: untranslated region, SP: signal peptide, L: linker, MITD: MHC class I trafficking signal.

First, we focused on indel mutations that cause the translation of novel amino acids and mined the sequence data of all three mouse tumor model systems accordingly (Table 3.1b). The sequencing reads were realigned the to the detected non-synonymous indel mutation sites in order to improve the local alignment by simultaneously using a mutated reference genome containing the indel and the wild-type reference. This step also allowed for the determination of the presence of the indels on an RNA level. Only the indels that were confirmed by the RNA sequencing data were processed further. In the case of the CT26 model, expression of the genes with the detected indels was determined afterwards (analysis by Martin Löwer). In total, 13 somatic indel mutations in expressed genes in the B16F10 melanoma model, 10 in CT26 colon cancer and 3 in 4T1 breast cancer were identified and validated by Sanger sequencing (Table 3.1 b, Table 3.4). 10 of these were insertions and 16 were deletions. The number of novel amino acids generated by these events ranged from 0 to 158, with a median of 9 new amino acids. The majority of indels led to frameshift mutations by insertion or deletion of a single nucleotide (Table 3.4). An example of this is featured by event B16_IND09 detected in the

B16 melanoma model, which affected gene Klf6 (Kruppel-like factor 6) on chromosome 13, where the insertion of one nucleotide into the coding region resulted in a frameshift mutation (Figure 3.5). As a consequence, 12 new amino acids were translated until a stop codon was finally reached. In two indel events, the reading frame was maintained as three nucleotides were inserted and therefore only one amino acid was added (B16_IND03, 4T1IND_01).

Table 3.4: Validated indel mutations. Indels were identified in NGS data and confirmed via Sanger sequencing. MHC class I or II binding prediction was performed with IEDB consensus V2.13. Immunogenicity was determined after RNA vaccination via IFN-γ ELISpot as described in section 2.2.2.3.

Indel	Gene symbol	Nucleotide change	Number of new aa	MHC I score (best prediction)	MHC II score (best prediction)	Immunogenic
B16_IND01	Dync1h1	-A	63	0.55	6.92	-
B16_IND02	Tbcd	-A	3	15	40.09	-
B16_IND03	Zfp598	+CAT	1	1.3	9.71	+
B16_IND04	Nipbl	+T	4	32	85.58	-
B16_IND05	Yod1	+G	8	2.1	60.59	-
B16_IND06	Dync2h1	+T	1	41.5	55.81	-
B16_IND07	Prtg	+C	158	0.2	0.65	+
B16_IND08	Col4a2	+C	68	1.7	5.49	-
B16_IND09	Klf6	+G	12	6.2	50.17	-
B16_IND10	Wdr33	+A	5	33	59.67	-
B16_IND11	Th1l	-T	0	5.7	72.94	-
B16_IND12	Cilp	-G	15	0.2	8.85	-
B16_IND13	Amotl2	-C	25	0.2	4.42	+
CT26_IND01	Pex3	-T	41	0.2	1.85	-
CT26_IND02	Man1a	-G	3	7.9	53.78	-
CT26_IND03	Fbxo48	-A	4	413	47.05	-
CT26_IND04	Nipsnap1	-C	44	0.5	23.18	+
CT26_IND05	Ewsr1	-C	27	0.4	8.33	-
CT26_IND06	Kcnma1	-T	6	2.35	37.65	-
CT26_IND07	Cyp2c65	-G	28	0.65	1.01	-
CT26_IND08	Ufl1	-ACTA	17	2.7	26.23	-
CT26_IND09	Auts2	-G	1	5	40.67	+
CT26_IND10	Lrrc49	-T	3	0.3	33.46	-
4T1_IND01	Mrpl37	+GAT	1	0.2	34.11	-
4T1_IND02	Man2a1	-T	34	0.3	5.70	+
4T1_IND03	Rnpep	+A	9	0.1	15.31	+

In order to analyze if the translation products of indel mutations can be recognized by T cells, mice were vaccinated with mutation-encoding RNA (10 from CT26, 13 from B16F10 and 3 from 4T1) and tested for the induction of a T-cell response via ELISpot as described in section 3.1.1.

This is exemplified for indel B16_IND07, which is the insertion of a single cytosine at the Prtg (protogenin homolog) locus, resulting in 158 novel amino acids in the translation product. The sequence contained both MHC class I, as well as MHC class II predicted candidate epitopes, as determined by the IEDB consensus algorithm. In a first step, putative neo-epitopes were narrowed down. Accordingly, peptide pools of 15-mer peptides overlapping for 11 amino acids and covering the entire stretch of 158 novel amino acids were used in an IFN-γ ELISpot to test for recognition by splenocytes of immunized mice (Figure 3.6a). Significant effector responses were detected against partially over-

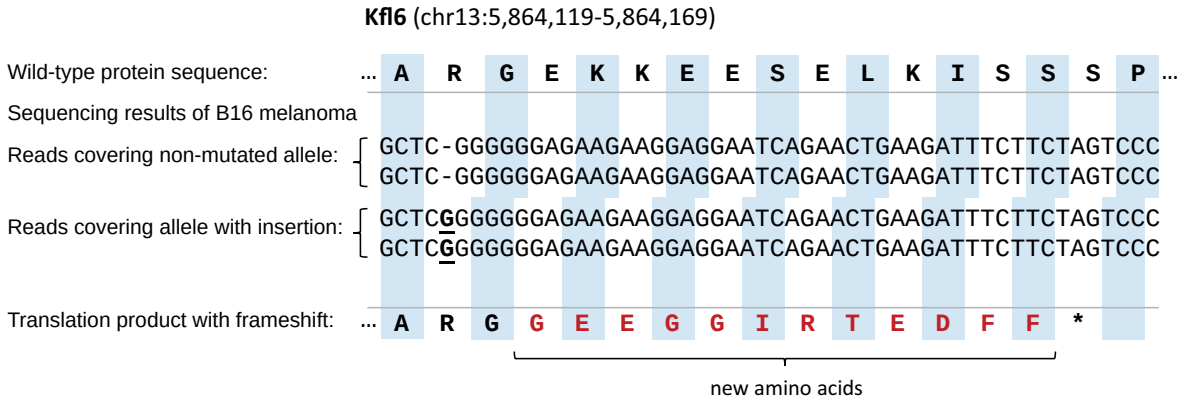

Figure 3.5: Exemplary effect of an indel mutation. Depiction of the insertion (underlined) detected at the Kfl6 locus in B16F10 melanoma and its effect on the translation product containing twelve new amino acids (red, *: stop codon).

lapping peptide pools 9 and 10 and against peptide pool 1 that does not overlap with the two other pools.

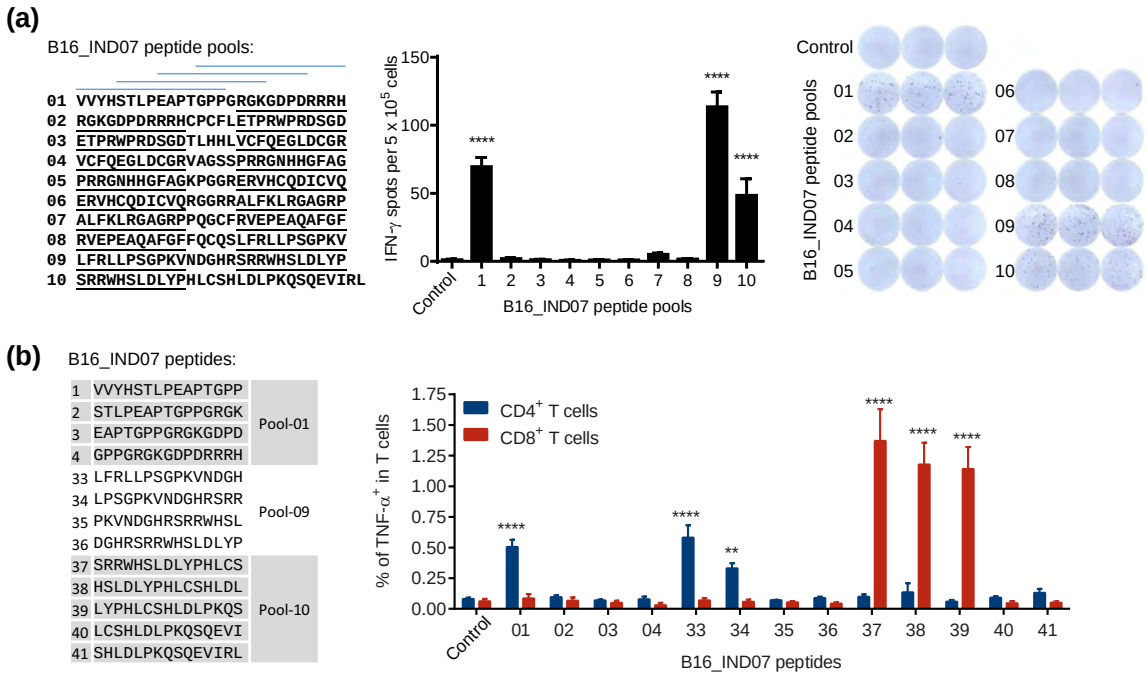

Abbildung 3.6: Immunogenicity testing of B16_IND07. a, Splenocytes of B16_IND07 RNA vaccinated C57BL/6 mice were tested via IFN-γ-ELISpot for recognition of irrelevant peptide (VSV-NP_{52-59}, control) or overlapping peptide pools (overlap underlined) consisting each of four (pools 1-9) or five (pool 10) 15-mer peptides as indicated by the blue horizontal lines and covering the complete B16_IND07 sequence (n=5, mean+s.e.m.). **b,** Intracellular TNF-α staining and T-cell subtyping was performed after stimulation of splenocytes with an irrelevant peptide (VSV-NP_{52-59}, control) or indicated 15-mer peptides of responding peptide pools (n=3, mean+s.e.m.). Definition of the minimal $CD8^+$ T-cell epitope. Overlapping 9-mer peptides and the best predicted 8-mer sequence were tested for induction of IFN-γ secretion via ELISpot. Mean+s.e.m. is shown.

In a second step, the peptide pools were deconvoluted and each single 15-mer peptide was tested for recognition by the induced immune response via intracellular flow cytometric staining of TNF-α

(Figure 3.6b). This approach allowed confirmation of T-cell reactivity by an orthogonal assay as well as differentiation between $CD4^+$ and $CD8^+$ T cells. $CD4^+$ T-cell reactivities against peptide 01 and against overlapping peptides 33, 34 as well as $CD8^+$ T-cell reactivities against overlapping peptides 37, 38, 39 were revealed. The 8-mer peptide SLDLYPHL was identified as minimal epitope for the neo-antigen-specific $CD8^+$ T-cell response, which had been predicted by the IEDB consensus MHC binding algorithm (Figure 3.7). Altogether, 26 indels were screened for recognition by T cells, of which 7 (27 %) were found to be immunogenic (Figure 3.10, Table 3.4).

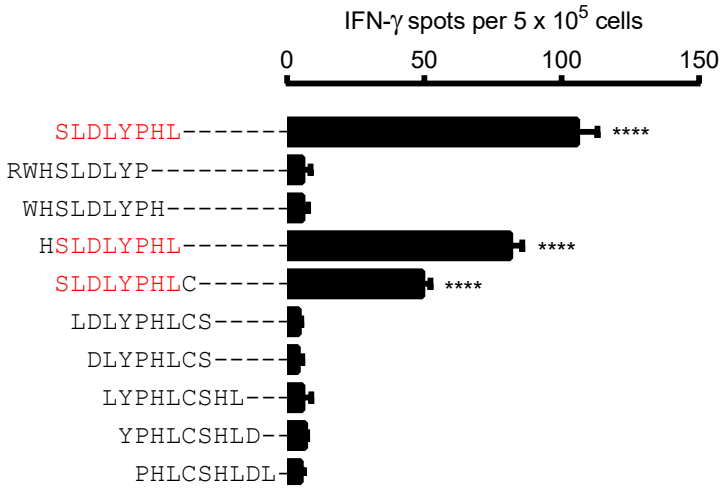

Abbildung 3.7: Definition of the minimal $CD8^+$ T-cell epitope of B16_IND07. Overlapping 9-mer peptides and the best predicted 8-mer sequence were tested for induction of IFN-γ secretion by splenocytes of a B16_IND07 RNA vaccinated C57BL/6 mouse via ELISpot. Mean+s.e.m. of triplicates are shown.

Next, we focused on gene fusions in paired-end RNA sequencing data of CT26 colon cancer using the deFuse algorithm, which uses discordantly aligned paired-end RNA-Seq reads to detect fusion events and reads with split alignment to the two fusion partners to determine the fusion breakpoint [168] (analysis by Martin Löwer). In total, deFuse revealed 1604 predicted potential fusion events in the CT26 tumor transcriptome data with predicted probabilities between 0.01 and 0.98. Only 164 predictions were reported with a probability of >0.66 and 11 of these events were selected for validation by Sanger sequencing. Five of these 11 were clearly validated as somatic fusion mutations (Figure 3.1c), while one predicted fusion event was not somatic and the Sanger results of the remaining fusion sites were inconclusive. One example is the fusion event CT26_F05 of the genes Reep5 (receptor accessory protein 5) and Pkd2l2 (polycystic kidney disease 2-like 2) (Figure 3.8, Table 3.5). In this case an originally intronic sequence derived from the Pkd2l2 locus was aberrantly translated and a frameshift was induced. This resulted in a stretch of eight somatically altered amino acids predicted to contain a $CD8^+$ T-cell epitope (Table 3.5).

In order to analyze if the translation products of fusion mutations can be recognized by T cells, cohorts of three BALB/c mice were vaccinated for each fusion mutation. For two of the five tested mutations (40 %, Figure 3.10), CT26-F01 and CT26-F03, specific immune responses against the respective fusion mutation were detected in the vaccinated mice (Figure 3.9, Table 3.5). CT26-F1 is

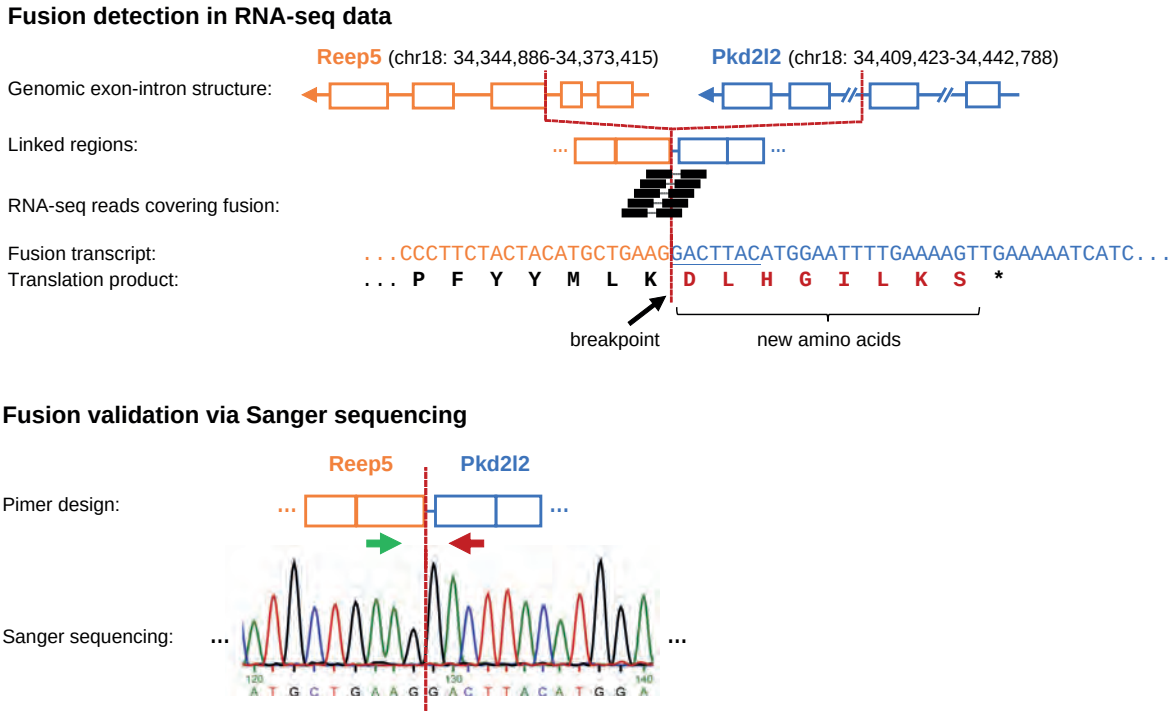

Figure 3.8: Exemplary detection and validation of of a gene fusion. Reep5-Pkd2l2 fusion detected in CT26 RNA-seq data. As a result of the fusion event a short intronic sequence (underlined in the fusion transcript sequence) was translated to a stretch of eight new amino acids (red, *: stop codon). Primers (green and red arrows) for validation of the detected fusions by Sanger sequencing were located at least 50 bp up- and downstream of the assumed fusion site (red dashed line) to generate 100-400 bp amplicons.

the fusion event of Btbd8 (BTB (POZ) domain containing 8) and A830010M20Rik (RIKEN cDNA A830010M20 gene) resulting in nine novel amino acids. The peptide CT26-F1.2, which contained six novel amino acids, provoked a strong T-cell response. CT26-F03, which is the fusion of Ezh2 (enhancer of zeste homolog 2) and A930035D04Rik (RIKEN cDNA A930035D04 gene) leads to 32 novel amino acids. A significant T-cell response was found against peptides CT26-F3.5 and CT26-F3.6 that solely encode for new amino acids.

Table 3.5: Validated fusion mutations. Fusions were identified in NGS data sets and confirmed by Sanger sequencing and PCR. MHC class I or II binding prediction was performed with IEDB consensus V2.13. Immunogenicity was determined by vaccinating mice with RNA encoding the respective mutations and assessment of induced T-cell responses in an IFN-γ ELISpot as described in section 2.2.2.3.

Fusion	Gene symbol 1	Gene symbol 2	Number of new aa	MHC I score (best prediction)	MHC II score (best prediction)	Immunogenic
CT26_F01	Btbd8	A830010M20Rik	9	0.8	0.94	+
CT26_F02	Acot7	Nphp4	9	0.8	17.21	-
CT26_F03	Ezh2	A930035D04Rik	32	0.4	0.66	+
CT26_F04	Arhgap26	Gm15337	1	13	99.00	-
CT26_F05	Reep5	Pkd2l2	8	0.2	17.96	-

The data in this section demonstrate that indels and gene fusions can be identified via NGS for personalized cancer immunotherapy. They are frequently immunogenic and can provide clusters of T-cell neo-epitopes.

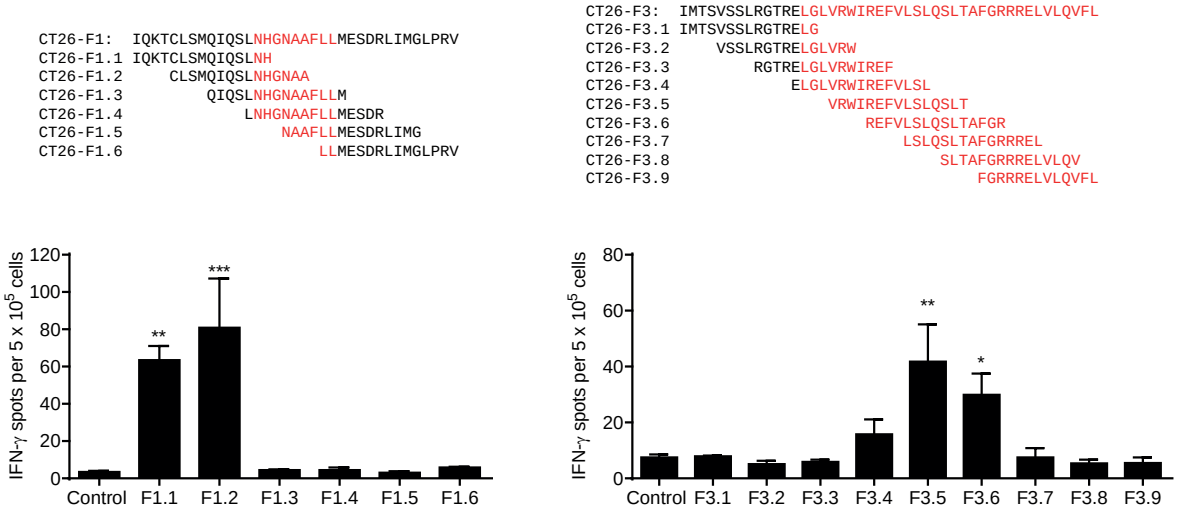

Abbildung 3.9: Immunogenicity testing of gene fusions CT26-F1 and CD26-F3. BALB/c mice (n=3) were vaccinated with RNA encoding fusion mutations. Splenocytes of immunized mice were tested *ex vivo* in an IFN-γ ELISpot for recognition of medium alone (control) or 15-mer peptides covering the vaccinated sequence.

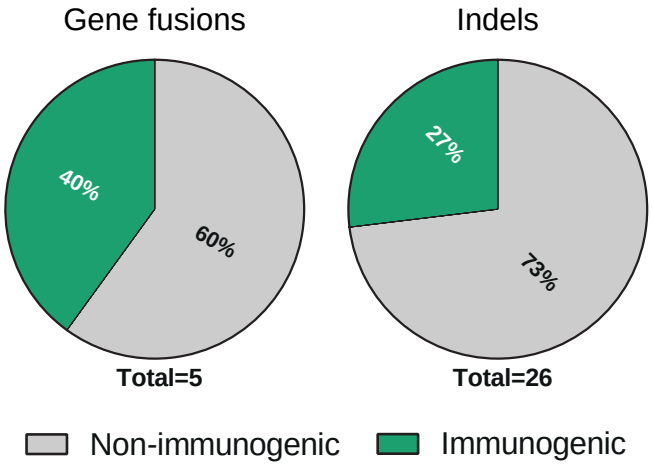

Abbildung 3.10: Prevalence of immunogenic indels and fusions.

3.2 Anti-Tumoral Efficacy of RNA based Neo-Epitope Vaccines

3.2.1 Monotope RNA Vaccine

CT26 colon carcinoma

In section 3.1, it was shown that tumor mutations are frequently immunogenic and that the majority of neo-epitope directed T cells are $CD4^+$. To investigate whether MHC class II-restricted cancer mutations are good vaccine targets *in vivo*, CT26-M90 was selected for a first therapeutic tumor experiment. As shown in Figure 3.11, CT26-M90 is highly expressed in the CT26 tumor. Stimulation of splenocytes with mutated peptide or RNA electroporated BMDC results in strong (>150 spots) T-cell responses. Moreover, T-cell responses against CT26-M90 were found after treatment of subcutaneous CT26-WT tumor bearing mice with an TLR7 agonist but not in untreated or irrelevant RNA treated mice (Supplementary Figure 5.1).

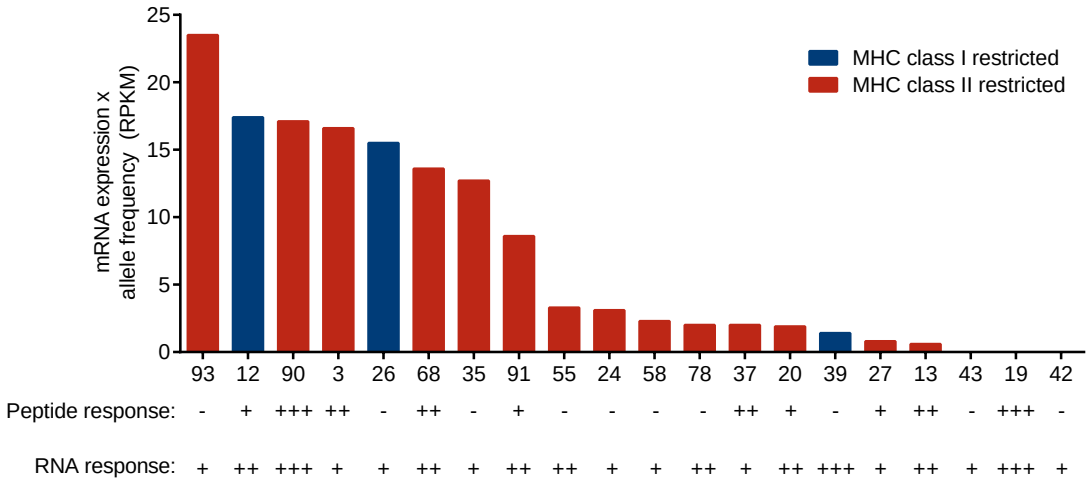

Abbildung 3.11: Immunogenicity and abundance of mutation-encoding transcripts in CT26. Expression levels of the mutated alleles of immunogenic CT26 mutations determined as RNA expression multiplied with the allele frequency of mutated RNA in reads per kilobase per million mapped reads (RPKM). Below, the strength of the T-cell response of splenocytes from RNA monotope vaccinated mice after stimulation with mutated peptides (Peptide response) or RNA electroporated BMDC (RNA response) as measured by ELISpot is anotated. 10<+<50, 50<++<100, +++>150 spots.

Subsequently, luciferase transgenic CT26 cells (CT26-Luc) were injected IV into the tail vain of naive BALB/c mice resulting in formation of tumor nodules in the lungs. Tumor growth was monitored regularly via *in vivo* bioluminescence imaging (BLI) of living animals vaccinated therapeutically with CT26-M90 RNA, irrelevant RNA or mice that were left untreated. Tumor growth measured as emitted photons per second (total flux, p/s) in mice treated with CT26-M90 RNA was significantly retarded compared to control animals (Figure 3.12, lower left and upper right). About two thirds of the neo-epitope RNA treated animals were still alive at day 110, while 80 % of control RNA treated mice died by day 50 (Figure 3.12, lower right).

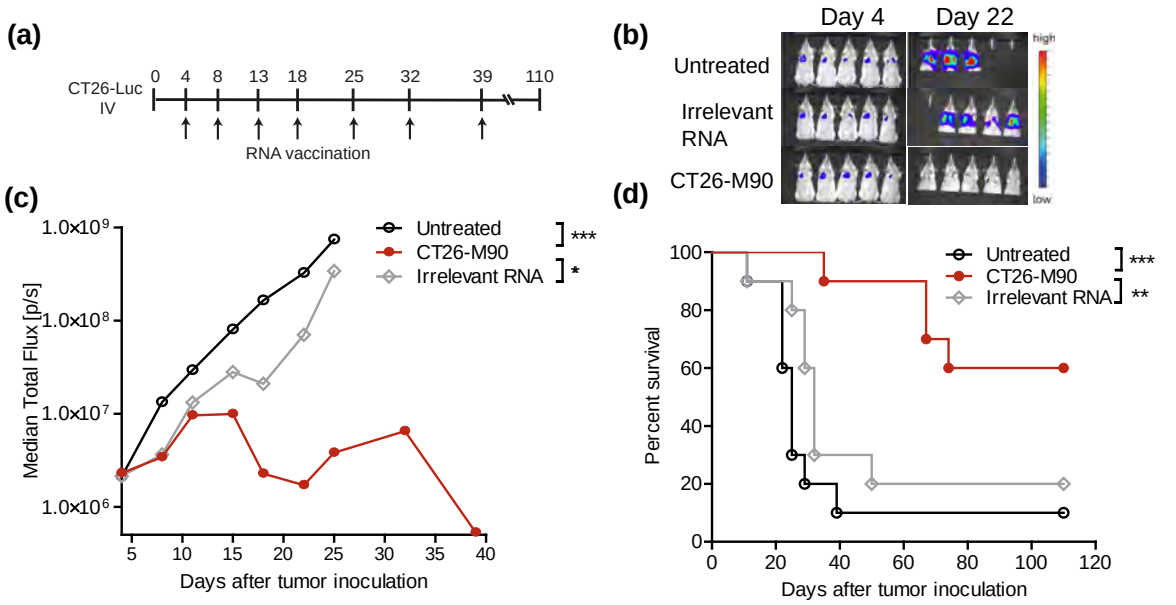

Figure 3.12: Efficient tumor control and survival benefit with an RNA vaccine encoding a single mutated CD4$^+$ T-cell epitope. BALB/c mice (n=10) developing lung metastases upon IV injection of CT26-Luc were treated with CT26-M90 or irrelevant RNA (SIINFEKL) or left untreated. The treatment shedule (**a**), exemplary BLI measurements (**b**) as well as the median tumor growth by BLI (**c**) and survival data (**d**) are shown.

Surviving CT26-M90 RNA treated mice showed strong memory T-cell responses 71 days after the last vaccination (110 days after tumor inoculation, Figure 3.13a). These mice were protected from a subsequent IV tumor challenge with CT26-WT cells as shown by reduced number of tumor nodules and lung weight as well as prolonged survival (Figure 3.13b).

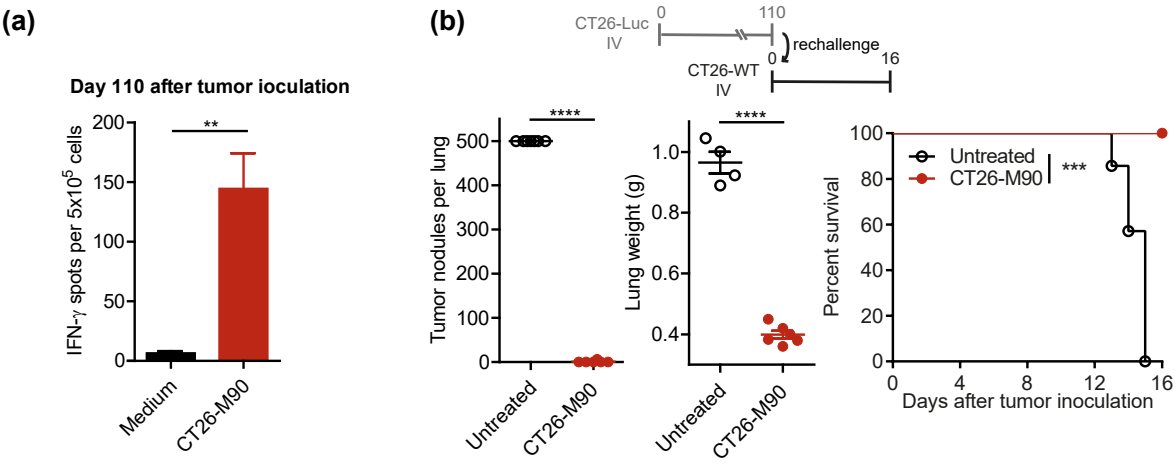

Figure 3.13: RNA vaccination against neo-epitopes induces long lasting T-cell memory and protection against a tumor rechallenge.a, CT26-M90 specific T-cell responses measured via ELISpot in the blood of surviving, CD26-M90 vaccinated mice (n=5) from the experiment shown in Figure 3.12 110 days after tumor inoculation (71 days after the last vaccination, mean ± s.e.m.). **b,** Tumor nodules per lung (mean ± s.e.m.), lung weight (mean ± s.e.m.) and survival of untreated mice (n=7) or survivors from the experiment shown in Figure 3.12 (n=6) after IV rechallenge with CT26-WT cells are depicted.

4T1 mammary carcinoma

Similarly to mutanome vaccination in the CT26 tumor model, monotope RNA vaccines were able to confer tumor control in the 4T1 tumor model. From the three tested monotope vaccines, therapeutic immunization of 4T1 tumor bearing BALB/c mice against 4T1-M31 and 4T1-M35 resulted significant reduction in tumor growth measured via BLI. However, tumor growth reduction was inferior compared to the CT26 tumor model confirming the general notion that 4T1 is a tough model for cancer immunotherapy (see section 4.3).

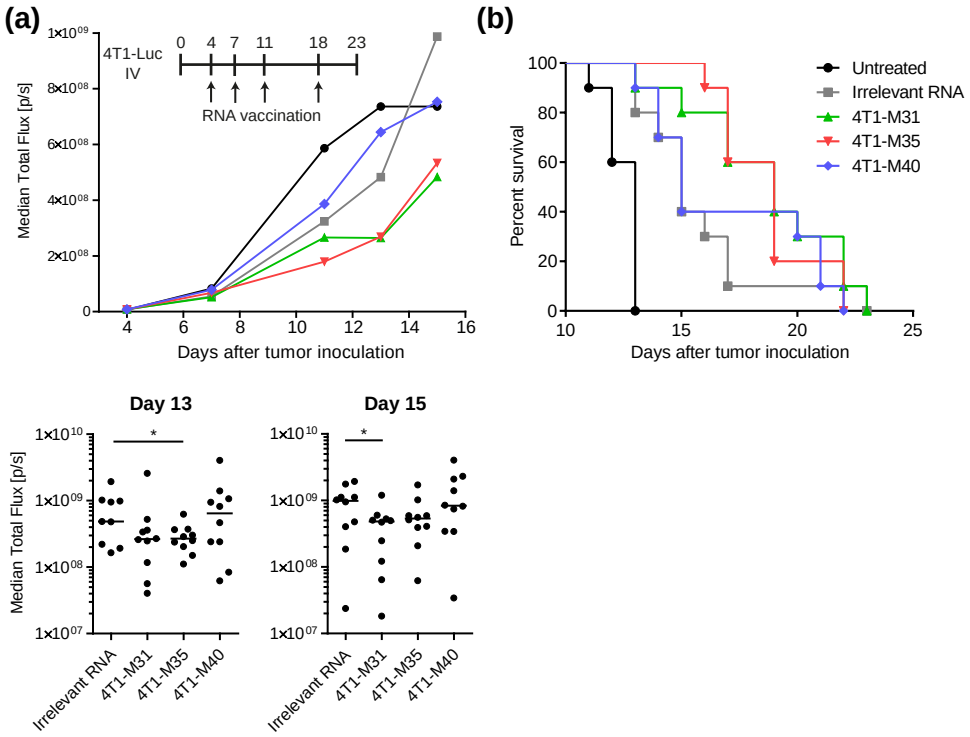

Figure 3.14: Mutanome vaccination in the 4T1-Luc tumor model. BALB/c mice (n=10) were inoculated IV with CT26-Luc tumor cells and left untreated or injected with irrelevant SIINFEKL or mutanome RNA. Tumor growth (BLI measurements, **a)** and survival data (**b)** are shown.

B16F10 melanoma

Anti-tumoral efficacy of RNA vaccines targeting B16F10 derived SNVs conferred therapeutic efficacy as shown by Sahin et al. [49,50]. To test whether vaccination against the identified immunogenic indels B16_IND03 and B16_IND07 could delay tumor growth, we performed therapeutic vaccination of B16F10 tumor bearing mice (Figure 3.15). Surprisingly, no anti-tumoral effect of vaccination against the two immunogenic indels could be detected. Subsequent analysis revealed that the expression of the mutated allele of B16_IND07 but not the wilde type allele was very low to absent (data not shown). B16_IND07, in comparison to B16_IND03, was highly immunogenic and contained several T-cell epitopes (Figure 3.6).

The data shown in this section demonstrate that RNA vaccination against a single neo-epitope can induce efficient tumor control, survival benefit and T-cell memory in mouse tumors.

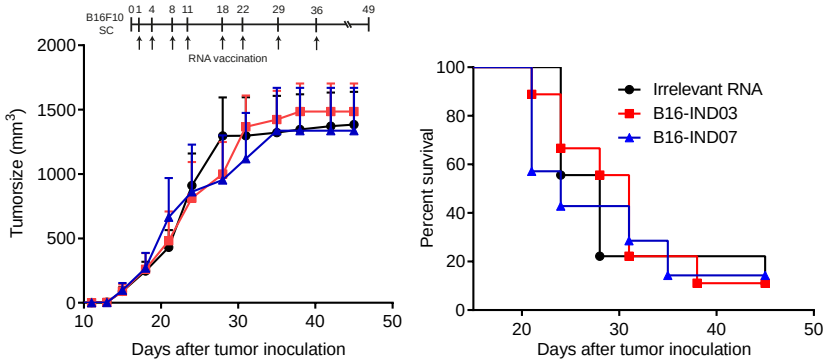

Figure 3.15: Therapeutic vaccination against B16-IND03 and -IND07. C57BL/6 mice (n=10) were inoculated SC with B16F10 tumor cells and injected with irrelevant VSV-NP_{52-59} or mutanome RNA. Tumor growth (mean + s.e.m.) and survival is depicted.

3.2.2 Pentatope RNA Vaccine

Even though tumor eradication was achieved in mice with a single mutation, to combine several mutations would be preferable to address tumor heterogeneity and immune editing, which could be factors leading to clinical failure of vaccines in humans [21, 146, 169–171]. Therefore, RNA monotopes encoding four MHC class II (CT26-M03, CT26-M20, CT26-M27, CT26-M68) and one MHC class I (CT26-M19) restricted mutation from the CT26 model (Table 3.3) and a synthetic RNA pentatope encoding all five neo-epitopes connected by 10-mer non-immunogenic glycine/serine linkers were engineered. In naive BALB/c mice the quantity of IFN-γ-producing T cells elicited by the pentatope was comparable (3 of 5) or even higher than that evoked by the respective monotope (Figure 3.16).

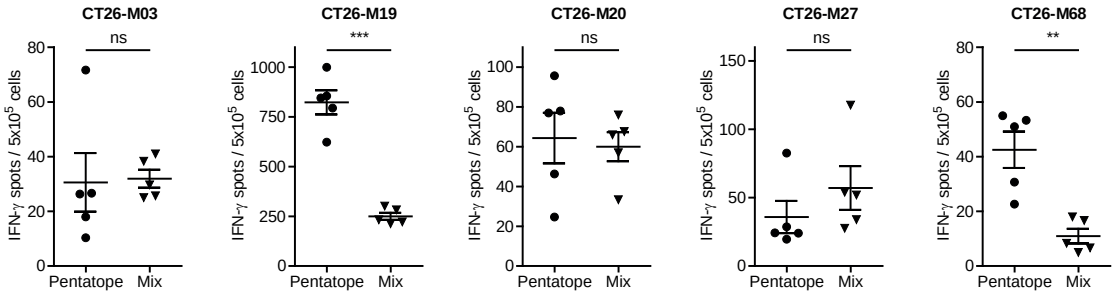

Figure 3.16: RNA pentatopes can induce stronger T-cell responses compared to RNA monotopes. BALB/c mice (n=5) were vaccinated either with pentatope (35 µg) or the corresponding mixture of five RNA monotopes (7 µg each). T-cell responses in peptide stimulated splenocytes of mice were measured *ex vivo* via ELISpot (medium control subtracted mean ± s.e.m.).

In BALB/c mice with CT26-Luc lung metastases vaccinated repeatedly with a mixture of two RNA pentatopes (3 MHC class I and 7 class II restricted epitopes, Supplementary Table 3.6) including the mutations tested in the previous experiment, tumor growth was significantly inhibited as revealed by luminescence imaging (Figure 3.17). At day 32, all mice in the RNA pentatope group were alive whereas 80 % of the control mice had already died.

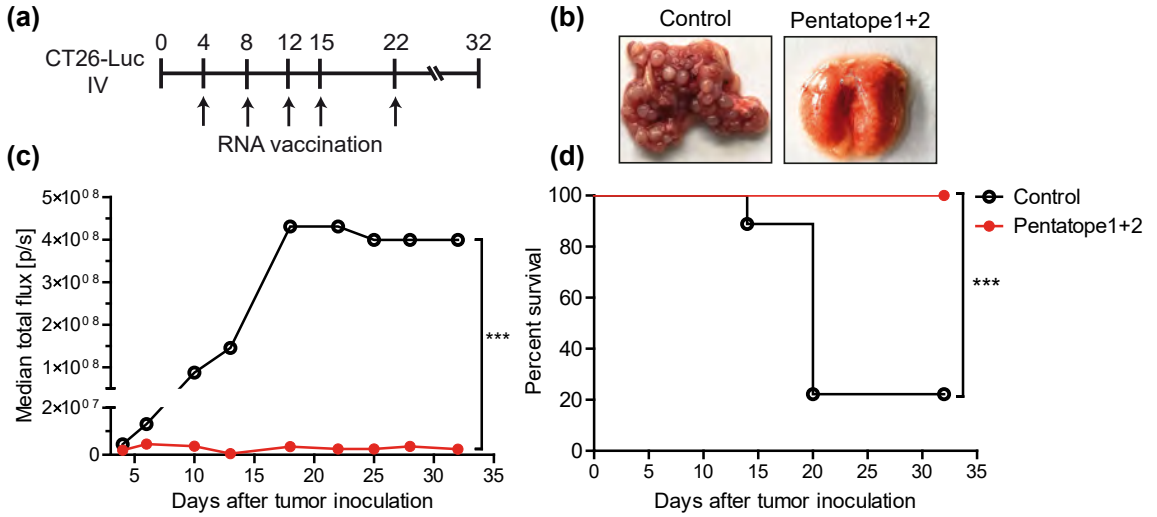

Figure 3.17: RNA pentatope immunization confers disease control and survival benefit in murine tumors. BALB/c mice (n=10) developing lung metastases upon IV injection of CT26-Luc were treated with a mixture of two pentatopes or left untreated (control). The treatment shedule (**a**), exemplary lungs from treated animals (**b**) as well as the median tumor growth by BLI (**c**) and survival data (**d**) are shown.

Table 3.6: CT26 mutated epitopes encoded in pentatope 1 and 2. Ten immunogenic mutated epitopes were used for generation of two pentatopes employed for therapeutic vaccination shown in Figure 3.17. WT, wild type; AA#, position of mutated amino acid; Mut, Mutation.

Pentatope	Mutation	Gene	Mutated sequence used for vaccination	Substitution (WT, AA#, Mut)	Reactive T cell subtype
1	CT26-M19	Tmem87a	QAIVRGCSMPGPWRSGRLLVSRRWSVE	G63R	$CD8^+$
1	CT26-M39	Als2	GYISRVTAGKDSYIALVDKNIMGYIAS	L675I	$CD8^+$
1	CT26-M13	Nphp3	AGTQCEYWASRALDSEHSIGSMIQLPQ	G234D	$CD4^+$
1	CT26-M55	Dkk2	EGDPCLRSSDCIDEFCCARHFWTKICK	G192E	$CD4^+$
1	CT26-M68	Steap2	VTSIPSVSNALNWKEFSFIQSTLGYVA	R388K	$CD4^+$
2	CT26-M20	Slc4a3	PLLPFYPPDEALEIGLELNSSALPPTE	T373I	$CD4^+$
2	CT26-M26	E2f8	VILPQAPSGPSYATYLQPAQAQMLTPP	I522T	$CD8^+$
2	CT26-M03	Slc20a1	DKPLRRNNSYTSYIMAICGMPLDSFRA	T425I	$CD4^+$
2	CT26-M37	Dhx35	EVIQTSKYYMRDVIAIESAWLLELAPH	T646I	$CD4^+$
2	CT26-M27	Agxt2l2	EHIHRAGGLFVADAIQVGFGRIGKHFW	E247A	$CD4^+$

Dissection of the anti-tumor activity of single RNA pentatopes in the CT26 model revealed that RNA pentatope 2 has a very strong anti-tumor activity, whereas pentatope 1 is modestly active (Figure 3.18). CT26-M19, the immune dominant MHC class I restricted T-cell epitope encoded on pentatope 1, however, does not control tumor growth on its own.

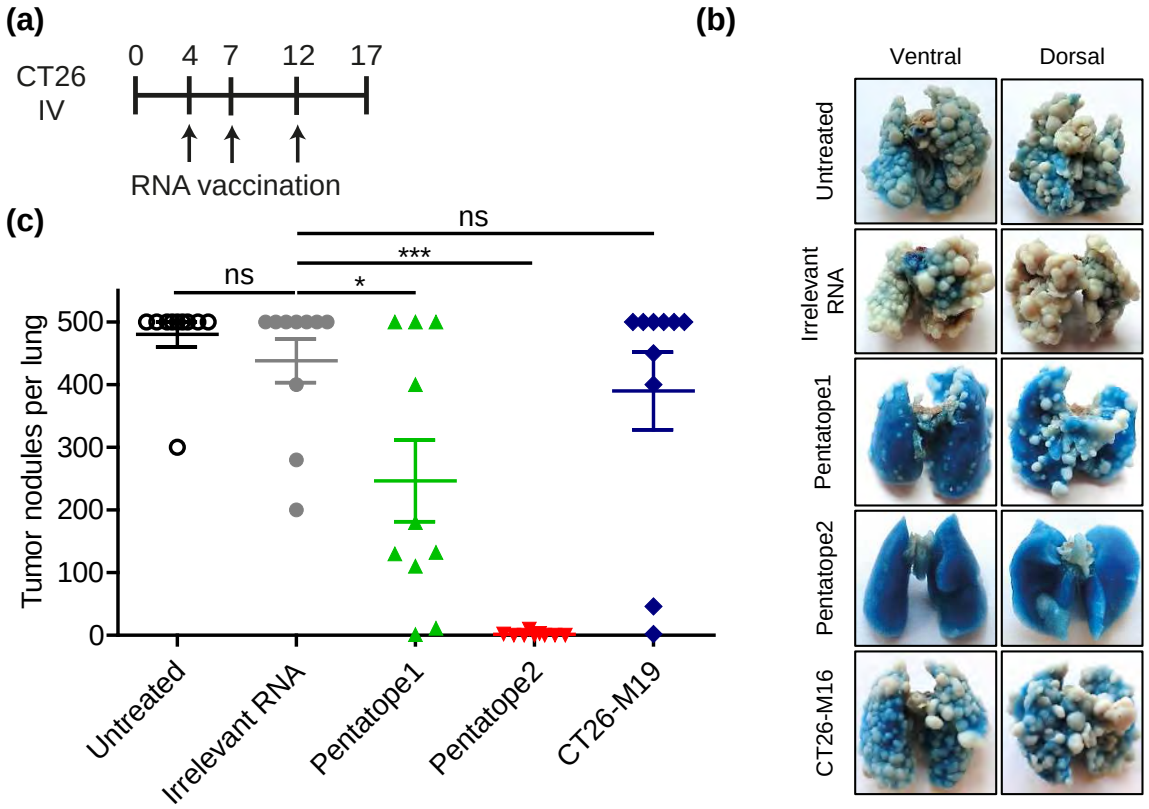

Figure 3.18: Pentatope 2 vaccination demonstrates a strong anti-tumoral effect. BALB/c mice (n=10) were inoculated IV with CT26 tumor cells and left untreated or injected with Pentatope 1, Pentatope 2, CT26-M19 or irrelevant (empty vector) RNA. The treatment shedule (**a**), exemplary ink-stained lungs from treated animals (**b**) as well as the number of tumor nodules per lung (mean ± s.e.m.) (**c**) are shown.

Dissecting the individual contribution of the neo-epitope specific T cells induced by pentatope 2 indicated that the combined vaccination rather than a single dominant response was responsible for the potent anti-tumoral effect (Figure 3.19). Whereas pentatope 2 vaccination induced strong tumor growth inhibition (tumor nodules per lung below the median of irrelevant RNA treated animals) in 10 of 10 mice, tumor growth control was comparably weak in CT26-M03 (6/10 mice), CT26-M20 (5/10 mice) and CT26-M37 (7/10 mice) vaccinated mice. CT26-M27 and -M26 vaccination alone did not induce tumor control probably due to induction of a rather weak immune response (Figure 3.11).

These data show that RNA pentatopes efficiently induce several neo-epitope specific T-cell responses simultaneously. RNA pentatope immunization confers disease control and survival benefit in murine tumors which, in the case of pentatope 2, results from the induction of several rather than one dominant neo-epitope specific T-cell responses.

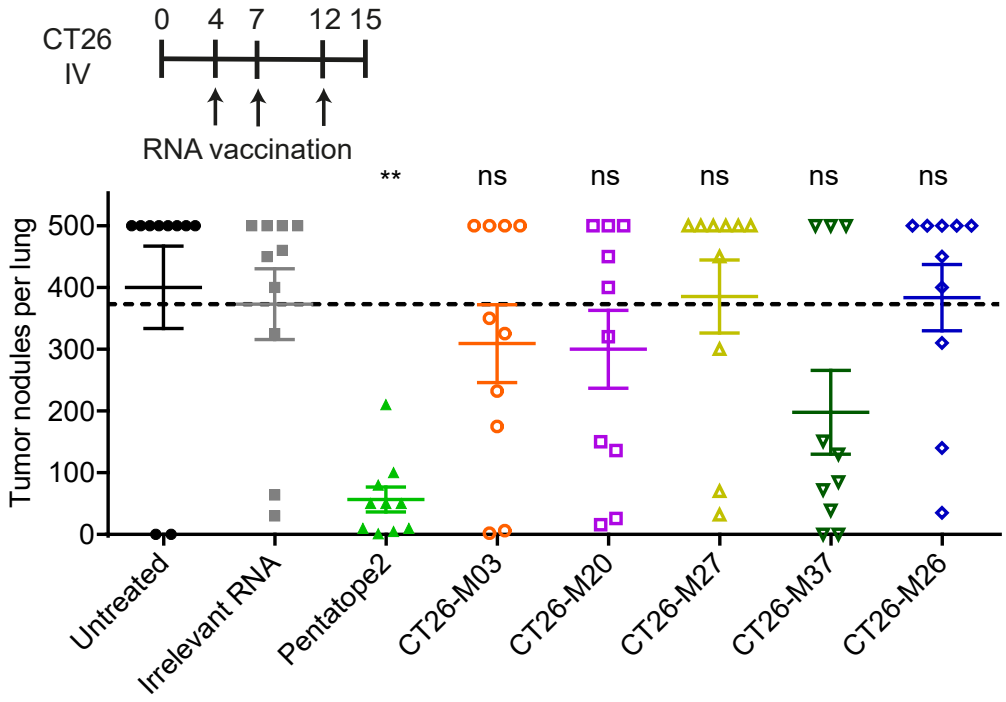

Figure 3.19: The anti-tumoral potency of pentatope 2 is a result of serveral neo-epitope specific T-cell responses. BALB/c mice (n=10) injected IV with CT26 cells were left untreated or injected with indicated RNAs (control: empty vector RNA). The number of tumor nodules per lung (mean ± s.e.m.) are shown. The dashed line represents the median number of tumor nodules measured in the irrelevant RNA group.

3.2.3 Mode of Action of a CD4 T-Cell Vaccine in the CT26 tumor model

It was shown that most immunogenic neo-epitopes are recognized by $CD4^+$ T-cells (Figure 3.2) and that therapeutic vaccination against one MHC class II restricted mutation conferred tumor control in CT26 (Figure 3.12). In addition, vaccination against five different mutations, 4 of 5 of which are MHC class II restricted, showed as well strong anti-tumoral efficacy (Figure 3.18 and 3.19). Whereas $CD8^+$ T-cells are known to directly kill tumor cells, the mode of action of anti-tumoral $CD4^+$ T-cells is less obvious. As described in section 1.2.1, $CD4^+$ T cells can mediate tumor control through activation of other cell types including macrophages, NK cells, B cells, DCs and $CD8^+$ T cells or act on tumor cell survival by intratumoral secretion of inflammatory cytokines like IFN-γ [157, 172, 173]. Moreover, direct killing of MHC class II positive tumor cells by $CD4^+$ T cells has been shown [174]. In order to gain insights into the mode of action of neo-epitope-specific $CD4^+$ T cells in CT26, the intratumoral composition of cell types after RNA vaccination was dissected. Lung sections of pentatope 2 or irrelevant RNA treated mice from Figure 3.18 were analyzed by immunofluorescence. Quantification of tumor area in tumor bearing animals (tumor free animals were excluded for analysis) confirmed the anti-tumoral effect of pentatope 2 (Figure 3.20). In addition, a significant increase of $CD4^+$ and $CD8^+$ T cells in tumor lesions of RNA pentatope 2 immunized mice and a lower FoxP3 to CD4 ratio ($FoxP3^+$, $CD4^+$ T-cells are T_{regs}) was found compared to tumors of mice treated with irrelevant RNA.

These findings were confirmed in independent experiments analyzing the lung tumors of mice shown in Figure 3.17b via immune histochemistry. An increased T-cell infiltration and a decreased FoxP3 to

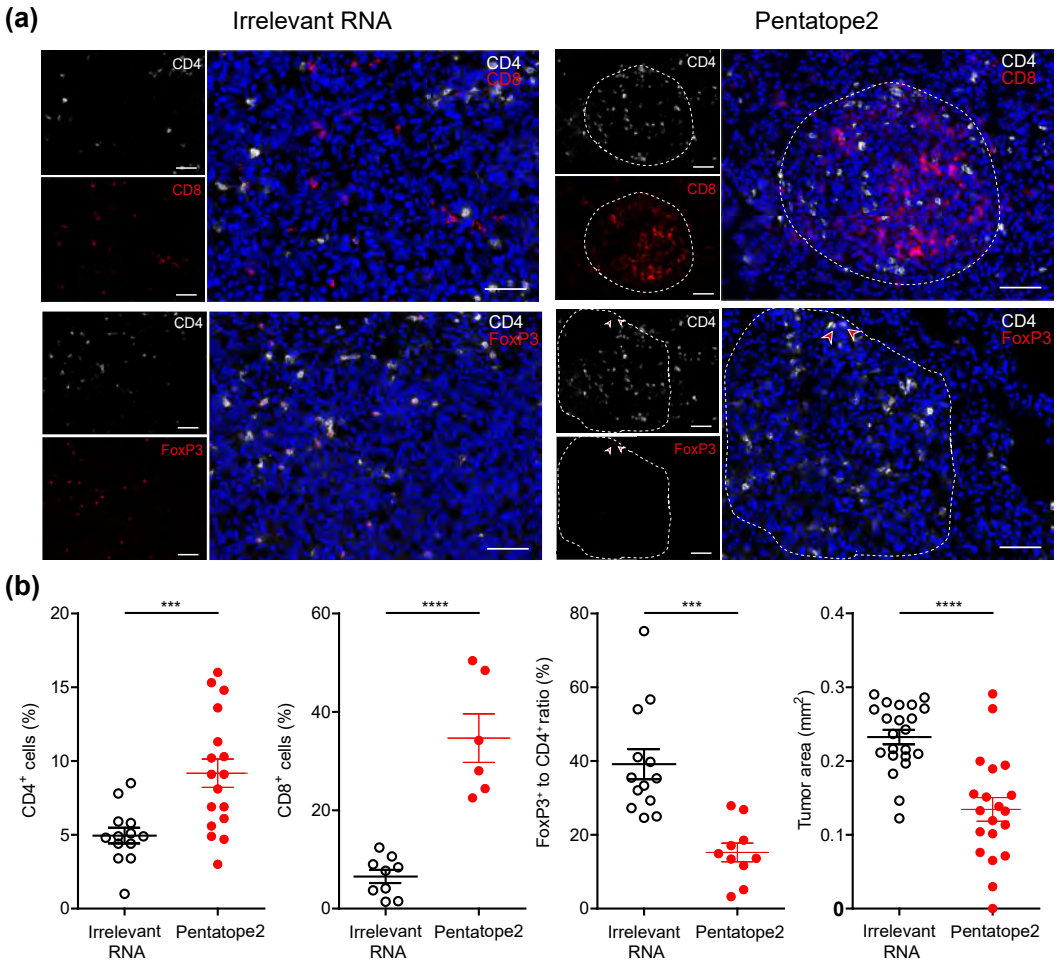

Figure 3.20: Immunofluorescence analysis of tumor infiltrating lymphocytes in pentatope2 vaccinated mice. a, lung tumor tissue harvested 17 days after tumor inoculation (see also Figure 3.18) and stained for CD4 and CD8 or CD4 and FoxP3. Scale bar: 50 µm. **b,** left, proportion of infiltrating cells in sections of irrelevant (CD4: n=13; CD8=9; FoxP3: n=13) or pentatope RNA (CD4: n=17; CD8: n=6; FoxP3: n=10) treated animals. Right, tumor area in sections of control (empty vector RNA, n=22) and pentatope2 (n=20) treated animals (mean ± s.e.m.).

CD4 ratio and tumor area was found accordingly (Figure 3.21).

We next analyzed the contribution of $CD4^+$ T cells, $CD8^+$ T cells and T_{regs} to the therapeutic effect of MHC class II restricted neo-epitope vaccines in more detail. It is known that T_{regs} play a crucial role in CT26 tumor growth and that depletion of T_{regs} results in tumor growth retardation [175]. In accordance to the literature, it was found that depletion of T_{regs} via anti-CD4 antibodies results in rejection of CT26-Luc tumors *in vivo* (Supplementary Figure 5.2). In order to study the role of $CD8^+$ T cells after CD4 neo-epitope vaccination, it was analyzed if the $CD8^+$ T cells were able to recognize CT26-WT tumors *ex vivo*. MACS-isolated $CD8^+$ T cells (CD4 depleted splenocytes, see section 2.2.2.4) from CT26 tumor bearing mice vaccinated against CT26-M90 strongly recognized CT26 tumor cells whereas $CD8^+$ T cells from irrelevant RNA vaccinated mice did not (Figure 3.22). $CD4^+$ T cells were unable to directly recognize CT26 tumor cells probably due to the lack of MHC class II expression even in the presence of IFN-γ (data not shown). The induction of tumor-specific $CD8^+$ T

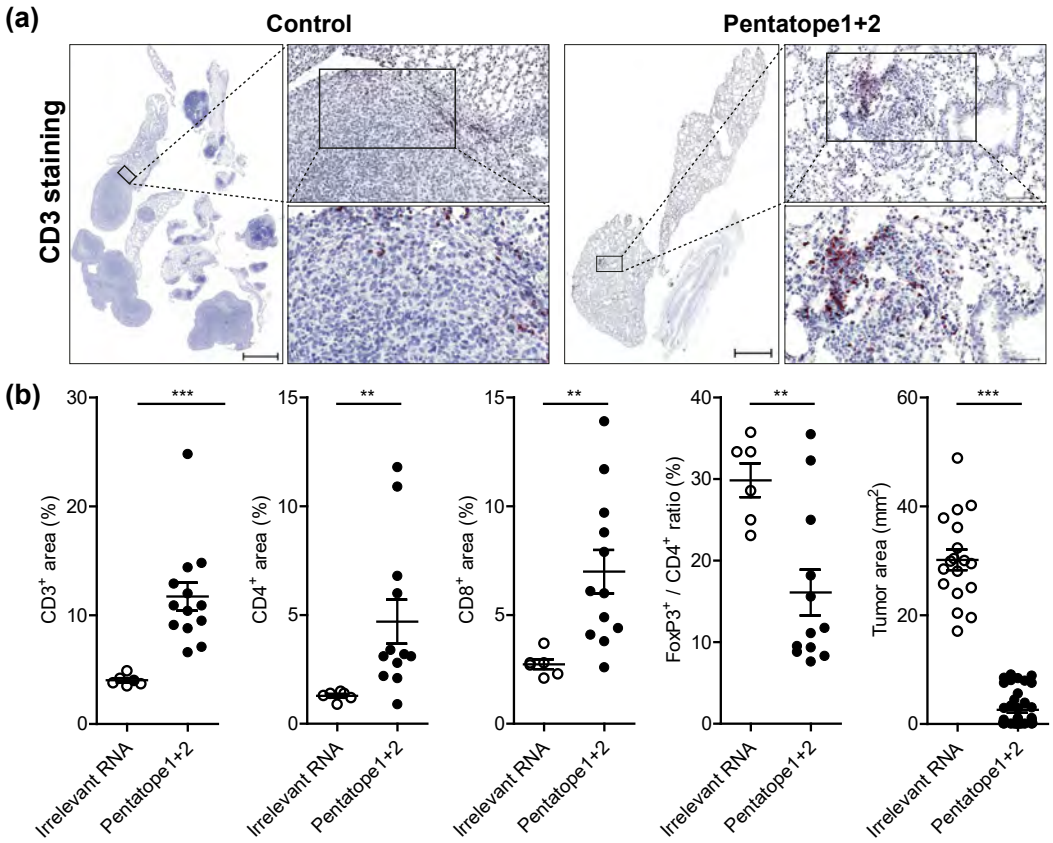

Figure 3.21: Immune histochemical analysis of tumor infiltrating lymphocytes in pentatope1+2 vaccinated mice. Upper panel, CD3 stained lung tissue sections. Scale bar: 1000 µm (scan), 100 µm (top), 50 µm (bottom). **b,** left, proportional lymphocyte areas in lung tumor tissue of control (n=6) or pentatope (CD3: n=14; CD4, CD8, FoxP3: n=12) treated animals. Right, tumor area (mean ± s.e.m) in sections of control (SIINFEKL RNA, n=18) and pentatope 1+2 (n=39) treated mice.

cells in CT26-M90 vaccinated mice was depending on CT26 tumors, as $CD8^+$ T cells from tumor-free, CT26-M90 vaccinated mice did not recognize CT26-WT tumor cells (Figure 3.23). Subsequent analysis showed that the CT26-WT responsive $CD8^+$ T cells were, at least in part, recognizing the gp70 derived CTL epitope AH1 ($gp70_{423\text{-}431}$) (Figure 3.27c).

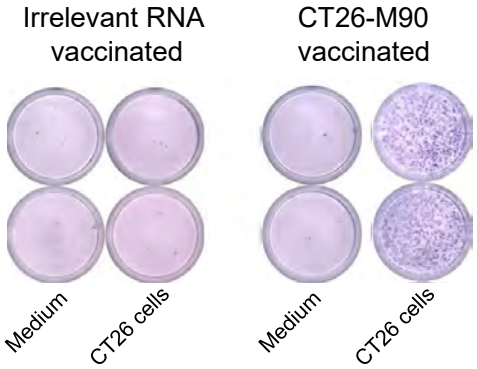

Figure 3.22: CD4 neo-epitope vaccination induces tumor-specific $CD8^+$ T cells. $CD8^+$ T cells (CD4 depleted splenocytes) isolated from CT26-WT tumor bearing mice (n=5) vaccinated with irrelevant (empty vector, left) or CT26-M90 (right) RNA were stimulated with CT26-WT cells or medium alone as control in an IFN-γ ELISpot. Exemplary results of one mouse are shown.

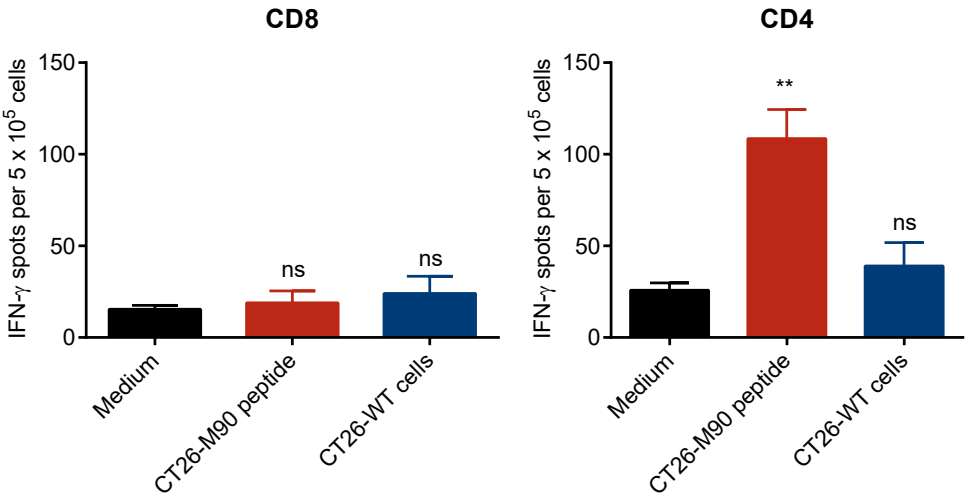

Figure 3.23: The induction of CT26 specific CD8$^+$ T cells after CT26-M90 vaccination is tumor dependant. CD8$^+$ T-cells isolated from CT26-M90 vaccinated, tumor-free mice (n=3) do not recognize CT26 cells *ex vivo*. Isolated CD4$^+$ T cells (CD8 depleted splenocytes) specific for CT26-M90 peptide are shown as control for the succesfull vaccination.

In conclusion of the experiments shown in Figure 3.21 and 3.22 it was hypothesized that tumor-specific CD4$^+$ T cells induced by RNA vaccination promote the formation of tumor-directed CD8$^+$ T cells. Antigen specific CD4$^+$ T helper cells promote the cross-priming of tumor-specific cytotoxic T-cell responses by CD40 ligand (CD40L) mediated activation of DCs. If CD4$^+$ T cells recognize their antigen on the same APC (cross-)presenting an MHC class I-restricted epitope, a diversified cytotoxic T-lymphocyte (CTL) response may result (a process called “DC licensing”) [157]. Thus, the anti-tumoral effect seen after induction of tumor-specific CD4$^+$ T cells would depend on CD40L signaling and CD8$^+$ T cells. Indeed, efficacy of pentatope 2 vaccination was significantly decreased upon CD40L blockade and completely lost after CD8$^+$ T cell depletion (Figure 3.24, CD8 depletion was determined to be >95 % by flow cytometry). This was independently confirmed in mice vaccinated with two different pentatopes (selected for MHC class II binding prediction and high expression levels, P_{ME}, see section 3.3) encoding solely MHC class II-restricted mutant epitopes (Figure 3.29, Figure 3.28, Table 3.8).

Off note, a direct tumor cell killing of CD4$^+$ T cells could not be demonstrated (no recognition of tumor cells in ELISpot, data not shown) consistent with the fact that CT26 tumor cells lack MHC class II expression even in the presence of IFN-γ (data not shown).

The data shown in this section demonstrate that CD4$^+$ T cells promote the cross-priming of tumor-specific cytotoxic T-cell responses by CD40 ligand mediated activation of DCs.

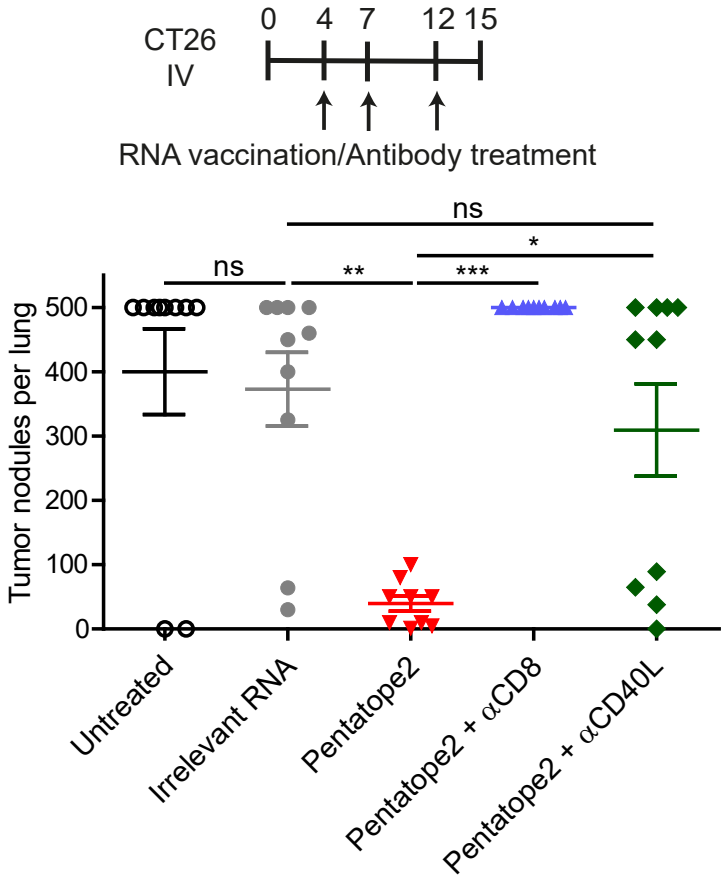

Figure 3.24: Efficacy of pentatope 2 vaccination depends on CD8$^+$ T cells and CD40L signaling. BALB/c mice (n=10) were inoculated IV with CT26 tumor cells and left untreated or injected with irrelevant (empty vector) or pentatope2 RNA in absence or presence of a CD8$^+$ T cell depleting antibody or a CD40L blocking antibody. Mean $\pm$ s.e.m. of tumor nodules per lung are shown.

3.3 Mutation Prioritization

The data shown in section 3.2 demonstrate that mutanome RNA vaccines induce T cells that target tumor lesions, recognize their mutated targets, reshape the cellular composition of the tumor microenvironment and result in efficient tumor control *in vivo*. However, tumors contain tens to thousands of expressed tumor mutations as potential vaccine targets (Figure 1.2). Thus, criteria are needed to select the therapeutically effective vaccine candidates out of the dozens or hundreds of mutations which are typically identified by NGS.

The current paradigm for selecting mutations for immunization is to employ MHC class I binding scores for enrichment of mutated epitope candidates [62, 63, 122, 147, 176] which can elicit $CD8^+$ T-cell responses and tumor rejection. We showed that MHC class I binding prediction resulted in an enrichment of immunogenic SNVs recognized by CD8 T cells in the CT26 tumor model (Figure 3.3). Moreover, immunogenic Indels had significantly better MHC class I binding scores compared to non-immunogenic ones (Figure 3.25). Our findings in section 3.1.1, however, indicate that MHC class II-presented neo-epitopes may be of higher interest for a personalized vaccination approach due to their relative abundance compared to MHC class I-restricted responses. As shown in Figure 3.2 the prevalence of MHC class II-restricted neo-epitopes is three to five times higher compared to $CD8^+$ T-cell epitopes despite the selection for predicted binding to MHC class I rather than MHC class II (for the 50 B16F10 and 48 CT26 mutations). Therefore, active prioritization of mutated sequences that are predicted to bind to MHC class II should further increase the immunogenicity rate.

In fact, a meta-analysis revealed that immunogenic SNVs have a significantly better MHC class II-binding score and area under the receiver operating characteristic (ROC) curve as compared to non-immunogenic ones (Figure 3.26a and b). This was also true for immunogenic indels without consideration of the actual subtype of the T-cell response (Figure 3.25). At a threshold of 10 for the MHC class II score a sensitivity of about 79 % and a specificity of 45 % was reached resulting in an odds ratio of 1.98 (< 10 vs. > 10, Figure 3.26c). Ultimately, this led to an enrichment factor of 152 % (< 10 vs. without).

Subsequently, 30 4T1-derived tumor mutations with MHC class II-binding scores below 10 were selected (Table 3.7). A pentatope RNA encoding five selected mutations per treatment group was used to vaccinate naive BALB/c mice (n=5) three times in an weekly interval. Five days after the last vaccination splenocytes, isolated $CD8^+$ T cells or $CD8^+$ T cell depleted splenocytes were stimulated *ex vivo* with mutated peptides and IFN-γ secretion was measured via ELISpot. 60 % of selected mutations were found to elicit $CD4^+$ T-cell responses, three of which were additionally recognized by $CD8^+$ T cells (Figure 3.26d, Table 3.7). Hence, MHC class II binding prediction almost doubled the fraction of immunogenic $CD4^+$ T-cell epitopes as compared to the initial screening of 38 mutations shown Figure 3.2.

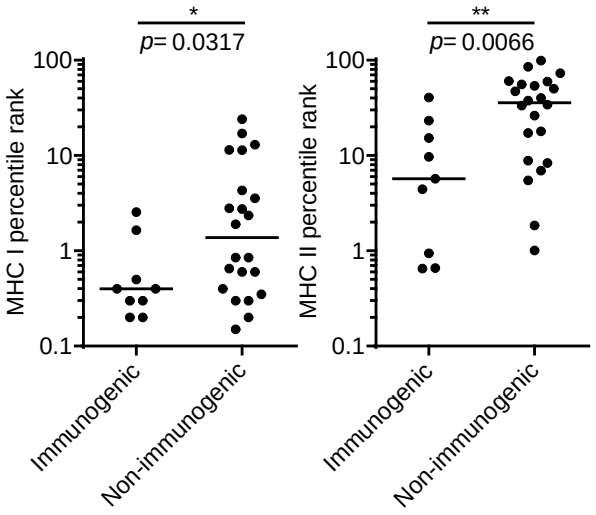

Figure 3.25: Immunogenic indels have significantly better MHC I and MHC II binding prediction. Retrospective analysis of MHC class I and MHC class II binding prediction of immunogenic compared to non-immunogenic indels was determined with IEDB consensus method version 2.12.

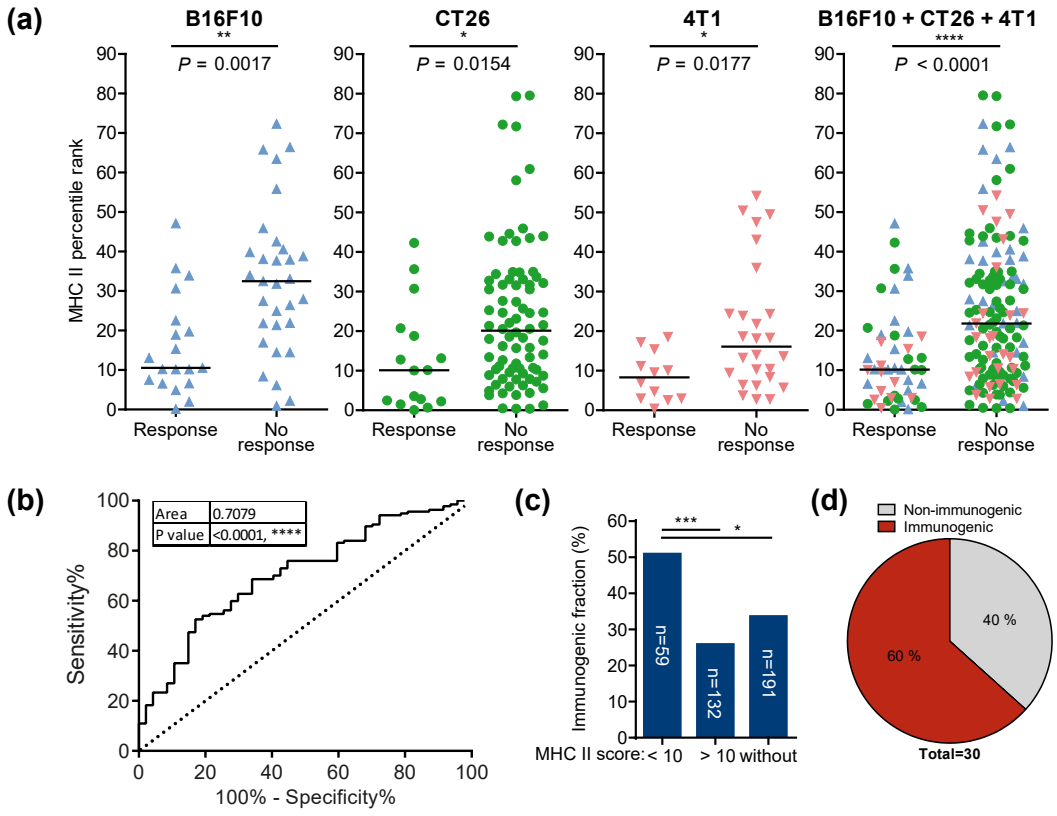

Figure 3.26: Immunogenic SNVs can be enriched via MHC class II binding prediction. (a) Comparison of median MHC II binding scores of immunogenic (Response) and non-immunogenic (No response) mutated 27-mers. **(b)** Receiver Operating Characteristic (ROC) curve comparing MHC II restricted and non-immunogenic or MHC I restricted mutations based on on their IEDB MHC class II binding score. Area: area under the ROC curve. **(c)** Frequency of immunogenic mutations (without) divided according to the predicted binding score (<10 and >10). **(d)** BALB/c mice (n=5) were vaccinated with one pentatope RNA per treatment group encoding five mutations with an MHC class II score below 10. Splenocytes were probed for recognition of mutated peptides via IFN-γ ELISpot.

Table 3.7: *In silico* prediction of 4T1 mutations with favorable MHC class II binding properties. 4T1 mutations with an MHC II percentile rank (IEDB consensus version 2.12) below 10 were selected. BALB/c mice (n=5) were vaccinated against five mutations encoded on one pentatope RNA (40 µg per mouse). IFN-γ secretion of splenocytes was determined via ELISpot as described in section 2.2.2.3. The subtype of responding T cells was determined by testing isolated $CD8^+$ (positive selection) and $CD4^+$ (negative selection) T cells (pooled cells from 5 mice, see section 2.2.2.5 and 2.2.2.4). WT, wild type; AA#, position of mutated amino acid; Mut, Mutation.

Mutation	Gene	Mutated sequence used for vaccination	Substitution (WT, AA#, Mut)	Reactive T cell subtype	MHC II score (best prediction)
4T1_M43	Fam168b	YPQQSPYAQQGTYCTQPLYAAPPHVIH	Y115C	CD4	6,9
4T1_M44	Fam168b	AQLSLFSPQQGTYCTQPLYAAPPHVIH	Y110C	CD4	6,9
4T1_M45	Rps6	IQRLVTPRVLQHKCRRIALKKQRTKKN	R189C	CD4	1,3
4T1_M46	Gyk	NAEESEIRYSTWKRAVMKSIGWVTTQS	K505R	CD4	4,3
4T1_M47	Txlna	FKHKDLQQQLVDANLQQAQEMLKEAEE	K340N	CD4	7,7
4T1_M48	Rbbp8	NLFGDVKGTGSLVSTKVKSRAVHGGCE	P609S	CD4	4,0
4T1_M49	Baiap2l1	TVTSRQSEIQKFIVDGCKEALLEEKRR	A179V	-	2,6
4T1_M50	Arhgef37	FQEEFEQVYKVYCTNYDQALLLVKAYQ	A123T	-	3,6
4T1_M51	Klhl10	NSVKRFDPVKKTWPQVAPMHSRRCYVS	H367P	CD4, CD8	6,9
4T1_M52	Cyp26a1	ETTASAATSLITYIGLYPHVLQKVREE	L316I	CD4	9,2
4T1_M53	Gnpat	VLREEASEILEEMRHKLRIGAIRFFAF	S110R	CD4	0,5
4T1_M54	Isoc1	EAALAEIPGVRSVLLFGVETHVCIQQT	V205L	-	8,1
4T1_M55	H2-Q6	PADITLTWQLNGEDLTQDMELVETRPA	E179D	-	8,9
4T1_M56	Chsy1	YILDLLLLYKKHKAKKMTVPVRRHAYL	G459A	CD4	1,0
4T1_M57	Pi4kb	GKRLATLPTKEQKAQRLISELSLLNHK	T17A	CD4	2,2
4T1_M58	Mrpl22	AKMIRGMSIDQALVQLEFNDKKGAQII	A98V	CD4	1,0
4T1_M59	Gpank1	CAARAGQGAAVRYILGRGAAWVGVCDL	L153I	CD4	8,7
4T1_M60	Btaf1	SIPPGQRHSIVSRLNNDPSIDVLLLTT	F1692L	CD4	9,2
4T1_M61	Agl	QLHESKIVRQAGVGTKGPNEYIQEIEF	A824G	-	2,9
4T1_M62	Abcc4	EATANVDPRTDELKQQKIREKFAQCTV	I1140K	-	9,8
4T1_M63	Nsmaf	TAILQSRLARTSFNKNRFQSVSEKLHM	D183N	-	8,2
4T1_M64	Klf5	NPHPSAVPQTSMKLFQGMPPCTYTMPS	Q259L	-	9,09
4T1_M65	Dctn2	PLSAGLQGACLMEMVELLQAKVSALDL	T261M	CD4	1,5
4T1_M66	Myh14	QLPIYTEAIVEMYQGKKRHEVPPHVYA	R159Q	CD4	9,5
4T1_M67	Arhgef19	SRRKELGKFAVFVRANMAELQVRDLSL	H645R	CD4	0,3
4T1_M68	Dusp1	GGLRALLREGAAQRLLLDCRSFFAFNA	C24R	-	4,3
4T1_M69	Shprh	VGSHRSSIKCAICHQTTSHKEVSYVFT	R1470H	-	4,9
4T1_M70	Mark2	EEFREAKPRSLRFPWSMKTTSSMEPNE	T639P	CD4, CD8	5,2
4T1_M71	Fpgt	TEYVYTDSLFYMDQKSAKKLLDFYKSE	H270Q	CD4, CD8	2,1
4T1_M72	D17H6S56E-3	SNLSRARLGLNESGWGRLWLEVPDSAA	A785G	-	8,0

As most cancers lack MHC class II expression, effective recognition of neo-epitopes by $CD4^+$ T cells should depend on presentation of released tumor antigens by APCs. This is most efficient for highly expressed antigens [177]. Thus, an algorithm combining good MHC class II binding with abundant expression of the RNA encoding the neo-epitope based on confirmed mutated RNA sequencing reads normalized to the overall read count (NVRC: normalized variant read counts) was implemented. To test the impact of predicted MHC class II binding affinity, CT26 mutanome data was ranked with this algorithm and the top ten mutations ("ME" mutations in Table 3.8) predicted to be the best MHC class II binders among the most abundant candidate epitopes (NVRC $\geq$60) were selected. The control comprised ten mutations with abundant expression only ("E" mutations in Table 3.8).

Table 3.8: *In silico* prediction of CT26 mutations with abundant expression and favorable MHC class II binding properties. CT26 mutations selected for high expression with (ME) or without (E) consideration of the MHC II percentile rank (IEDB consensus version 2.5). (WT, wild type; AA#, position of mutated amino acid; Mut, Mutation).

Mutation	Gene	Mutated sequence used for vaccination	Substitution (WT, AA#, Mut)	Expression (NVRC)	MHC II score (best prediciton)
CT26-E1	Asns	DSVVIFSGEGSDEFTQGYIYFHKAPSP	L370F	1428,05	45,45
CT26-E2	Cd34	PQTSPTGILPTTSNSISTSEMTWKSSL	D120N	1150,85	23,76
CT26-E3	Actb	WIGGSILASLSTFHQMWISKQEYDESG	Q353H	974,16	8,30
CT26-E4	Tmbim6	SALGSLALMIWLMTTPHSHETEQKRLG	A73T	825,51	2,96
CT26-E5	Glud1	DLRTAAYVNAIEKIFKVYNEAGVTFT	V546I	619,54	8,04
CT26-E16	Eif4g2	KLCLELLNVGVESNLILKGVILLIVDK	K108N	327,79	20,99
CT26-E17	Sept7	NVHYENYRSRKLATVTYNGVDNNKNKG	A314T	316,98	6,47
CT26-E18	Fn1	YTVSVVALHDDMENQPLIGIQSTAIPA	S1710N	303,62	17,41
CT26-E19	Brd2	KPSTLRELERYVLACLRKKPRKPYTIR	S703A	301,83	7,86
CT26-E20	Uchl3	KFMERDPDELRFNTIALSAA	A224T	301,78	9,75
CT26-ME1	Aldh18a1	LHSGQNHLKEMAISVLEARACAAAGQS	P154S	67,73	0,05
CT26-ME2	Ubqln1	DTLSAMSNPRAMQVLLQIQQGLQTLAT	A62V	84,08	0,24
CT26-ME3	Ppp6r1	DGQLELLAQGALDNALSSMGALHALRP	D309N	139,80	0,44
CT26-ME4	Trip12	WKGGPVKIDPLALMQAIERYLVVRGYG	V1328M	83,09	0,49
CT26-ME5	Pcdhgc3	QDINDNNPSFPTGKMKLEISEALAPGT	E139K	86,16	0,54
CT26-ME6	Cad	SDPRAAYFRQAENDMYIRMALLATVLG	G2139D	152,86	0,55
CT26-ME7	Smarcd1	MDLLAFERKLDQTVMRKRLDIQEALKR	I161V	125,85	0,60
CT26-ME8	Ddx27	ITTCLAVGGLDVKFQEAALRAAPDILI	S297F	61,82	0,62
CT26-ME9	Snx5	KARLKSKDVKLAEAHQQECCQKFEQLS	T341A	120,27	0,73
CT26-ME10	Lin7c	GEVPPQKLQALQRALQSEFCNAVREVY	V41A	71,24	1,09

These neo-epitopes were used without any further pre-validation (e.g. Sanger sequencing) or immunogenicity testing to engineer two RNA pentatopes for each group (P_{ME} and P_E pentatopes). Naive BALB/c mice were inoculated IV with luciferase transgenic CT26-Luc cells and vaccinated three days later either with the two P_E or with the P_{ME} pentatopes. Tumor growth in mice was tracked via *in vivo* imaging of lungs after IV injection of D-Luciferin. Established lung metastases were completely rejected in almost all P_{ME} vaccinated mice whereas P_E pentatopes were not able to control tumor growth (Figure 3.27a). In accordance, in mice with established CT26-Luc lung tumors, P_{ME} induced a much stronger T-cell response as compared to P_E pentatopes which was measured via IFN-γ ELISpot assay at day 41 (n=5, randomly selected) (Figure 3.27b). In support of the supposed mode of action (see section 3.2.3), $CD8^+$ T cell responses against gp70-AH1, a well characterized immunodominant CTL epitope of the endogenous murine leukemia virus-related cell surface antigen were detected in the blood and spleen of mice immunized with P_{ME} but not P_E pentatopes (Figure 3.27c).

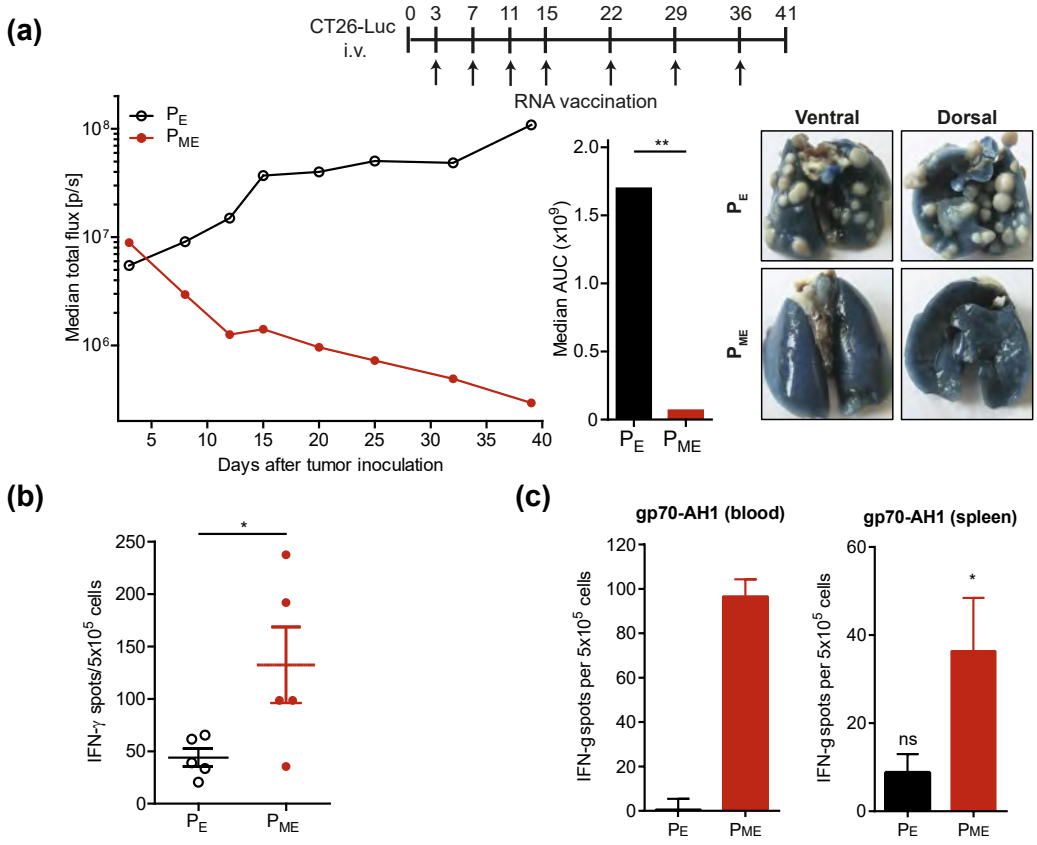

Figure 3.27: Vaccine targets selected for *in silico* predicted favorable MHC class II binding and abundant expression confer potent anti-tumor control. (a) Highly expressed mutations were selected with ("ME") or without (Ë") considering MHC class II binding score. Ten mutations (two pentatopes) per category were used for vaccination of CT26-Luc tumor bearing mice (n=10). Tumor growth, area under the curve at day 40 and ink treated lungs are shown. **(b)** Mice (n=5) were analyzed for T-cell responses against the RNA pentatopes via ELISpot (mean ±+s.e.m. subtracted by an irrelevant RNA control). **(c)** T-cell responses against $gp70_{423\text{-}431}$ (gp70-AH1) determined via ELISpot in blood (pooled from 5 mice at day 20) and spleen (n=5). Background (medium control) subtracted mean ± s.e.m. are shown.

Subsequent analysis of immune responses after P_{ME} vaccination of naive mice proved the presence of multiple immunogenic MHC class II neo-epitopes in the P_{ME} RNA pentatopes (Figure 3.28). Interestingly, especially the top three ranked mutations were immunogenic and showed a decrease in the T-cell response according to their prediction score.

An independent study in CT26-WT tumor bearing mice confirmed the strong therapeutic anti-tumor activity of the pentatope P_{ME} and, in agreement with the studies depicted in section 3.2.3, showed loss of the anti-tumor effect upon CD40L blockade and anti-CD8 treatment (Figure 3.29).

The data presented in this section demonstrate that considering MHC class II binding prediction and expression levels of the mutated allele can improve the selection of relevant mutated vaccine targets.

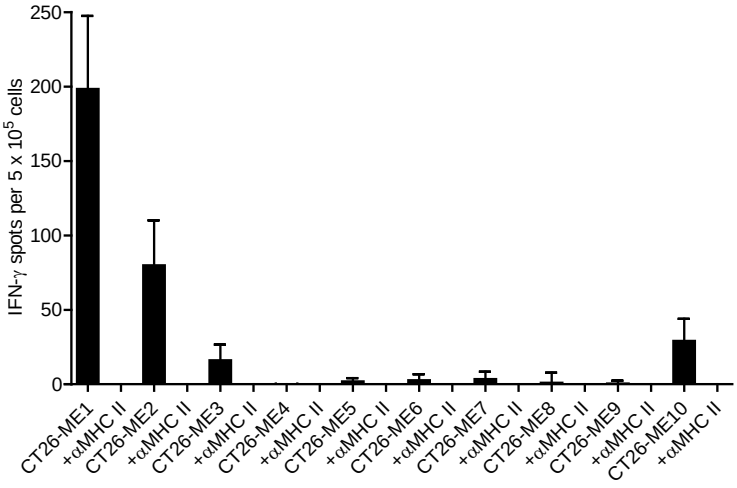

Figure 3.28: Immunogenicity testing of P_{ME} pentatopes encoded mutations. Splenocytes of P_{ME} RNA vaccinated BALB/c mice (n=6) were tested ex vivo for recognition of peptides representing the mutated 27mer sequences represented in P_{ME} pentatopes with or without addition of an MHC class II blocking antibody. Mean + s.e.m. of background (medium control) subtracted responses are shown.

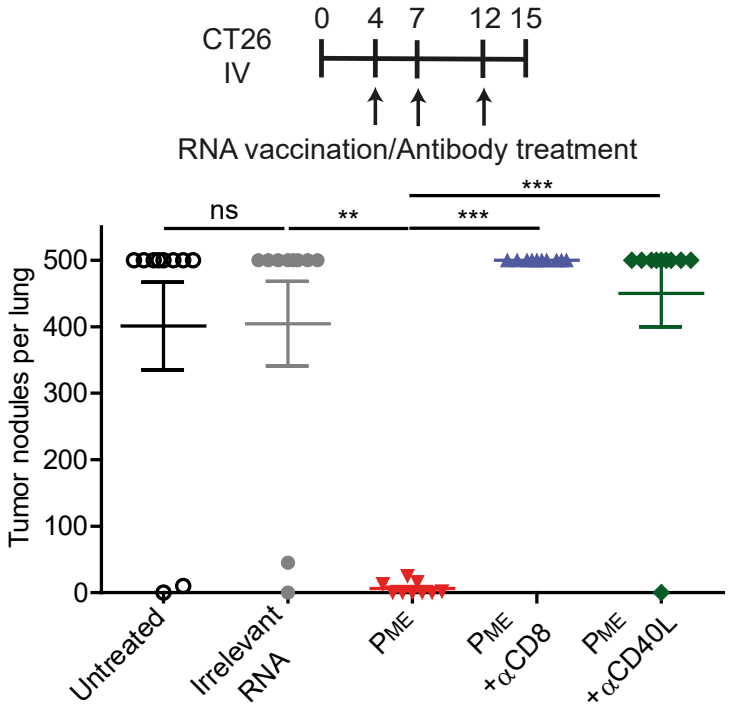

Figure 3.29: MHC II-restricted mutanome vaccines depend on $CD8^+$ T cells and CD40L signaling. CT26 tumor nodules per lung of untreated mice or mice (n=10) injected with irrelevant (empty vector) or P_{ME} RNA (± CD8 depletion or CD40L blocking). Mean ± s.e.m. of tumor nodules per lung are shown.

4 Discussion

The results of this study show that tumor mutations, in particular SNVs, indels and gene fusions are frequently immunogenic and that MHC class II-restricted T-cell neo-epitopes are more abundant than previously assumed (Figure 3.2 and 3.10). Neo-epitopes can be targeted by customized RNA-based monotope or poly-neo-epitope vaccines with substantial therapeutic effects in mouse tumor models (Figure 3.12, 3.18, 3.17 and 3.24). Such pentatope vaccines are equally efficient or even superior in the induction of T-cell responses compared to monotopes (Figure 3.16). Notably, CD4 neo-epitope vaccination was shown to affect the tumor microenvironment by decreasing the ratio of $FoxP3^+$ to $CD4^+$ T cells and augmenting $CD4^+$ and $CD8^+$ T-cell infiltration (Figure 3.20 and Figure 3.21). $FoxP3^+$ regulatory T cells play a crucial role in suppressing the host immune response against CT26 (Supplementary Figure 5.2). In addition, anti-tumoral efficacy of neo-epitope specific $CD4^+$ T cells in CT26 tumors was shown to depend on $CD8^+$ T cells and CD40L signaling (Figure 3.24). Finally, a meta-analysis revealed that immunogenic SNVs and indels have a significantly better binding prediction for MHC class II than their non-immunogenic counterparts. Vaccination against mutations selected for favorable MHC class II binding prediction and abundant mutated mRNA expression resulted in tumor-control without prior validation or immunogenicity testing (Figure 3.27).

4.1 Mutation Specific T-Cell Immunotherapy

Cancer vaccines: past failures, present potential and future hopes

Despite considerable efforts, so far only one cancer vaccine has been approved by the FDA and EMA. Treatment of prostate cancer patients with sipuleucel-T, a cellular vaccine consisting of PBMCs treated with the antigen prostatic acid phosphatase and fused to GM-CSF, resulted only in a minor survival benefit of 4.1 month (compared to a placebo group) and no reported effect on tumor growth [178]. One might argue that the so far largely disappointing outcome of clinical vaccination trials [145] was due to targeting of the wrong antigens (see also sections1.2.1 and 4.1) with ineffective vaccine formats.

Present studies on neo-epitope vaccines, as shown in this thesis and by other studies in mouse models [62, 63, 126], have demonstrated unprecedented therapeutic potential. But still, one should raise the question how efficient a monotherapy with a cancer vaccine can be. Studies in human melanoma and gastrointestinal cancers detect preexisting immune responses in the majority of cancer patients [123, 124]. Thus, these T-cell responses are either insufficient in frequency or potency to control tumor growth and/or the tumor has established mechanisms to protect its destruction by the

immune system. In the former case, cancer vaccination is a promising therapy. In the latter case, however, vaccination probably might not be efficient as a monotherapy alone. Immune evasion of tumors by suppression of an ongoing immune response seems to be especially important in immunogenic tumors [179] like melanoma. This might be one reason for the high response rates of melanoma patients to antibodies such as anti-CTLA-4 and anti-PD-1 that tackle tumor-induced T-cell suppression. On the other hand, checkpoint blockade was also shown to expand preexisting tumor-specific T-cell responses [115, 116]. To which extent the efficacy of these antibodies is mediated by the T-cell expansion in comparison to the reversion of T-cell suppression is unknown. Probably both mechanisms are indispensable. Successful cancer immunotherapy might on the one hand need to enhance effector cell frequencies and on the other hand enable their unhindered trafficking and infiltration to the tumor as well as the recognition and killing of cancer cells (Figure 4.1). In this regard, Beckhove and colleagues demonstrated that ACT of $CD8^+$ T cells was only efficient if combined with neoadjuvant local low-dose irradiation reverting the immunosuppressive tumor microenvironment and allowing the efficient T-cell migration to the tumor [180]. Nonetheless, it was shown in this thesis that neoantigen-specific $CD4^+$ T-cell responses induced after RNA vaccination alone were sufficient to revert immunosuppression, increase T-cell migration and infiltration as well as tumor cell killing (section 3.2.3). The RNA as vaccine format might in fact play a crucial role here by causing inflammation and maturation of APCs through stimulation of pattern recognition receptors [158]. Therapeutic RNA vaccination at late time points, however, was inefficient in controlling CT26 (Supplementary Figure 5.3) and B16F10 (data not shown) tumor growth. In the IV tumor model, mice start dying at day 15-17 post-inoculum. Initiation of an immune response usually takes about 4-5 days, and in the case of the CT26 model even longer due to the dependence of the anti-tumoral effect on the subsequent priming of $CD8^+$ T cells. Thus, when vaccination is started late, the formation of an effective $CD8^+$ T-cell response might simply take to long to affect the tumor growth. An additional explanation might be that the T-cell influx into the tumor is dependent on the initial inflammation caused by the injection of tumor cells. In such cases, therapeutic efficacy might be restored if vaccination is combined with additional synergistic interventions such as local low-dose irradiation that induce an inflammation in the tumor. However, this explanation seems unlikely for the IV tumor model as tumor formation (lung) and injection of tumor cells (tail vein) are spaced apart.

The future treatment of cancer will probably be dominated by the combination of several synergistic immunotherapies and supportive “conventional” therapies such as anti-angiogenic- and radiotherapy [27]. As T-cell responses are key for this treatment model, neo-epitopes specific vaccines ought to be one important pillar of such a combination therapy (see also section 4.2).

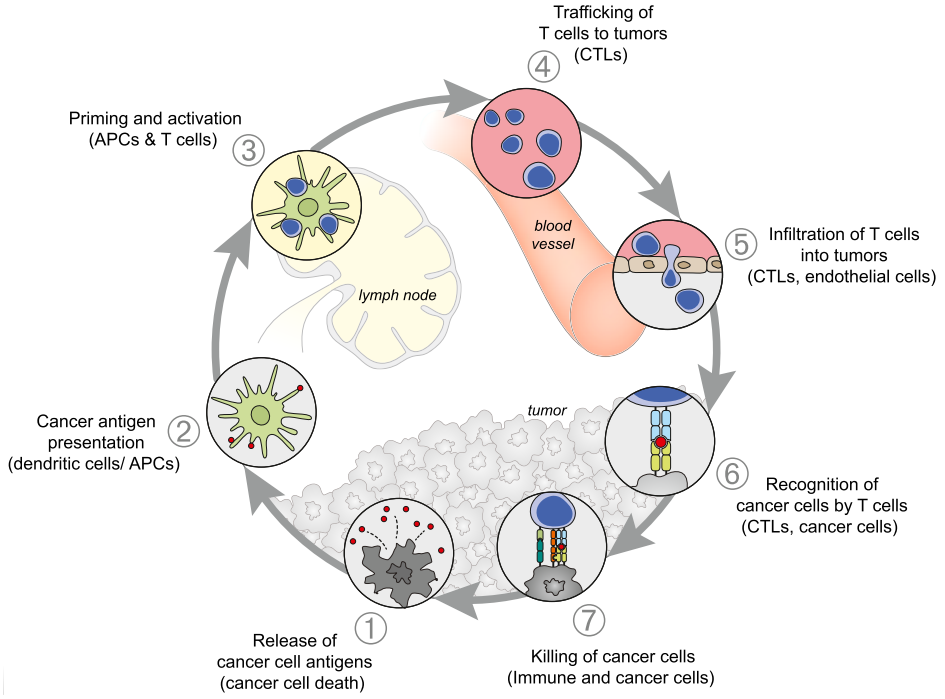

Figure 4.1: The cancer-immunity cycle (adopted from Chen and Mellman [23]).

Mutations as superior tumor antigens

It has been known for decades that the immune system is able to recognize and destroy tumor cells [15, 18, 19]. Nevertheless, only in the last years, a better picture of the molecular T-cell targets on cancer cells has evolved. Recent studies indicate that mutations are a dominant source of tumor rejection antigens (reviewed in [131, 181, 182]). Notwithstanding their unique expression in a single patients' tumor, mutations seem ideal targets for specific T-cell immunotherapy due to the expected lack of tolerance and toxicity (section 1.2.1). However, despite the accumulating evidence pointing out the importance of mutation-specific T-cell responses in cancer (section 1.2.3), comprehensive studies that prove the superiority of neo-antigens compared to TAAs or cancer germline antigens are lacking. Especially for SNVs, central tolerance might play a role due to their resemblance to the wild type sequence (see section 1.2.1.2). Thus, the SNV-specific T-cell repertoire might be sculpt, discarding high-affinity clones that recognize the wild type protein as well. In comparison to shared antigens, SNVs-specific T-cell responses theoretically have a chance to be completely unaffected by tolerance for example if the point mutation serves as an anchor for MHC binding. Moreover, it is a matter of debate if the induction of T-cell responses against point mutations are generally safe. In most cases, SNV-specific immune responses showed, at least to some extent, activity against the wild type peptide as well [50]. Therefore, auto-immune side effects are conceivable (especially if very high frequencies are induced for example through adoptive cell transfer) although no toxicities of neo-epitope specific RNA vaccination has been observed in mice. Even if point mutations are not generally superior to shared antigens in terms of immunogenicity, their mere abundance compared to TAAs makes them indispensable targets for T-cell immunotherapy. In comparison to SNVs, mutations that introduce longer stretches of novel amino acids such as indels and fusions are rather scarce

but due to the lack of a resembling wild type sequences, tolerance and auto-immunity should not play a role. Moreover, as shown here, they harbor a chance of containing several T-cell epitopes simultaneously which renders them even more interesting vaccine candidates. Hence, it is not a surprise that mismatch repair deficiency of cancers results in a higher T-cell infiltration [99, 100] and a better overall prognosis due to the accumulation of frameshift mutations which induce $CD8^+$ T-cell responses [100, 183].

4.2 Antigenicity Rate and Dominance of $CD4^+$ T-Cell Responses

Therapeutically relevant mutations are frequently antigenic but not immunogenic

Here, it was shown that 25 % to almost 50 % of mutations induced IFN-γ secretion by T cells after RNA vaccination of mice (antigenicity rate, section 3.1). Approximately 80 % of those T cells were $CD4^+$. In comparison, a study by Schumacher and colleagues estimated that 0.5 % of all mutations are spontaneously recognized by $CD4^+$ T cells in humans (immunongenicity rate) [123,181]. The differences in these results indicate that only a fraction of antigenic mutations spontaneously elicit T-cell responses. However, as shown for CT26-M90 in this thesis, vaccination against SNVs that are not spontaneously immunogenic induce immunotherapeutically relevant T-cell responses (Figure 3.12, Supplementary Figure 5.1). Therefore, mutanome vaccines targeting 10 (IVAC Mutanome phase I clinical trial in melanoma, NCT02035956) to 20 (TNBC-MERIT phase I trial in triple negative breast cancer, NCT02316457) mutations should elicit at minimum 2-4 relevant neo-epitope-directed T-cell responses. This response rate can be further enhanced if selection criteria such as MHC class II binding prediction are employed (see section 4.5). As a result, it should be possible to treat even tumors with low mutational burden such as thyroid or prostate cancer (see Figure 1.2) with an individualized vaccine against cancer.

In addition, mutanome vaccination might be an attractive combination partner for immune checkpoint blockade. As indicated earlier, ACT or PD-1/PD-L1 blockade therapies require preexisting T-cell responses [115, 184] and seem to be especially successful in tumors with a high mutational load that have a higher chance for spontaneous immune responses [128–130] (Figure 4.2). Hence, a logical conclusion would be that further induction of tumor-specific T cells by vaccination or indirect measures like immunogenic cell death through low-dose irradiation, chemotherapy as well as oncolytic virotherapy would expand the functional range to tumor types with lower numbers of mutations. Indeed, it was shown that the efficiency of PD-1 immunotherapy was significantly improved by oncolytic virotherapy due to broadening of neo-antigen specific T-cell responses [127].

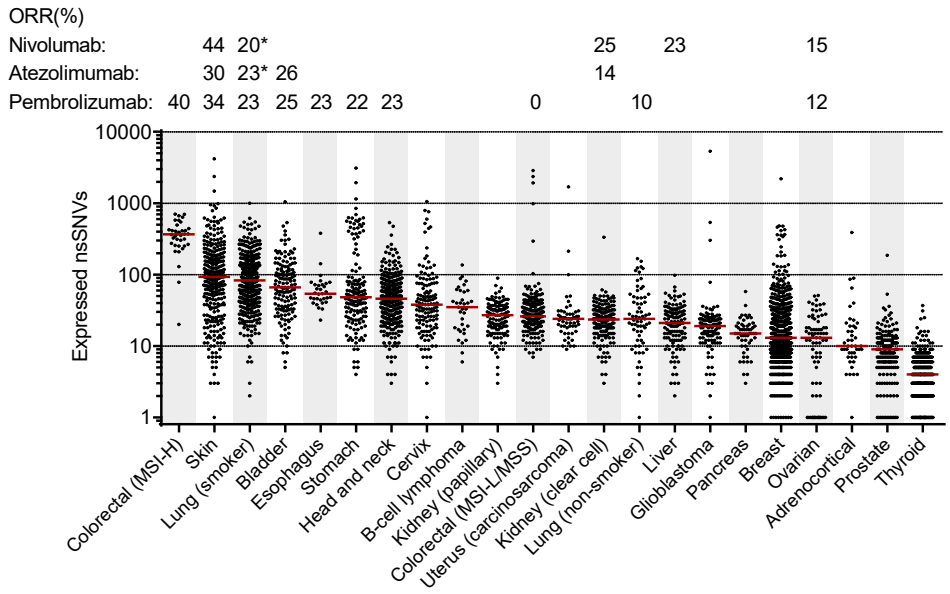

Figure 4.2: Number of expressed tumor mutations and response rates of PD-1/PD-L1 blockade in human tumor types. Non-synonymous SNVs (nsSNVs) derived from human cancer samples (TCGA) were retrieved as described in [49]. The overall response rates (ORR) after nivolumab (anti-PD-1), atezolimumab (anti-PD-L1) and pembrolizumab (anti-PD-1) treatment were retrieved from: [28, 98, 113, 116, 137–143, 185–188]. *No differentiation between smoker and non-smoker.

Neo-antigen specific responses are dominated by CD4⁺ T cells

Surprisingly, only a rather low fraction of antigenic SNV derived neo-epitopes were MHC class I restricted (Figure 3.2). To ensure optimal antigen presentation of encoded proteins for CD4⁺ T-cell epitopes, the target sequence in our vaccine was flanked with a signal peptide (signal peptide, SP or secretion domain, SEC) and the transmembrane and cytosolic domain (MHC class I trafficking domain, MITD) of MHC class I. The fusion protein is routed into the ER membrane from which it travels via the Golgi apparatus and the endosomal pathway to the cell membrane and back, until it is degraded and loaded onto MHC class I or MHC class II molecules. Processing and loading of MHC class II epitopes takes place in endosomes and lysosomes [189]. Thus, routing of proteins into the endosomal pathway by SP and MITD increases their processing and presentation on MHC class II. In contrast, MHC class I epitopes are processed in the cytosolic proteasome (Figure 4.3). Routing of the fusion protein into the ER theoretically should hamper its processing and require transport into the cytosol (e.g. via the endoplasmic-reticulum-associated protein degradation (ERAD) pathway). Therefore, one might assume that the dominance of CD4⁺ T-cell responses observed here was a bias caused by the vaccine design. Surprisingly, though, it was clearly shown that flanking antigens with SP and MITD results in enhanced CD4⁺ and CD8⁺ T-cell responses [159] thereby ruling out that the dominance of CD4⁺ T-cell responses was a bias caused by the vaccine design. The mechanism by which MHC class I epitopes are processed after targeting into the ER, however, is still unclear. Moreover, vaccination with long 27-mer peptides led to similarly low frequencies of CD8⁺ T-cell responses [50].

Except for the analysis shown here, no comprehensive study so far analyzed the antigenicity rate of MHC class I (and class II) restricted neo-epitopes. Srivastava and colleagues found frequent CD8⁺ T-

cell neo-epitopes after vaccinating mice with predicted minimal peptide epitopes [62]. Minimal $CD8^+$ T-cell epitopes can bind to MHC class I without further processing by the proteasome. Therefore, it needs to be shown that those minimal epitopes are correctly processed from the mutated proteins by the tumor cells or APCs which was only done for one neo-epitope. Importantly, only a small part of this study was reproducible: two of eight mutations elicited immune responses using either peptide or RNA vaccines (including the one for which correct processing was demonstrated, data not shown).

Rosenberg et al. found several spontaneous $CD8^+$ T-cell responses in TILs and blood of melanoma patients [106, 124]. They tested more than 1,400 tumor mutations for the recognition by patient-derived T cells. In total, only 12 $CD8^+$ (0.8 %) and 6 $CD4^+$ (0.4 %) T-cell neo-eptitopes were found which seems to be in accordance with the prediction made by Schumacher. In comparison, the antigenicity rate of MHC class I restricted neo-epitopes in our studies was almost one log higher (4-12 %), probably for the same reasons stated above (Figure 3.2).

In light of the binding properties of MHC class I in comparison to MHC class II, it is not surprising that CD8 epitopes are outnumbered by $CD4^+$ T-cell epitopes. MHC class I molecules bind peptides with very defined properties: a length between 8-11 amino acids with conserved anchor residues important for binding. In contrast, MHC class II binding is more variable (open ends of binding groove allow big variability in the length of epitopes, binding core is not well defined, flanking residues contribute to binding) [81]. Correspondingly, also for viral antigens, epitope screening approaches unveil predominantly $CD4^+$ T-cell epitopes [190, 191].

Antigenicity rates of indels and fusions

Comparing the antigenicity rate of point mutations to indels and fusion, one would assume higher frequencies among the latter groups as longer stretches of novels amino acid can potentially harbor multiple T-cell epitopes. The overall immunogenicity rate of SNVs, however, is 32 % compared to 29 % for indels and fusions (without considering SNVs selected for MHC class II binding prediction). Yet, one should take into account that in total only 31 indels and fusion were tested as to more than 200 SNVs. Looking more closely, there is a trend that the immunogenicity rate of indels and fusions positively correlates with the number of novel amino acids. The median number of new amino acids for immunogenic indels and fusions is 25 compared to 8 for non-immunogenic mutations. 77 % (seven of nine) of immunogenic indels and fusions result in equally or more than the overall median of nine new amino acids, corresponding to only 45 % (10 of 22) for non-immunogenic alterations.

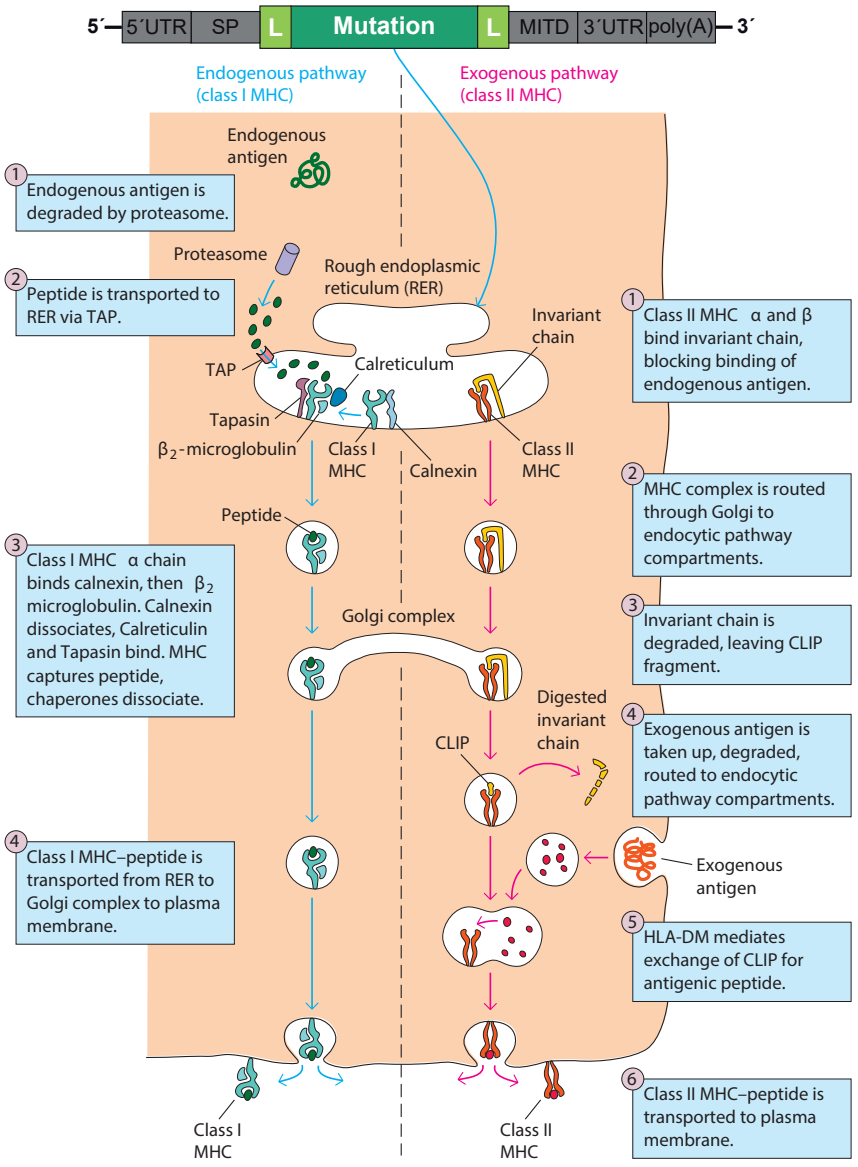

Figure 4.3: Antigen processing and presentation pathways (modified after [192]).

4.3 Anti-Tumoral Effect of Neo-Epitope Vaccines

SNV-specific CD4⁺ T cells induce tumor control through distinct mechanisms

RNA vaccination induced CD4$^+$ T-cell responses against point mutations was shown to induce potent tumor control and protective T-cell memory in B16F10 [49, 50] and CT26 (Figure 3.12, 3.17, 3.24 and 3.13). The spontaneous arising B16 cell line originated in 1954 and was selected for the ability to form lung nodules *in vivo* after IV injection (B16F10) [193]. B16F10 is considered as rather non-immunogenic with low MHC class I expression (and no MHC class II expression) [179]. In comparison, CT26 is an N-nitroso-N-methylurethane-induced BALB/c undifferentiated colon carcinoma which was cloned to generate CT26-WT [194]. CT26-WT is comparably immunogenic and has considerable MHC class I expression but is known to induce an immunosuppressive microenvironment

(e.g. T_{regs}) [175, 179, 194]. Notably, mutanome vaccination was successful in both tumor models besides considerable differences.

In B16F10, the anti-tumoral effect was directly mediated through $CD4^+$ T-cells depending on IFN-γ and in part on NK cells but independent of $CD8^+$ T cells (which is in accordance with the low MHC class I expression levels) [49]. $CD4^+$ T-cell-derived IFN-γ directly results in tumor growth inhibition *in vitro*, MHC class I upregulation, inflammation and NK cell activation (data not shown). Moreover, it was shown in our group that the inflammatory response mediated by the neo-epitope-specific $CD4^+$ T-cells increases the influx of effector T cells and dampens MDSC and T_{reg} infiltration in B16F10 (data not shown).

In contrast, MHC class II neo-epitope vaccination in CT26 was completely dependent on the $CD4^+$ T-cell mediated induction of a $CD8^+$ T-cell response. Here, $CD4^+$ T cells act on the intramural T_{regs} to effector T-cell ratio and, via CD40L signaling, on DCs to activate and prime $CD8^+$ T-cells that kill the immunogenic, MHC class I-high tumors. In addition to MHC class I expression, the high number of neo-antigens and the high expression of the murine leukaemia virus-related cell surface antigen gp70 probably renders CT26 immunogenic and makes epitope spreading more likely. From this perspective, CT26 is resembling highly mutated, immunogenic tumor types such as human melanoma and other carcinogen induced cancers such as smoking induced lung cancer or bladder cancer (Figure 1.2).

Similar to B16F10, CT26 cells lack MHC class II expression even under the influence of IFN-γ (data not shown). Thus $CD4^+$ T-cells need to recognize neo-epitopes on APCs either in the tumor or the draining lymph node. Most likely $CD8^+$ T-cell priming takes place in the draining lymph node due to its optimal spatial properties to bring together APCs and lymphocytes. Conceivably, tumor-antigens are draining through the lymphatic vessels into the lymph node, are taken up by APCs and presented to primed $CD4^+$ T cells and naive $CD8^+$ T cells. In addition, some APCs might reside in the tumor where they present tumor antigens to the neo-epitope specific $CD4^+$ T cells that subsequently cause inflammation and influx of lymphocytes. In theory, priming of naive, tumor-specific $CD8^+$ T cells could also take place inside the tumor, however, this is much more unlikely due to the low chance that all three cells meet there at once.

4T1 derived myeloid cells challenge immunotherapy

The 4T1 cell line derived from a spontaneously arising mammary tumor of a $MMTV^+$ BALB/c mouse [195]. It is highly tumorigenic and can spontaneously metastasize from the primary tumor to multiple distant sites including lymph nodes, blood, liver, lung, brain, and bone [196]. 4T1 displays a comparably low mutational load (similarly to human breast cancer) and a significant immunosuppressive microenvironment. Moreover, 4T1 cells induce a strong induction and infiltration of myeloid cells (including suppressive M2 macrophages and $Gr\text{-}1^+$ $CD11b^+$ MDSCs) through the production of various cytokines and chemokines such as G-CSF, GM-CSF, RANTES, MIP-1α and β [197–200]. Myeloid cells can comprise more than 80 % of PBLs and more than 70 % of $CD45^+$ cells in the spleen of 4T1 tumor bearing mice compared to less than 15 % and 5 %, respectively, in healthy mice [201]. Thus, 4T1 is considered a “tough” model for immunotherapeutic interventions

and mutanome vaccination as monotherapy showed only minor effects (Figure 3.14). Further experiments will explore vaccination against additional 4T1 mutations as well as combinations with tumor microenvironment-targeting substances.

Indels and gene fusions are often scarcely expressed

Vaccination against indels and gene fusions was so far not therapeutically successful (see exemplarily Figure 3.15), despite the induction of strong T-cell responses, which might be in part due to a very low expression on mRNA level (this is the case for B16_IND07). As discussed in section 1.2.1.1, cells tend to downregulate expression of aberrant mRNA through nonsense-mediated mRNA decay. Alternatively, epigenetic alterations might arrest the expression of longer stretches of mutated DNA. Thus, combination with epigenetic modulators [202] or substances that block NMD [203] might help to overcome this problem. In the case of B16_IND03, the second immunogenic indel in the B16F10 tumor model, expression levels were good but the immunogenicity was very weak. Nevertheless, indels and fusions remain interesting targets as several studies showed that cancer patients can develop profound T-cell responses against the respective mutated proteins [95, 100, 119, 204, 205].

4.4 Vaccine Targets Beyond SNVs, Indels and Fusions

In section 1.2.3 and 3.2 it was illustrated that mutated tumor antigens play a pivotal role in spontaneous and immunotherapy induced T-cell responses in cancer. As SNVs are the most abundant cancer mutations, research so far has focused mainly on this subtype. Alterations that introduce several new amino acids are even more interesting from an immunological point of view, as they may simultaneously harbor multiple T-cell neo-epitopes. For this reason we investigated indel and fusion mutations.

Several other potential antigen classes exist that might induce high avidity T-cell responses without causing on-target off-tumor toxicity. As an example splice site mutations that alter the open reading frame of the protein might introduce long stretches of new amino acids (see Figure 1.3). Moreover, epigenetic changes leading to private (or shared) overexpressed or cancer germline antigens may play a more important role than previously anticipated. NGS or mass spectrometry-based identification should potentially be able to reveal these antigen types as well by searching for differentially overexpressed genes. Indeed, a study discovered several shared TAAs antigens via HLA ligandome analysis in chronic lymphocytic leukemia (CLL) patients and could show that they can be recognized by T cells which in turn was correlated with increased patient survival [206]. However, especially in the case of private over-expressed mutations, a careful examination of potential side effects is necessary.

Yet another source of tumor antigens are post-transcriptional (e.g. splice variants [207]), translational and post-translational alterations. For example modified cystein [208, 209] or asparagine [210] residues which alter the TCR binding affinity have been shown to induce specific immune responses. Moreover, it has been demonstrated that novel antigens can be generated from the proteasome via "peptide splicing" (two distant parts of a protein are excised and ligated together to form a novel

peptide) [211, 212]. Identification of such antigens is rather difficult, thus their therapeutic evaluation is so far scarce.

4.5 Predicting Relevant Vaccine Targets

Tumors contain up to thousands of mutations that represent potential T-cell targets (Figure 1.2). Thus, selecting relevant neo-epitopes is a key challenge for individualized immunotherapy. As discussed below, several factors influence if a mutation is properly presented by tumor cells or APCs and recognized by tumor-specific T cells and thus need to be addressed for efficient selection of neo-epitope candidates.

Increasing the antigenicity rate: MHC binding prediction

As shown in section 3.3 utilizing MHC class II binding significantly enhances the immunogenicity rate of SNVs. Moreover, only when MHC class I binding prediction was employed, CD8 neo-epitopes were found in the CT26 tumor model (Figure 3.3). In accordance, immunogenic indels had significant better MHC class I and II binding predictions compared to their non-immunogenic counterparts (Figure 3.25). Although MHC class I binding prediction is crucial for the identification of CTL neo-epitopes [213], the rate of immunogenic CD4 neo-epitopes after MHC class II binding prediction is about ten times higher than the rate of CD8 epitopes after MHC class I binding prediction. Thus, although MHC class I binding prediction is thought to be superior to MHC class II binding prediction [81], in the case of neo-epitopes, the latter seems to be more efficient due to the abundance of CD4 epitopes. In order to increase the prediction of CD8 neo-epitopes, one might prefer mutations that affect an anchor position in the epitope [62], the TCR binding affinity [63] or the processing and presentation of the neo-epitope (Figure 1.4). However, so far no convincing evidence was published supporting these theories. Moreover, algorithms that predict TCR binding or processing of epitopes are so far not as reliable as MHC binding prediction and therefore should be used with care.

MHC binding prediction primarily enhances the immunogenicity rate. In addition, a higher binding affinity to MHC molecules, and thus a better binding score, is thought to correlate with increased T-cell frequencies and tumor-cell killing by CTLs [76, 214].

Predicting the abundance of peptide:MHC complexes on tumor cells and APCs

The efficiency of antigen processing, antigen half-life, expression levels and the abundance of MHC class I molecules are additional factors that influence the amount of peptide:MHC class I complexes on the cell surface of tumor cells [63, 215] and their recognition and rejection by $CD8^+$ T cells [216–218]. Antigen abundance might be even more important for the anti-tumoral effect of $CD4^+$ T cells as most tumor cells lack MHC class II expression. $CD4^+$ T-cells probably recognize their cognate antigen on APCs in the tumor and draining lymph nodes. APCs need to take up tumor antigens from dying tumor cells or tumor exosomes. Therefore, mutated proteins that are expressed abundantly or preferentially taken up by APCs should enhance the anti-tumor effect of neo-antigen specific T cells. As an example, it was shown that a CD20 mAb against a lymphoma cell line resulted in the induction

of a T-cell response which was dependent on the formation of immune complexes selectively taken up by DCs [219]. Accordingly, highly expressed mutations with preferential MHC class II binding prediction were shown to induce potent tumor control (Figure 3.27). In addition to enhancing the likelihood of T-cell recognition during the effector phase, expression levels and enrichment of tumor antigens in APCs potentially increase the likelihood for spontaneous T-cell responses. Hence, these parameters might be valuable markers for the prediction of spontaneous T-cell responses.

Driver mutations as preferential vaccine targets

A matter of debate is if the products of mutated genes that are crucial in the proliferation, survival and metastasis of tumor cells or mutations implicated with oncogenesis ("driver mutations") are superior T-cell targets compared to bystander mutations ("passenger mutations"). It is hypothesized that driver mutations are less easily lost by the malignant cells and thus reduce the likelihood of immune escape. However, the great majority of neo-antigen specific T-cell responses identified so far recognize passenger mutations. Moreover, targeting of the oncogenic V600E mutation in B-Raf using the small-molecule kinase inhibitor Vemurafenib shows that tumor cells can readily escape by mutating Ras (N-Ras) or by upregulation of receptor tyrosine kinase (RTK)-mediated activation of alternative survival pathways [220]. Nevertheless, driver mutations might be interesting T-cell targets from a different perspective: alterations involved in the formation of cancer should be common to all tumor cells. It was shown that branched evolution of cancer results in mutational heterogeneity between metastasis and the primary tumor and even within tumor regions (tumor heterogeneity) [146,169,170]. Databases collecting known driver genes and driver mutations can serve as a source for prioritizing potential neo-epitopes. Otherwise identification of broadly expressed mutations via NGS is difficult as only a small proportion of the tumor is analyzed which is even contaminated with healthy tissue.

Spontaneous immune responses as an indication for therapeutic relevance

In addition to *in silico* methods, selection of relevant vaccine targets can be supported by experimental procedures. Preexisting neo-antigen specific T-cell responses identified i*n vitro* not only prove the immunogenicity of the target but corroborate that the cognate antigen is sufficiently expressed, processed and presented.

4.6 Challenges and Hurdles of Personalized Cancer Vaccination

Besides the prediction of relevant vaccine candidates (section 4.5), several challenges and hurdles of personalized cancer vaccination such as an immunosuppressive tumor microenvironment, tumor heterogeneity or immune editing exist which are discussed in more detail below.

T-cell frequency and memory

High avidity, high frequency and long-lasting memory of tumor-specific T cells is necessary to permanently eradicate tumors. We observed that T-cell frequencies induced with most neo-epitope or TAA specific vaccines (irrespective of the format) stay below 5 % despite repetitive vaccination (data

not shown). In some cases, this might be enough to shrink tumors or prevent recurrence after minimal residual disease. However, large established tumors are probably difficult to treat with such T-cell frequencies. Understanding the reason for this might help to overcome this limitation. It is thought that the naive T-cell precursor frequency is dictating the magnitude of an immune response [221,222]. Effector T-cell responses induced via vaccination, however, are rather short lived and might not contribute significantly to the overall amount of induced T cells. Thus, broadening the naive T-cell pool against the respective antigen or inducing long lived T cells with a better potential to proliferate might help to increase the T-cell frequency. In this regard, memory T cells and in particular stem cell memory T cells (T_{SCM}) were shown to be long-lived and have a high proliferative potential [223, 224]. Additionally, preferential induction of T_{SCM} cells might further boost long-term memory, although potent induction of T-cell memory was already demonstrated after RNA neo-epitope vaccination (Figure 3.13).

Alternatively, adoptive cell transfer of *in vitro* expanded or TCR-transduced neo-antigen specific T-cell might be helpful to increase the frequency of tumor-specific T cells (Figure 4.4).

Tumor induced immunosuppression, immunoediting and immune escape

Cancer is an extremely complex disease which is, despite major advances in the last years, far from being completely understood. Dissecting the resistance mechanisms of tumors to T-cell responses and developing biomarkers will help to decide if vaccination alone might be efficient in a particular patient or if combinations with other drugs are needed. Several resistance mechanisms of tumors including recruitment of suppressive immune cells (MDSCs, T_{regs}, TAMs etc.), production of suppressive molecules (PD-L1, IDO, FAS-L, ROS etc.) and generation of an aberrant vasculature that affects T-cell infiltration and function have been observed in cancer patients (reviewed in [24, 225], see also Table 1.1), however, a comprehensive understanding of the frequency, distribution and importance of those single escape mechanisms is lacking. In addition, T-cell function and survival in the tumor might be severely compromised by an unphysiologic pH and hypoxia. Combining individualized vaccines against cancer with agents that modulate the suppressive tumor microenvironment might be beneficial for a subpopulation of patients.

Tumor-specific T cells were shown to induce evolutionary pressure on tumor cells selecting tumor clones with low immunogenicity (immunoediting [21]) ultimately leading to immune escape (see section 1.2). For this reason, pentatope vaccines are especially attractive as multiple T-cell targets reduce the risk of immune escape.

Regarding tumors that lost expression of MHC class I which is known to regularly occur [226], one might prefer the selection of predicted MHC class II restricted neo-eptiopes for vaccination. However, even though tumors are MHC class I negative, $CD8^+$ T cells might induce tumor control through targeting of the tumor vasculature which cross-presents tumor antigens from dying tumor cells or tumor exosomes or by secretion of IFN-γ and other inflammatory cytokines after recognition of their cognate antigen on APCs or stromal cells [172, 227].

Tumor heterogeneity

As mentioned before (section 4.5), heterogeneity of tumors [146] might prevent the complete destruction of all malignant cells. If only a fraction of tumor cells are expressing the antigen, those malignant cells might survive and cause disease relapse. This can be especially problematic for $CD8^+$ T-cell responses as they directly kill tumor cells whereas $CD4^+$ T cells usually recognize their cognate antigen on APCs and indirectly affect tumor growth through IFN-γ or the induction of NK cells, B cells, DCs, macrophages, or a diverse set of $CD8^+$ T cells. For immunogenic tumors with high numbers of tumor antigens (such as CT26), this is probably not a prominent problem, as epitope spreading readily broadens the T-cell response. Nonetheless, the risk of disease relapse can be reduced if antigens are targeted that are expressed on the majority of tumor cells (e.g. driver mutations). NGS of several metastases or sequencing of circulating tumor derived DNA [228] could help identifying those broadly expressed mutations. Moreover, targeting several neo-epitopes via pentatopes increases the chance to target most tumor subclones.

Clinical studies in well chosen patients are needed

Individualized vaccines against cancer were shown to be effective in B16F10 and CT26 tumors of murine origin. Due to the large fraction of immunogenic mutations, this therapy should be applicable to almost all human cancer types. Nevertheless, even though mouse tumor models are established systems to study the efficacy of a drug, clinical trials with well chosen patients need to be performed. Importantly, patients should not be pretreated with immunosupressive drugs such as corticosteroids, myelosuppressive chemotherapy and high-dose radiotherapy or suffer from systemic immune suppression (e.g. HIV). Only patients with an intact immune system are able to mount strong immune responses that can affect tumor growth. In this regard, the patients age might be a crucial factor. With age the risk of developing cancer severely increases while the capacity of the immune system decreases.

Moreover, the tumor type might influence the efficacy of individualized vaccines. Tumor entities largely differ in the amount of mutations (Figure 1.2), immunosuppression and accessibility by immune cells. At this point of time, it is unclear which cancer patients are most likely to benefit from neo-epitope vaccines. A high mutational load increases the amount of potential targets and the chance of high-avidity and highly expressed neo-epitopes. However, tumor types with high mutational load (e.g. melanoma) have a higher chance of preexisting T-cell responses that trigger immunosupression and immune escape (e.g. mutated MHC class I) therefore potentially exacerbating the success of T-cell vaccines and ACT. In comparison, tumor types with a low mutational load have a lower chance of preexisting immune responses. Thus, these tumors were less likely exposed to T-cell pressure which potentially would have induced immunosupression and immune escape. On the other hand, the number of good vaccine targets might be lower in these tumors. Especially difficult might be the treatment of cancers that tend to be immunosuppressive and lack high numbers of neo-epitopes (e.g. pancreatic cancer). Regarding the accessibility of tumors, cancer in tissues that are naturally highly infiltrated by T cells (e.g. the lung and gut) might be more suitable for neo-epitope vaccination as compared to tumors in immune privileged sites (e.g. the CNS or the eye).

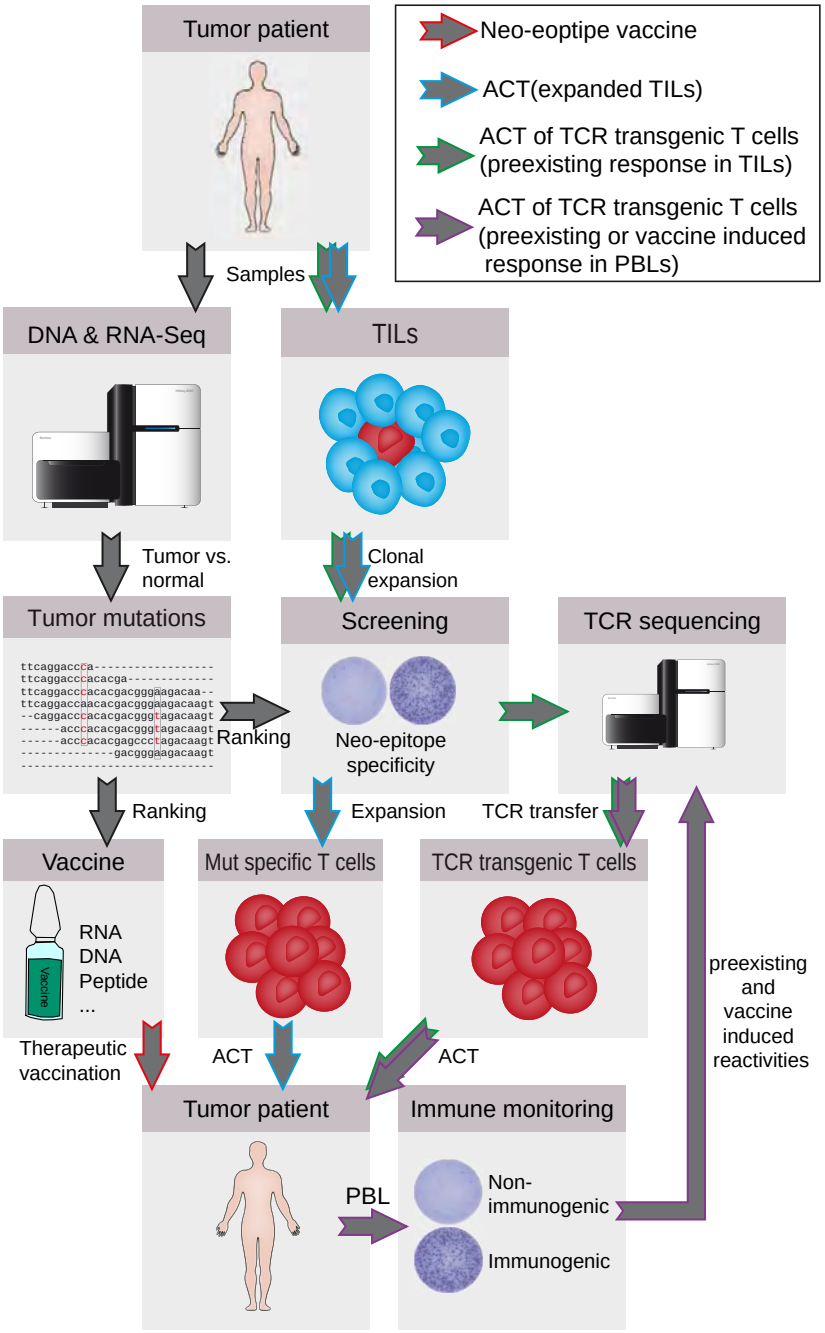

Figure 4.4: Personalized neo-antigen specific vaccination and ACT. The flow chart describes the schematic procedure for personalized mutanome vaccination and ACT. Tumor and healthy tissue are subjected to Exome and RNA sequencing in order to identify tumor mutations (black arrows). Selected mutations can constitute targets for personalized vaccination (red arrow). For expansion and transfer of neo-antigen specific T cells, TIL clones are tested for recognition of selected tumor mutations. Responding clones will be further expanded and infused (blue arrow). For ACT of TCR transgenic T cells, TCRs of responding T cell clones are identified via RNA sequencing (green arrow). Alternatively, sorted neo-antigen specific T cells from the blood patients with spontaneous or vaccine induced T-cell responses are subjected to TCR sequencing (purple arrow). TCR transgenic T cells can then be generated and infused for personalized ACT. ACT: adoptive cell transfer, TCR: T-cell receptor, PBLs: peripheral blood lymphocytes, TILs: tumor-infiltrating leukocytes.

4.7 Relevance of this Thesis

The lifetime risk of developing cancer is almost 50 % with one out of four patients dying of the disease [229]. Despite meaningful efforts, standard of care treatments are unsatisfactory for many tumor types. The recent clinical success of cancer immunotherapies such as adoptive cell transfer of T cells and immune checkpoint blocking antibodies exemplifies the potency of tumor-specific T cells against cancer. Especially mutated antigens seem to constitute important targets of anti-tumoral T cells due to lack of tolerance and their high abundance. Addressing these mutated targets directly with vaccines requires an individualized, patient-centered therapy. Our group pioneered the concept of tailored neo-epitope vaccines for cancer treatment and showed for the first time its feasability in mouse models. The presented approach integrates several highly innovative technologies into a process for a universally applicable, but truly individualized tumor therapy and therefore initiates a paradigm shift in cancer treatment.

In this thesis, it was shown that cancer mutations represent a rich source of tumor-specific antigens. Combining NGS, computational immunology as well as customized RNA vaccines allowed the identification of a novel immunological principle. We showed that a considerable fraction of non-synonymous cancer mutations is immunogenic and unexpectedly pre-dominantly recognized by highly potent $CD4^+$ T cells. Notably, the superiority of multi-epitope vaccines was established. In combination with an advanced selection algorithm based on MHC class II binding prediction and expression levels of the mutated allele, therapeutic tumor control without prior immunogenicity testing or target validation was possible. Several experiments showed *in vitro* as well as *in vivo* that the therapeutic efficacy of neo-epitope specific $CD4^+$ T cells in the CT26 tumor model depends on CD40L-mediated licensing of DCs and the subsequent priming of tumor-specific $CD8^+$ T cells.

The preclinical data in mouse tumor models presented here established the feasibility of individualized cancer vaccines and raised hopes that this concept will be effective in humans as well. The results shown in this thesis paved the way and directly influenced the design (in particular the vaccine format and mutation selection) of clinical studies in melanoma and triple-negative breast cancer patients (NCT02035956, NCT02316457).

References

[1] Kaatsch, P., Spix, C., Katalinic, A. & Hentschel, S. *Krebs in Deutschland 2007/2008.* (Robert Koch-Institut und die Gesellschaft der epidemiologischen Krebsregister in Deutschland e.V., Berlin, 2012), 8. edn. 1

[2] Hanahan, D., Weinberg, R. a. & Francisco, S. The Hallmarks of Cancer. *Cell* **100**, 57–70 (2000). 1

[3] Linzer, D. I. & Levine, A. J. Characterization of a 54K dalton cellular SV40 tumor antigen present in SV40-transformed cells and uninfected embryonal carcinoma cells. *Cell* **17**, 43–52 (1979). 1

[4] Jacks, T. *et al.* Effects of an Rb mutation in the mouse. *Nature* **359**, 295–300 (1992). 1

[5] Nishisho, I. *et al.* Mutations of chromosome 5q21 genes in FAP and colorectal cancer patients. *Science* **253**, 665–669 (1991). 1

[6] Chang, E. H., Gonda, M. A., Ellis, R. W., Scolnick, E. M. & Lowy, D. R. Human genome contains four genes homologous to transforming genes of Harvey and Kirsten murine sarcoma viruses. *Proc. Natl. Acad. Sci. U. S. A.* **79**, 4848–52 (1982). 1

[7] Jones, P. a. & Baylin, S. B. The fundamental role of epigenetic events in cancer. *Nat. Rev. Genet.* **3**, 415–28 (2002). 1

[8] Wan, G., Mathur, R., Hu, X., Zhang, X. & Lu, X. miRNA response to DNA damage. *Trends Biochem. Sci.* **36**, 478–84 (2011). 1

[9] Rosen, H. R. Chronic Hepatitis C Infection. *N. Engl. J. Med.* **364**, 2429–2438 (2011). 1

[10] Hodgson, J. T. & Darnton, A. The quantitative risks of mesothelioma and lung cancer in relation to asbestos exposure. *Ann. Occup. Hyg.* **44**, 565–601 (2000). 1

[11] Hanahan, D. & Weinberg, R. a. Hallmarks of cancer: the next generation. *Cell* **144**, 646–674 (2011). URL `http://www.ncbi.nlm.nih.gov/pubmed/21376230`. 2

[12] Coley, W. B. The treatment of malignant tumors by repeated inoculations of erysipelas. With a report of ten original cases. 1893. *Am J Med Sci* **105**, 487–510 (1893). 2

[13] Coley, W. B. II. Contribution to the Knowledge of Sarcoma. *Ann. Surg.* **14**, 199–220 (1891). 2

[14] Ehrlich, P. Ueber den jetzigen stand der Karzinomforschung. *Ned.Tijdschr. Geneeskd.* **5**, 273–290 (1909). 2

[15] Gorer, P. A., Lyman, S. & Snell, G. D. Studies on the genetic and antigenic basis of tumour transplantation. Linkage between a histocompatibility gene and 'fused' in mice. *Proc. R. Soc. London B Biol. Sci.* **135**, 499–505 (1948). 2, 65

[16] Little, C. & Strong, L. Genetic studies on the transplantation of two adenocarcinomata. *J. Exp. Zool.* **41**, 93–114 (1924). 2

[17] Strong, L. C. The establishment of the C3H inbred strain of mice for the study of spontaneous carcinoma of the mammary gland. *Genetics* **20**, 586 (1935). 2

[18] Foley, E. J. Antigenic properties of methylcholanthrene-induced tumors in mice of the strain of origin. *Cancer Res.* **13**, 835–837 (1953). 2, 65

[19] Prehn, R. T. & Main, J. M. Immunity to methylcholanthrene-induced sarcomas. *J. Natl. Cancer Inst.* **18**, 769–778 (1957). 2, 65

[20] Burnet, M. Cancer-A Biological Approach: I. The Processes Of Control. II. The Significance of Somatic Mutation. *Br. Med. J.* **1**, 779–86 (1957). 2

[21] Dunn, G. P., Bruce, A. T., Ikeda, H., Old, L. J. & Schreiber, R. D. Cancer immunoediting: from immunosurveillance to tumor escape. *Nat. Immunol.* **3**, 991–998 (2002). 2, 49, 74

[22] Shankaran, V. *et al.* IFNγ and lymphocytes prevent primary tumour development and shape tumour immunogenicity. *Nature* **410**, 1107–1111 (2001). 2

[23] Chen, D. S. S. & Mellman, I. Oncology meets immunology: The cancer-immunity cycle. *Immunity* **39**, 1–10 (2013). 3, 65

[24] Motz, G. T. & Coukos, G. The parallel lives of angiogenesis and immunosuppression: cancer and other tales. *Nat. Rev. Immunol.* **11**, 702–711 (2011). 3, 74

[25] Rabinovich, G. a., Gabrilovich, D. & Sotomayor, E. M. Immunosuppressive strategies that are mediated by tumor cells. *Annu. Rev. Immunol.* **25**, 267–96 (2007). 3

[26] Whiteside, T. L. The tumor microenvironment and its role in promoting tumor growth. *Oncogene* **27**, 5904–12 (2008). 3

[27] Melero, I. *et al.* Evolving synergistic combinations of targeted immunotherapies to combat cancer. *Nat. Rev. Cancer* **15**, 457–72 (2015). 3, 64

[28] Larkin, J. *et al.* Combined Nivolumab and Ipilimumab or Monotherapy in Untreated Melanoma. *N. Engl. J. Med.* **373**, 23–34 (2015). 3, 14, 67

[29] Klein, L., Hinterberger, M., Wirnsberger, G. & Kyewski, B. Antigen presentation in the thymus for positive selection and central tolerance induction. *Nat. Rev. Immunol.* **9**, 833–844 (2009). 4

[30] Linette, G. P. *et al.* Cardiovascular toxicity and titin cross-reactivity of affinity-enhanced T cells in myeloma and melanoma. *Blood* **122**, 863–71 (2013). 4

[31] Kawashima, I. *et al.* Identification of HLA-A3-restricted cytotoxic T lymphocyte epitopes from carcinoembryonic antigen and HER-2/neu by primary in vitro immunization with peptide-pulsed dendritic cells. *Cancer Res* **59**, 431–435 (1999). 4

[32] Schmitz, M. *et al.* Generation of survivin-specific CD8+ T effector cells by dendritic cells pulsed with protein or selected peptides. *Cancer Res* **60**, 4845–4849 (2000). 4

[33] Weinzierl, A. O. *et al.* A cryptic vascular endothelial growth factor T-cell epitope: identification and characterization by mass spectrometry and T-cell assays. *Cancer Res.* **68**, 2447–54 (2008). 4

[34] Vonderheide, R. H., Hahn, W. C., Schultze, J. L. & Nadler, L. M. The telomerase catalytic subunit is a widely expressed tumor-associated antigen recognized by cytotoxic T lymphocytes. *Immunity* **10**, 673–679 (1999). 4

[35] Kang, X. *et al.* Identification of a tyrosinase epitope recognized by HLA-A24-restricted, tumor-infiltrating lymphocytes. *J Immunol* **155**, 1343–1348 (1995). 4, 5

[36] Jäger, D. *et al.* Identification of a tissue-specific putative transcription factor in breast tissue by serological screening of a breast cancer library. *Cancer Res.* **61**, 2055–61 (2001). 4, 10

[37] Bioley, G. *et al.* Melan-A/MART-1-specific CD4 T cells in melanoma patients: identification of new epitopes and ex vivo visualization of specific T cells by MHC class II tetramers. *J Immunol* **177**, 6769–6779 (2006). 4

[38] Wang, R. F., Parkhurst, M. R., Kawakami, Y., Robbins, P. F. & Rosenberg, S. A. Utilization of an alternative open reading frame of a normal gene in generating a novel human cancer antigen. *J Exp Med* **183**, 1131–1140 (1996). 4

[39] GOLD, P. & FREEDMAN, S. O. Demonstration of tumor-specific antigens in human colonic carcinomata by immunological tolerance and absorption techniques. *J. Exp. Med.* **121**, 439–62 (1965). 4

[40] van der Bruggen, P. *et al.* A gene encoding an antigen recognized by cytolytic T lymphocytes on a human melanoma. *Science* **254**, 1643–7 (1991). 4, 10

[41] van der Bruggen, P. *et al.* A peptide encoded by human gene MAGE-3 and presented by HLA-A2 induces cytolytic T lymphocytes that recognize tumor cells expressing MAGE-3. *Eur. J. Immunol.* **24**, 3038–43 (1994). 4

[42] Boel, P. *et al.* BAGE: a new gene encoding an antigen recognized on human melanomas by cytolytic T lymphocytes. *Immunity* **2**, 167–175 (1995). 4

[43] Chen, Y. T. *et al.* A testicular antigen aberrantly expressed in human cancers detected by autologous antibody screening. *Proc. Natl. Acad. Sci. U. S. A.* **94**, 1914–8 (1997). 4, 10

[44] Bosch, G. J., Joosten, A. M., Kessler, J. H., Melief, C. J. & Leeksma, O. C. Recognition of BCR-ABL positive leukemic blasts by human CD4+ T cells elicited by primary in vitro immunization with a BCR-ABL breakpoint peptide. *Blood* **88**, 3522–3527 (1996). 4, 5, 6

[45] Wang, R. F., Wang, X., Atwood, A. C., Topalian, S. L. & Rosenberg, S. A. Cloning genes encoding MHC class II-restricted antigens: mutated CDC27 as a tumor antigen. *Science* **284**, 1351–1354 (1999). 4

[46] Gjertsen, M. K., Bjorheim, J., Saeterdal, I., Myklebust, J. & Gaudernack, G. Cytotoxic CD4+ and CD8+ T lymphocytes, generated by mutant p21-ras (12Val) peptide vaccination of a patient, recognize 12Val-dependent nested epitopes present within the vaccine peptide and kill autologous tumour cells carrying this mutation. *Int. J. Cancer* **72**, 784–90 (1997). 4, 5

[47] Ito, D. *et al.* Immunological characterization of missense mutations occurring within cytotoxic T cell-defined p53 epitopes in HLA-A*0201+ squamous cell carcinomas of the head and neck. *Int. J. Cancer* **120**, 2618–24 (2007). 4, 5

[48] Wölfel, T. *et al.* A p16INK4a-insensitive CDK4 mutant targeted by cytolytic T lymphocytes in a human melanoma. *Science* **269**, 1281–1284 (1995). 4, 12

[49] Kreiter, S. *et al.* Mutant MHC class II epitopes drive therapeutic immune responses to cancer. *Nature* **520**, 692–696 (2015). 4, 6, 16, 18, 20, 36, 48, 67, 69, 70

[50] Castle, J. C. *et al.* Exploiting the mutanome for tumor vaccination. *Cancer Res.* **72**, 1081–1091 (2012). 4, 19, 36, 48, 65, 67, 69

[51] zur Hausen, H. Papillomaviruses in human cancers. *Proc Assoc Am Physicians* **111**, 581–587 (1999). 4

[52] Lee, M. S. *et al.* Hepatitis B vaccination and reduced risk of primary liver cancer among male adults: a cohort study in Korea. *Int J Epidemiol* **27**, 316–319 (1998). 4

[53] Parkhurst, M. R. *et al.* T cells targeting carcinoembryonic antigen can mediate regression of metastatic colorectal cancer but induce severe transient colitis. *Mol. Ther.* **19**, 620–6 (2011). 5

[54] Bos, R. *et al.* Balancing between antitumor efficacy and autoimmune pathology in T-cell-mediated targeting of carcinoembryonic antigen. *Cancer Res.* **68**, 8446–55 (2008). 5

[55] Palmer, D. C. *et al.* Effective tumor treatment targeting a melanoma/melanocyte-associated antigen triggers severe ocular autoimmunity. *Proc. Natl. Acad. Sci. U. S. A.* **105**, 8061–6 (2008). 5

[56] van den Berg, J. H. *et al.* Case report of a fatal Serious Adverse Event upon administration of T cells transduced with a MART-1 specific T cell receptor. *Mol. Ther.* 1–10 (2015). 5

[57] Gotter, J., Brors, B., Hergenhahn, M. & Kyewski, B. Medullary epithelial cells of the human thymus express a highly diverse selection of tissue-specific genes colocalized in chromosomal clusters. *J. Exp. Med.* **199**, 155–166 (2004). 5

[58] Kenter, G. G. *et al.* Vaccination against HPV-16 oncoproteins for vulvar intraepithelial neoplasia. *N. Engl. J. Med.* **361**, 1838–47 (2009). 5

[59] Vormehr, M. *et al.* Mutanome directed cancer immunotherapy. *Curr. Opin. Immunol.* **39**, 14–22 (2015). 6, 19

[60] Alexandrov, L. B. *et al.* Signatures of mutational processes in human cancer. *Nature* **500**, 415–421 (2013). 6, 36

[61] Popp, M. W.-L. & Maquat, L. E. Organizing principles of mammalian nonsense-mediated mRNA decay. *Annu. Rev. Genet.* **47**, 139–65 (2013). 6

[62] Duan, F. *et al.* Genomic and bio-informatic profiling of mutational neo-epitopes reveals new rules to predict anti-cancer immunogenicity. *J. Exp. Med.* **211**, 2231–2248 (2014). 8, 19, 57, 63, 68, 72

[63] Yadav, M. *et al.* Predicting immunogenic tumour mutations by combining mass spectrometry and exome sequencing. *Nature* **515**, 572–576 (2014). 8, 19, 57, 63, 72

[64] Spierings, E. *et al.* The minor histocompatibility antigen HA-3 arises from differential proteasome-mediated cleavage of the lymphoid blast crisis (Lbc) oncoprotein. *Blood* **102**, 621–629 (2003). 8

[65] Pierce, R. a. *et al.* The HA-2 minor histocompatibility antigen is derived from a diallelic gene encoding a novel human class I myosin protein. *J. Immunol.* **167**, 3223–3230 (2001). 8, 12

[66] Kessler, J. H. & Melief, C. J. M. Identification of T-cell epitopes for cancer immunotherapy. *Leukemia* **21**, 1859–1874 (2007). 10, 11

[67] Rammensee, H., Bachmann, J., Emmerich, N. P., Bachor, O. a. & Stevanović, S. SYFPEITHI: database for MHC ligands and peptide motifs. *Immunogenetics* **50**, 213–219 (1999). 10, 11, 26

[68] Skipper, J. C. *et al.* An HLA-A2-restricted tyrosinase antigen on melanoma cells results from posttranslational modification and suggests a novel pathway for processing of membrane proteins. *J Exp Med* **183**, 527–534 (1996). 10

[69] Sahin, U. *et al.* Human neoplasms elicit multiple specific immune responses in the autologous host. *Proc. Natl. Acad. Sci. U. S. A.* **92**, 11810–11813 (1995). 10

[70] Chen, Y. T. *et al.* Identification of multiple cancer/testis antigens by allogeneic antibody screening of a melanoma cell line library. *Proc Natl Acad Sci U S A* **95**, 6919–6923 (1998). 10

[71] SEREX-defined Antigens - Cancer Immunity Database (2015-10-27). URL `http://cancerimmunity.org/serex/tumor-type/`. 10

[72] Linnemann, T. *et al.* Mimotopes for tumor-specific T lymphocytes in human cancer determined with combinatorial peptide libraries. *Eur J Immunol* **31**, 156–165 (2001). 10

[73] Siewert, K. *et al.* Unbiased identification of target antigens of CD8+ T cells with combinatorial libraries coding for short peptides. *Nat Med* **18**, 824–828 (2012). 10

[74] Human Genome Project Completion: Frequently Asked Questions (2015-09-22). URL `http://www.genome.gov/11006943`. 11

[75] Check Hayden, E. Technology: The $1,000 genome. *Nature* **507**, 294–295 (2014). 11

[76] van der Burg, S. H., Visseren, M. J., Brandt, R. M., Kast, W. M. & Melief, C. J. Immunogenicity of peptides bound to MHC class I molecules depends on the MHC-peptide complex stability. *J Immunol* **156**, 3308–3314 (1996). 11, 72

[77] Vita, R. *et al.* The immune epitope database (IEDB) 3.0. *Nucleic Acids Res.* **43**, D405–D412 (2014). 11, 26, 35

[78] Hoof, I. *et al.* NetMHCpan, a method for MHC class i binding prediction beyond humans. *Immunogenetics* **61**, 1–13 (2009). 11

[79] Reche, P. A., Glutting, J.-P. & Reinherz, E. L. Prediction of MHC class I binding peptides using profile motifs. *Hum Immunol* **63**, 701–709 (2002). 11

[80] Trolle, T. *et al.* Automated benchmarking of peptide-MHC class I binding predictions. *Bioinformatics* 1–8 (2015). 11

[81] Nielsen, M., Lund, O., Buus, S. r. & Lundegaard, C. MHC class II epitope predictive algorithms. *Immunology* **130**, 319–28 (2010). 11, 68, 72

[82] Zaks, T. Z. & Rosenberg, S. A. Immunization with a peptide epitope (p369-377) from HER-2/neu leads to peptide-specific cytotoxic T lymphocytes that fail to recognize HER-2/neu+ tumors. *Cancer Res* **58**, 4902–4908 (1998). 11

[83] Nijman, H. W. *et al.* p53, a potential target for tumor-directed T cells. *Immunol Lett* **40**, 171–178 (1994). 11

[84] Disis, M. L., Smith, J. W., Murphy, A. E., Chen, W. & Cheever, M. A. In vitro generation of human cytolytic T-cells specific for peptides derived from the HER-2/neu protooncogene protein. *Cancer Res* **54**, 1071–1076 (1994). 11

[85] Kuttler, C. *et al.* An algorithm for the prediction of proteasomal cleavages. *J Mol Biol* **298**, 417–429 (2000). 11

[86] Kesmir, C., Nussbaum, A. K., Schild, H., Detours, V. & Brunak, S. Prediction of proteasome cleavage motifs by neural networks. *Protein Eng* **15**, 287–296 (2002). 11

[87] Bhasin, M. & Raghava, G. P. S. Pcleavage: an SVM based method for prediction of constitutive proteasome and immunoproteasome cleavage sites in antigenic sequences. *Nucleic Acids Res* **33**, W202—-W207 (2005). 11

[88] Holzhütter, H. G., Froemmel, C. & Kloetzel, P. M. A theoretical approach towards the identification of cleavage-determining amino acid motifs of the 20 S proteasome. *J Mol Biol* **286**, 1251–1265 (1999). 11

[89] Calis, J. J. a. *et al.* Properties of MHC Class I Presented Peptides That Enhance Immunogenicity. *PLoS Comput. Biol.* **9** (2013). 12

[90] Pascolo, S. *et al.* A MAGE-A1 HLA-A A*0201 epitope identified by mass spectrometry. *Cancer Res* **61**, 4072–4077 (2001). 12

[91] Kessler, J. H. *et al.* Efficient identification of novel HLA-A(*)0201-presented cytotoxic T lymphocyte epitopes in the widely expressed tumor antigen PRAME by proteasome-mediated digestion analysis. *J Exp Med* **193**, 73–88 (2001). 12

[92] Asemissen, A. M. *et al.* Identification of a highly immunogenic HLA-A*01-binding T cell epitope of WT1. *Clin Cancer Res* **12**, 7476–7482 (2006). 12

[93] Boon, T. & Kellermann, O. Rejection by syngeneic mice of cell variants obtained by mutagenesis of a malignant teratocarcinoma cell line. *Proc. Natl. Acad. Sci. U. S. A.* **74**, 272–275 (1977). 12

[94] den Haan, J. M. *et al.* Identification of a graft versus host disease-associated human minor histocompatibility antigen. *Science* **268**, 1476–1480 (1995). 12

[95] De Rijke, B. *et al.* A frameshift polymorphism in P2X5 elicits an allogeneic cytotoxic T lymphocyte response associated with remission of chronic myeloid leukemia. *J. Clin. Invest.* **115**, 3506–3516 (2005). 12, 71

[96] Dolstra, H. *et al.* A human minor histocompatibility antigen specific for B cell acute lymphoblastic leukemia. *J. Exp. Med.* **189**, 301–8 (1999). 12

[97] Lennerz, V. *et al.* The response of autologous T cells to a human melanoma is dominated by mutated neoantigens. *Proc. Natl. Acad. Sci. U. S. A.* **102**, 16013–8 (2005). 12

[98] Le, D. T. *et al.* PD-1 Blockade in Tumors with Mismatch-Repair Deficiency. *N. Engl. J. Med.* **372**, 2509–2520 (2015). 12, 15, 67

[99] Gryfe, R. *et al.* Tumor microsatellite instability and clinical outcome in young patients with colorectal cancer. *N. Engl. J. Med.* **342**, 69–77 (2000). 12, 66

[100] Maby, P. *et al.* Correlation between Density of CD8+ T-cell Infiltrate in Microsatellite Unstable Colorectal Cancers and Frameshift Mutations: A Rationale for Personalized Immunotherapy. *Cancer Res.* **75**, 3446–3455 (2015). 12, 66, 71

[101] Galon, J. *et al.* Type, density, and location of immune cells within human colorectal tumors predict clinical outcome. *Science* **313**, 1960–1964 (2006). 12

[102] Brown, S. D. *et al.* Neo-antigens predicted by tumor genome meta-analysis correlate with increased patient survival. *Genome Res.* **24**, 743–750 (2014). 14

[103] Dudley, M. E. *et al.* Cancer regression and autoimmunity in patients after clonal repopulation with antitumor lymphocytes. *Science* **298**, 850–854 (2002). 14

[104] Dudley, M. E. *et al.* Adoptive cell transfer therapy following non-myeloablative but lymphodepleting chemotherapy for the treatment of patients with refractory metastatic melanoma. *J. Clin. Oncol.* **23**, 2346–2357 (2005). 14

[105] Lu, Y.-C. *et al.* Mutated PPP1R3B is recognized by T cells used to treat a melanoma patient who experienced a durable complete tumor regression. *J. Immunol.* **190**, 6034–6042 (2013). 14

[106] Tran, E. *et al.* Cancer immunotherapy based on mutation-specific CD4+ T cells in a patient with epithelial cancer. *Science* **344**, 641–645 (2014). 14, 68

[107] Maus, M. V., Grupp, S. a., Porter, D. L. & June, C. H. Antibody-modified T cells: CARs take the front seat for hematologic malignancies. *Blood* **123**, 2625–35 (2014). 14

[108] Maus, M. V. *et al.* Adoptive immunotherapy for cancer or viruses. *Annu. Rev. Immunol.* **32**, 189–225 (2014). 14

[109] Postow, M. a. *et al.* Nivolumab and ipilimumab versus ipilimumab in untreated melanoma. *N. Engl. J. Med.* **372**, 2006–17 (2015). 14

[110] Wolchok, J. D. *et al.* Nivolumab plus ipilimumab in advanced melanoma. *N. Engl. J. Med.* **369**, 122–33 (2013). 14

[111] Ansell, S. M. *et al.* PD-1 Blockade with Nivolumab in Relapsed or Refractory Hodgkin's Lymphoma. *N. Engl. J. Med.* **372**, 311–319 (2014). 14

[112] Topalian, S. L. *et al.* Safety, activity, and immune correlates of anti-PD-1 antibody in cancer. *N. Engl. J. Med.* **366**, 2443–54 (2012). 14, 15

[113] Robert, C. *et al.* Pembrolizumab versus Ipilimumab in Advanced Melanoma. *N. Engl. J. Med.* **372**, 2521–3532 (2015). 14, 67

[114] Pardoll, D. M. The blockade of immune checkpoints in cancer immunotherapy. *Nat. Rev. Cancer* **12**, 252–264 (2012). 14

[115] Tumeh, P. C. *et al.* PD-1 blockade induces responses by inhibiting adaptive immune resistance. *Nature* **515**, 568–571 (2014). 14, 15, 64, 66

[116] Herbst, R. S. *et al.* Predictive correlates of response to the anti-PD-L1 antibody MPDL3280A in cancer patients. *Nature* **515**, 563–567 (2014). 14, 15, 64, 67

[117] Kvistborg, P. *et al.* Anti-CTLA-4 therapy broadens the melanoma-reactive CD8+ T cell response. *Sci. Transl. Med.* **6**, 254ra128 (2014). 14

[118] Corbière, V. *et al.* Antigen spreading contributes to MAGE vaccination-induced regression of melanoma metastases. *Cancer Res.* **71**, 1253–1262 (2011). 14

[119] Huang, J. *et al.* T cells associated with tumor regression recognize frameshifted products of the CDKN2A tumor suppressor gene locus and a mutated HLA class I gene product. *J. Immunol.* **172**, 6057–64 (2004). 14, 71

[120] van der Bruggen, P Stroobant, V., Vigneron, N. & Van den Eynde, B. Peptide database: T cell-defined tumor antigens (2015-12-12). *Cancer Immun* (2013). URL `http://www.cancerimmunity.org/peptide/`. 14

[121] Zhou, J., Dudley, M. E., Rosenberg, S. a. & Robbins, P. F. Persistence of multiple tumor-specific T-cell clones is associated with complete tumor regression in a melanoma patient receiving adoptive cell transfer therapy. *J. Immunother.* **28**, 53–62 (2005). 14

[122] Robbins, P. F. *et al.* Mining exomic sequencing data to identify mutated antigens recognized by adoptively transferred tumor-reactive T cells. *Nat. Med.* **19**, 747–752 (2013). 14, 57

[123] Linnemann, C. *et al.* High-throughput epitope discovery reveals frequent recognition of neo-antigens by CD4+ T cells in human melanoma. *Nat. Med.* **21**, 81–85 (2015). 14, 63, 66

[124] Tran, E. *et al.* Immunogenicity of somatic mutations in human gastrointestinal cancers. *Science* aad1253 (2015). 14, 63, 68

[125] Cohen, C. J. *et al.* Isolation of neoantigen-specific T cells from tumor and peripheral lymphocytes. *J. Clin. Invest.* **125**, 3981–3991 (2015). 14

[126] Gubin, M. M. *et al.* Checkpoint blockade cancer immunotherapy targets tumour-specific mutant antigens. *Nature* **515**, 577–581 (2014). 14, 18, 63

[127] Woller, N. *et al.* Viral Infection of Tumors Overcomes Resistance to PD-1-immunotherapy by Broadening Neoantigenome-directed T-cell Responses. *Mol. Ther.* **10**, 1630–1640 (2015). 14, 15, 66

[128] Snyder, A. *et al.* Genetic Basis for Clinical Response to CTLA-4 Blockade in Melanoma. *N. Engl. J. Med.* **371**, 2189–2199 (2014). 14, 66

[129] Rizvi, N. A. *et al.* Mutational landscape determines sensitivity to PD-1 blockade in non-small cell lung cancer. *Science* **348**, 124–128 (2015). 14, 15, 66

[130] Van Allen, E. M. *et al.* Genomic correlates of response to CTLA-4 blockade in metastatic melanoma. *Science* **350**, 207–211 (2015). 14, 66

[131] Gubin, M. M. & Schreiber, R. D. The odds of immunotherapy success. *Science* **350**, 158–159 (2015). 14, 65

[132] Hinrichs, C. S. & Rosenberg, S. a. Exploiting the curative potential of adoptive T-cell therapy for cancer. *Immunol. Rev.* **257**, 56–71 (2014). 14

[133] Restifo, N. P., Dudley, M. E. & Rosenberg, S. A. Adoptive immunotherapy for cancer: harnessing the T cell response. *Nat Rev Immunol* **12**, 269–281 (2012). 14

[134] Hodi, F. & O'Day, S. Improved survival with ipilimumab in patients with metastatic melanoma. *N Engl J Med* **363**, 711–723 (2010). 14

[135] Hamid, O. *et al.* Safety and tumor responses with lambrolizumab (anti-PD-1) in melanoma. *N. Engl. J. Med.* **369**, 134–44 (2013). 14

[136] Lynch, T. J. *et al.* Ipilimumab in combination with paclitaxel and carboplatin as first-line treatment in stage IIIB/IV non-small-cell lung cancer: Results from a randomized, double-blind, multicenter phase II study. *J. Clin. Oncol.* **30**, 2046–2054 (2012). 15

[137] Garon, E. B. *et al.* Pembrolizumab for the treatment of non-small-cell lung cancer. *N. Engl. J. Med.* **372**, 2018–28 (2015). 15, 67

[138] Plimack, E. R. *et al.* Pembrolizumab (MK-3475) for advanced urothelial cancer: Updated results and biomarker analysis from KEYNOTE-012. *J. Clin. Oncol.* **33**, (suppl; abstr 4502) (2015). 15, 67

[139] Powles, T. *et al.* MPDL3280A (anti-PD-L1) treatment leads to clinical activity in metastatic bladder cancer. *Nature* **515**, 558–562 (2014). 15, 67

[140] Doi, T. *et al.* Pembrolizumab (MK-3475) for patients (pts) with advanced esophageal carcinoma: Preliminary results from KEYNOTE-028. *J. Clin. Invest.* **33**, (suppl; abstr 4010) (2015). 15, 67

[141] Seiwert, T. Y. *et al.* Inflamed-phenotype gene expression signatures to predict benefit from the anti-PD-1 antibody pembrolizumab in PD-L1+ head and neck cancer patients. *J. Clin. Oncol.* **33**, (suppl; abstr 6017) (2015). 15, 67

[142] Motzer, R. J. *et al.* Nivolumab versus Everolimus in Advanced Renal-Cell Carcinoma. *N. Engl. J. Med.* 1–11 (2015). 15, 67

[143] El-Khoueiry, A. B. *et al.* Phase I/II safety and antitumor activity of nivolumab in patients with advanced hepatocellular carcinoma (HCC): CA209-040. *J. Clin. Oncol.* **33**, (suppl; abstr LBA101) (2015). 15, 67

[144] Melief, C. J. M., van Hall, T., Arens, R., Ossendorp, F. & van der Burg, S. H. Therapeutic cancer vaccines. *J. Clin. Invest.* **125**, 3401–12 (2015). 15

[145] Melero, I. *et al.* Therapeutic vaccines for cancer: an overview of clinical trials. *Nat. Rev. Clin. Oncol.* **11**, 509–524 (2014). 15, 63

[146] Gerlinger, M. *et al.* Intratumor heterogeneity and branched evolution revealed by multiregion sequencing. *N. Engl. J. Med.* **366**, 883–92 (2012). 15, 49, 73, 75

[147] Matsushita, H. *et al.* Cancer exome analysis reveals a T-cell-dependent mechanism of cancer immunoediting. *Nature* **482**, 400–404 (2012). 15, 18, 57

[148] Löwer, M. *et al.* Confidence-based somatic mutation evaluation and prioritization. *PLoS Comput. Biol.* **8**, e1002714 (2012). 16

[149] Vormehr, M. *et al.* Mutanome Engineered RNA Immunotherapy : Towards Patient-Centered Tumor Vaccination. *J. Immunol. Res.* **2015**, 6 (2015). 16, 17, 19

[150] Nothnagel, M. *et al.* Technology-specific error signatures in the 1000 Genomes Project data. *Hum. Genet.* **130**, 505–516 (2011). 16

[151] Taub, M. A., Corrada Bravo, H. & Irizarry, R. A. Overcoming bias and systematic errors in next generation sequencing data. (2010). 16

[152] Weide, B. *et al.* Direct injection of protamine-protected mRNA: results of a phase 1/2 vaccination trial in metastatic melanoma patients. Tech. Rep. 5 (2009). 17

[153] Rittig, S. M. *et al.* Intradermal vaccinations with RNA coding for TAA generate CD8+ and CD4+ immune responses and induce clinical benefit in vaccinated patients. *Mol. Ther.* **19**, 990–999 (2011). 17

[154] Heiser, A. *et al.* Autologous dendritic cells transfected with prostate-specific antigen RNA stimulate CTL responses against metastatic prostate tumors. *J. Clin. Invest.* **109**, 409–417 (2002). 17

[155] Holtkamp, S. *et al.* Modification of antigen-encoding RNA increases stability, translational efficacy, and T-cell stimulatory capacity of dendritic cells. *Blood* **108**, 4009–17 (2006). 17, 26

[156] Kuhn, A. N. *et al.* Phosphorothioate cap analogs increase stability and translational efficiency of RNA vaccines in immature dendritic cells and induce superior immune responses in vivo. *Gene Ther.* **17**, 961–971 (2010). 17

[157] Schoenberger, S. P., Toes, R. E., van der Voort, E. I., Offringa, R. & Melief, C. J. T-cell help for cytotoxic T lymphocytes is mediated by CD40-CD40L interactions. *Nature* **393**, 480–483 (1998). 17, 52, 55

[158] Sahin, U., Kariko, K. & Tureci, O. mRNA-based therapeutics - developing a new class of drugs. *Nat Rev Drug Discov* **13**, 759–780 (2014). 17, 18, 64

[159] Kreiter, S. *et al.* Increased antigen presentation efficiency by coupling antigens to MHC class I trafficking signals. *J. Immunol.* **180**, 309–318 (2008). 17, 18, 26, 67

[160] Hubo, M. *et al.* Costimulatory molecules on immunogenic versus tolerogenic human dendritic cells. *Front. Immunol.* **4**, 1–14 (2013). 18

[161] Kreiter, S. *et al.* Intranodal vaccination with naked antigen-encoding RNA elicits potent prophylactic and therapeutic antitumoral immunity. *Cancer Res.* **70**, 9031–9040 (2010). 18

[162] Diken, M. *et al.* Selective uptake of naked vaccine RNA by dendritic cells is driven by macropinocytosis and abrogated upon DC maturation. *Gene Ther.* **18**, 702–708 (2011). 18

[163] Granstein, R. D., Ding, W. & Ozawa, H. Induction of anti-tumor immunity with epidermal cells pulsed with tumor- derived RNA or intradermal administration of RNA. *J. Invest. Dermatol.* **114**, 632–636 (2000). 18

[164] Wolff, J. A. *et al.* Direct gene transfer into mouse muscle in vivo. *Science* **247**, 1465–1468 (1990). 18

[165] Blum, J. S., Wearsch, P. a. & Cresswell, P. Pathways of antigen processing. *Annu. Rev. Immunol.* **31**, 443–73 (2013). 18

[166] Lutz, M. B. *et al.* An advanced culture method for generating large quantities of highly pure dendritic cells from mouse bone marrow. *J. Immunol. Methods* **223**, 77–92 (1999). 27

[167] Castle, J. C. *et al.* Immunomic, genomic and transcriptomic characterization of CT26 colorectal carcinoma. *BMC Genomics* **15**, 190 (2014). 36

[168] McPherson, A. *et al.* deFuse: an algorithm for gene fusion discovery in tumor RNA-Seq data. *PLoS Comput. Biol.* **7**, e1001138 (2011). 43

[169] Gundem, G. *et al.* The evolutionary history of lethal metastatic prostate cancer. *Nature* **520**, 353–7 (2015). 49, 73

[170] Yates, L. R. *et al.* Subclonal diversification of primary breast cancer revealed by multiregion sequencing. *Nat. Med.* **21** (2015). 49, 73

[171] Koebel, C. M. *et al.* Adaptive immunity maintains occult cancer in an equilibrium state. *Nature* **450**, 903–7 (2007). 49

[172] Qin, Z. & Blankenstein, T. CD4+ T cell–mediated tumor rejection involves inhibition of angiogenesis that is dependent on IFN gamma receptor expression by nonhematopoietic cells. *Immunity* **12**, 677–86 (2000). 52, 74

[173] Bouwer, A. L. *et al.* NK cells are required for dendritic cell-based immunotherapy at the time of tumor challenge. *J. Immunol.* **192**, 2514–21 (2014). 52

[174] Quezada, S. a. *et al.* Tumor-reactive CD4(+) T cells develop cytotoxic activity and eradicate large established melanoma after transfer into lymphopenic hosts. *J. Exp. Med.* **207**, 637–50 (2010). 52

[175] Casares, N. *et al.* CD4+/CD25+ regulatory cells inhibit activation of tumor-primed CD4+ T cells with IFN-gamma-dependent antiangiogenic activity, as well as long-lasting tumor immunity elicited by peptide vaccination. *J. Immunol.* **171**, 5931–5939 (2003). 53, 70

[176] Van Rooij, N. *et al.* Tumor exome analysis reveals neoantigen-specific T-cell reactivity in an ipilimumab-responsive melanoma. *J. Clin. Oncol.* **31**, e439–442 (2013). 57

[177] Shen, Z., Reznikoff, G., Dranoff, G. & Rock, K. L. Cloned dendritic cells can present exogenous antigens on both MHC class I and class II molecules. *J. Immunol.* **158**, 2723–30 (1997). 59

[178] Kantoff, P. W. *et al.* Sipuleucel-T immunotherapy for castration-resistant prostate cancer. *N. Engl. J. Med.* **363**, 411–22 (2010). 63

[179] Lechner, M. G. *et al.* Immunogenicity of murine solid tumor models as a defining feature of in vivo behavior and response to immunotherapy. *J. Immunother.* **36**, 477–89 (2013). 64, 69, 70

[180] Klug, F. *et al.* Low-Dose Irradiation Programs Macrophage Differentiation to an iNOS(+)/M1 Phenotype that Orchestrates Effective T Cell Immunotherapy. *Cancer Cell* **24**, 589–602 (2013). 64

[181] Schumacher, T. N. & Schreiber, R. D. Neoantigens in cancer immunotherapy. *Science* **348**, 69–74 (2015). 65, 66

[182] Gubin, M. M., Artyomov, M. N., Mardis, E. R. & Schreiber, R. D. Tumor neoantigens: building a framework for personalized cancer immunotherapy. *J. Clin. Invest.* **125**, 1–9 (2015). 65

[183] Saeterdal, I. *et al.* Frameshift-mutation-derived peptides as tumor-specific antigens in inherited and spontaneous colorectal cancer. *Proc. Natl. Acad. Sci. U. S. A.* **98**, 13255–13260 (2001). 66

[184] Herbst, R. S. *et al.* Predictive correlates of response to the anti-PD-L1 antibody MPDL3280A in cancer patients. *Nature* **515**, 563–567 (2014). 66

[185] Brahmer, J. *et al.* Nivolumab versus Docetaxel in Advanced Squamous-Cell Non-Small-Cell Lung Cancer. *N. Engl. J. Med.* **373**, 123–135 (2015). 67

[186] Varga, A. *et al.* Antitumor activity and safety of pembrolizumab in patients (pts) with PD-L1 positive advanced ovarian cancer: Interim results from a phase Ib study. *J. Clin. Oncol.* **33**, (suppl; abstr 5510) (2015). 67

[187] Hamanishi, J. *et al.* Durable tumor remission in patients with platinum-resistant ovarian cancer receiving nivolumab. *J. Clin. Oncol.* **33**, (suppl; abstr 5570) (2015). 67

[188] Muro, K. *et al.* Printer-friendly version . Relationship between PD-L1 expression and clinical outcomes in patients (Pts) with advanced gastric cancer treated with the anti-PD-1 monoclonal antibody pembrolizumab (Pembro; MK-3475) in KEYNOTE-012. *J. Clin. Oncol.* **33**, (suppl 3; abstr 3) (2015). 67

[189] Honey, K. & Rudensky, A. Y. Lysosomal cysteine proteases regulate antigen presentation. *Nat. Rev. Immunol.* **3**, 472–82 (2003). 67

[190] Wang, M. *et al.* HLA class I binding 9mer peptides from influenza A virus induce CD4 T cell responses. *PLoS One* **5**, e10533 (2010). 68

[191] Leen, A. M. *et al.* Identification of hexon-specific CD4 and CD8 T-cell epitopes for vaccine and immunotherapy. *J. Virol.* **82**, 546–54 (2008). 68

[192] Goldsby, R., Kindt, T. J., Osborne, B. A. & Kuby, J. *Immunology* (W. H. Freeman, Cranbury, 2002), 5 edn. 69

[193] Fidler, I. J. Selection of successive tumour lines for metastasis. *Nat. New Biol.* **242**, 148–9 (1973). 69

[194] Wang, M. *et al.* Active immunotherapy of cancer with a nonreplicating recombinant fowlpox virus encoding a model tumor-associated antigen. *J. Immunol.* **154**, 4685–92 (1995). 69, 70

[195] Dexter, D. L. *et al.* Heterogeneity of Tumor Cells from a Single Mouse Mammary Tumor of Tumor Cells from a Single Mouse Mammary Tumor1. *Cancer Res.* **38**, 3174–3181 (1978). 70

[196] Ostrand-Rosenberg, S. *et al.* Cell-based vaccines for the stimulation of immunity to metastatic cancers. *Immunol. Rev.* **170**, 101–14 (1999). 70

[197] DuPré, S. a., Redelman, D. & Hunter, K. W. The mouse mammary carcinoma 4T1: characterization of the cellular landscape of primary tumours and metastatic tumour foci. *Int. J. Exp. Pathol.* **88**, 351–60 (2007). 70

[198] Sinha, P., Clements, V. K. & Ostrand-Rosenberg, S. Reduction of Myeloid-Derived Suppressor Cells and Induction of M1 Macrophages Facilitate the Rejection of Established Metastatic Disease. *J. Immunol.* **174**, 636–645 (2005). 70

[199] Sinha, P., Clements, V. K., Fulton, A. M. & Ostrand-Rosenberg, S. Prostaglandin E2 promotes tumor progression by inducing myeloid-derived suppressor cells. *Cancer Res.* **67**, 4507–4513 (2007). 70

[200] Ostrand-Rosenberg, S. & Sinha, P. Myeloid-derived suppressor cells: linking inflammation and cancer. *J Immunol* **182**, 4499–4506 (2009). 70

[201] DuPre', S. a. & Hunter, K. W. Murine mammary carcinoma 4T1 induces a leukemoid reaction with splenomegaly: association with tumor-derived growth factors. *Exp. Mol. Pathol.* **82**, 12–24 (2007). 70

[202] Kim, K. *et al.* Eradication of metastatic mouse cancers resistant to immune checkpoint blockade by suppression of myeloid-derived cells. *Proc. Natl. Acad. Sci. U. S. A.* **111**, 1–6 (2014). 71

[203] Pastor, F., Kolonias, D., Giangrande, P. H. & Gilboa, E. Induction of tumour immunity by targeted inhibition of nonsense-mediated mRNA decay. *Nature* **465**, 227–30 (2010). 71

[204] Linnebacher, M. *et al.* Frameshift peptide-derived T-cell epitopes: a source of novel tumor-specific antigens. *Int. J. Cancer* **93**, 6–11 (2001). 71

[205] Coulie, P. G. *et al.* A mutated intron sequence codes for an antigenic peptide recognized by cytolytic T lymphocytes on a human melanoma. *Proc. Natl. Acad. Sci. U. S. A.* **92**, 7976–80 (1995). 71

[206] Kowalewski, D. J. *et al.* HLA ligandome analysis identifies the underlying specificities of spontaneous antileukemia immune responses in chronic lymphocytic leukemia (CLL). *Proc. Natl. Acad. Sci. U. S. A.* **112**, E166–75 (2015). 71

[207] Warren, E. H. *et al.* An antigen produced by splicing of noncontiguous peptides in the reverse order. *Science* **313**, 1444–1447 (2006). 71

[208] Meadows, L. *et al.* The HLA-A*0201-restricted H-Y antigen contains a posttranslationally modified cysteine that significantly affects T cell recognition. *Immunity* **6**, 273–281 (1997). 71

[209] Pierce, R. A. *et al.* Cutting edge: the HLA-A*0101-restricted HY minor histocompatibility antigen originates from DFFRY and contains a cysteinylated cysteine residue as identified by a novel mass spectrometric technique. *J. Immunol.* **163**, 6360–6364 (1999). 71

[210] Skipper, J. C. *et al.* An HLA-A2-restricted tyrosinase antigen on melanoma cells results from posttranslational modification and suggests a novel pathway for processing of membrane proteins. *J. Exp. Med.* **183**, 527–34 (1996). 71

[211] Berkers, C. R. *et al.* Peptide Splicing in the Proteasome Creates a Novel Type of Antigen with an Isopeptide Linkage. *J. Immunol.* **195**, 4075–84 (2015). 72

[212] Berkers, C. R. *et al.* Definition of Proteasomal Peptide Splicing Rules for High-Efficiency Spliced Peptide Presentation by MHC Class I Molecules. *J. Immunol.* **195**, 4085–95 (2015). 72

[213] Fritsch, E. F. *et al.* HLA-Binding Properties of Tumor Neoepitopes in Humans. *Cancer Immunol. Res.* **2**, 522–529 (2014). 72

[214] Engels, B. *et al.* Relapse or Eradication of Cancer Is Predicted by Peptide-Major Histocompatibility Complex Affinity. *Cancer Cell* **23**, 516–526 (2013). 72

[215] Bassani-Sternberg, M., Pletscher-Frankild, S., Jensen, L. J. & Mann, M. Mass spectrometry of human leukocyte antigen class I peptidomes reveals strong effects of protein abundance and turnover on antigen presentation. *Mol. Cell. Proteomics* **14**, 658–73 (2015). 72

[216] Wherry, E. J., Puorro, K. A., Porgador, A. & Eisenlohr, L. C. The induction of virus-specific CTL as a function of increasing epitope expression: responses rise steadily until excessively high levels of epitope are attained. *J. Immunol.* **163**, 3735–45 (1999). 72

[217] Spiotto, M. T. *et al.* Increasing tumor antigen expression overcomes "ignorance" to solid tumors via crosspresentation by bone marrow-derived stromal cells. *Immunity* **17**, 737–47 (2002). 72

[218] Riker, A. I. *et al.* Threshold levels of gene expression of the melanoma antigen gp100 correlate with tumor cell recognition by cytotoxic T lymphocytes. *Int. J. Cancer* **86**, 818–26 (2000). 72

[219] Dilillo, D. J. & Ravetch, J. V. Differential Fc-Receptor Engagement Drives an Anti- tumor Vaccinal Effect Differential Fc-Receptor Engagement Drives an Anti-tumor Vaccinal Effect. *Cell* **161**, 1035–1045 (2015). 73

[220] Nazarian, R. *et al.* Melanomas acquire resistance to B-RAF(V600E) inhibition by RTK or N-RAS upregulation. *Nature* **468**, 973–977 (2010). 73

[221] Moon, J. J. *et al.* Naive CD4(+) T cell frequency varies for different epitopes and predicts repertoire diversity and response magnitude. *Immunity* **27**, 203–13 (2007). 74

[222] Jenkins, M. K. & Moon, J. J. The Role of Naive T Cell Precursor Frequency and Recruitment in Dictating Immune Response Magnitude. *J. Immunol.* **188**, 4135–4140 (2012). 74

[223] Gattinoni, L., Kebanoof, C. a. & Nicholas P Restifo. Paths to stemness: building the ultimate antitumour T Cell. *Nat. Rev. Cancer* **12**, 671–684 (2012). 74

[224] Oliveira, G. *et al.* Tracking genetically engineered lymphocytes long-term reveals the dynamics of T cell immunological memory. *Sci Transl Med* **7**, 317ra198– (2015). 74

[225] Munn, D. H. & Bronte, V. Immune suppressive mechanisms in the tumor microenvironment. *Curr. Opin. Immunol.* **39**, 1–6 (2015). 74

[226] Shukla, S. a. *et al.* Comprehensive analysis of cancer-associated somatic mutations in class I HLA genes. *Nat. Biotechnol.* **33**, 1152–1158 (2015). 74

[227] Santoro, S. P. *et al.* T cells bearing a chimeric antigen receptor against prostate-specific membrane antigen mediate vascular disruption and result in tumor regression. *Cancer Immunol. Res.* **3**, 68–84 (2015). 74

[228] Garcia-Murillas, I. *et al.* Mutation tracking in circulating tumor DNA predicts relapse in early breast cancer. *Sci. Transl. Med.* **7**, 302ra133 (2015). 75

[229] Lifetime Risk of Developing or Dying From Cancer (2016-02-13). URL `http://www.cancer.org/`. 77

5 Supplements

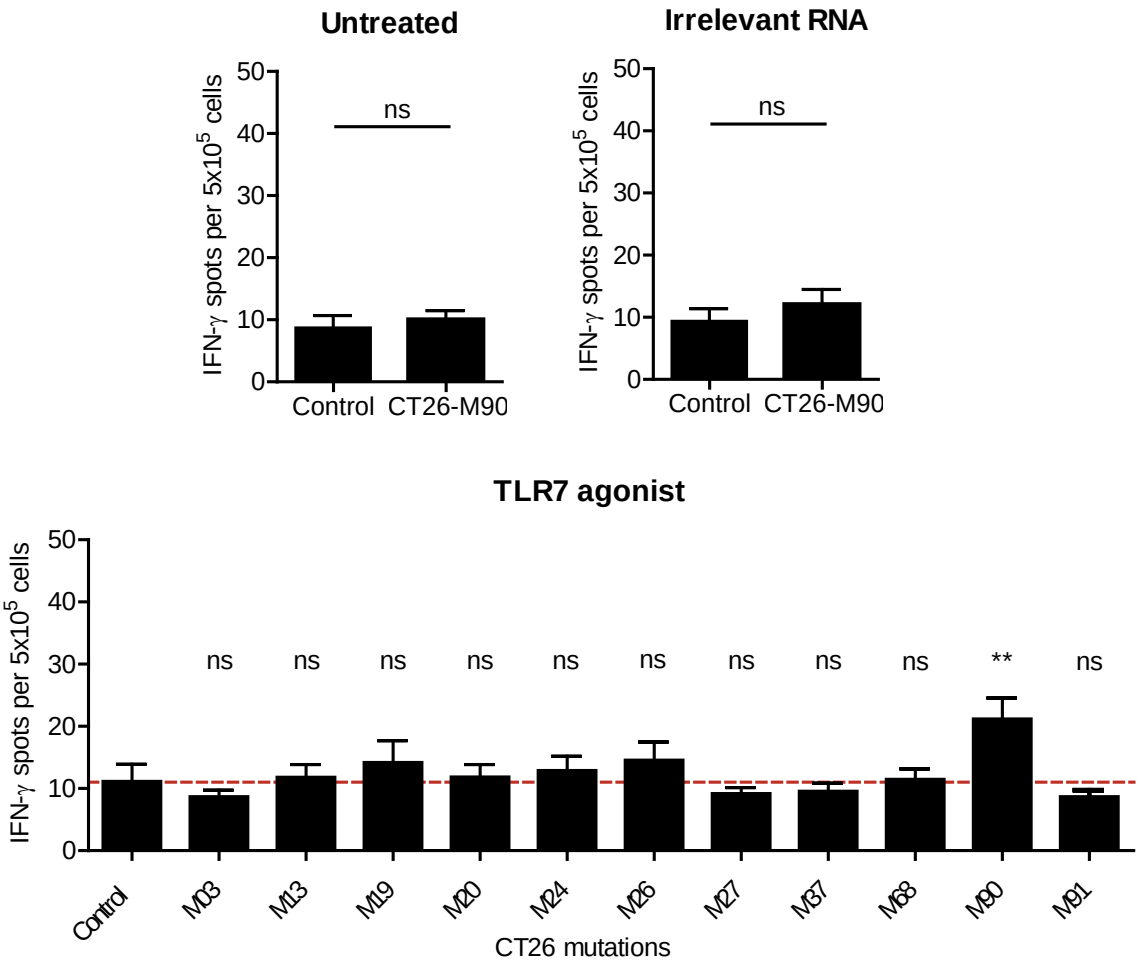

Figure 5.1: Induction of CT26-M90 specific T cells after treatment with an TLR7 agonist. Detection of immune responses in splenocytes of untreated, irrelevant RNA or Toll-like receptor (TLR) 7 agonist treated mice against immunogenic CT26 mutations. Splenocytes of subcutaneous CT26-WT tumor bearing BALB/c mice (untreated/irrelevant RNA: n=5, TLR7 agonist: n=9) were tested by ELISpot for recognition of synthetic peptides (mean $\pm$ s.e.m.).

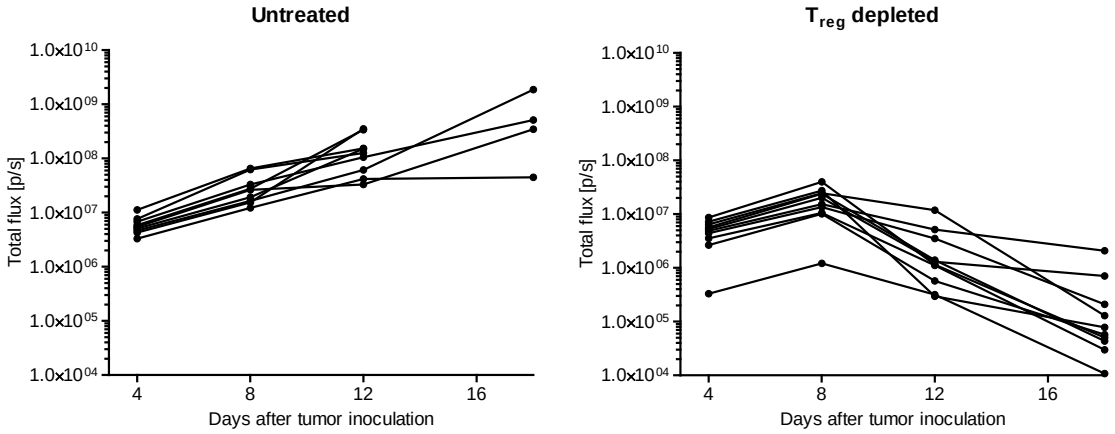

Figure 5.2: T_{reg} depletion results in rejection of CT26 tumors. BLI measurements of CT26-Luc tumor bearing mice (n=10) that were left untreated or treated with an depleting antibody against CD4 at day 4, 8, 12 and 18 after tumor inoculation. Efficiency of CD4 depletion was >90 % as determined by flow cytometry.

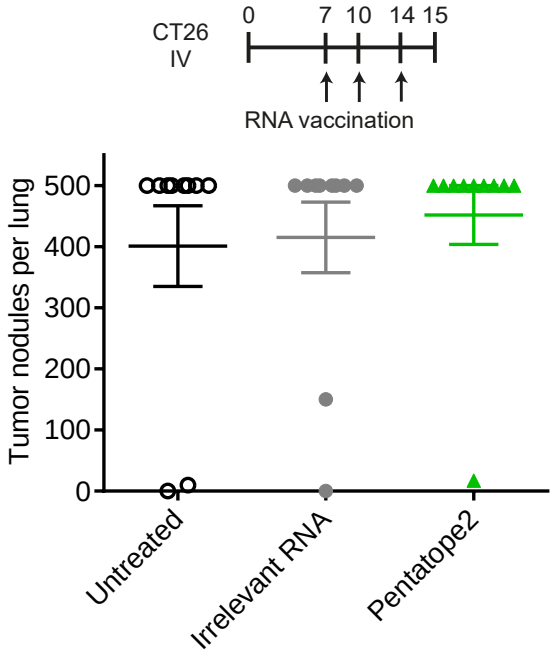

Figure 5.3: Late RNA vaccination against pentatope2 is inefficient. BALB/c mice (n=10) were inoculated IV with CT26 tumor cells and left untreated or injected with irrelevant or pentatope2 RNA starting at day 7 after tumor inoculation. Tumor nodules per lung a shown.